Traction Awareness Through Haptic Feedback for the Teleoperation of UGVs

Rute Isabel Soares da Luz

Thesis to obtain the Master of Science Degree in

Aerospace Engineering

Supervisors: Prof. Rodrigo Martins de Matos Ventura
Prof. José Luís Cardoso da Silva

Examination Committee

Chairperson: José Fernando Alves da Silva
Supervisor: Rodrigo Martins de Matos Ventura
Member of the Committee: Carlos António Roque Martinho

June 2018

ACKNOWLEDGMENTS

Resumo

Teleoperação de Veículos Terrestres não Tripulados está dependente de vários factores devido ao facto de que o operador humano está fisicamente separado do robô. Esta tese foca-se em situações em que o veículo perde a tração e o robô é incapaz de cumprir os comandos do operador humano. Em situações como esta, a falta de consciência sobre a situação do robô pode levar a uma resposta incorreta e ineficiente ao estado atual do veículo, geralmente confundindo e frustrando o operador humano. O uso exclusivo de informação visual para executar simultaneamente uma tarefa e estar ciente de possíveis impedimentos à operação do veículo, tal como a perca de tração, pode tornar-se uma tarefa muito exigente para um único operador humano. Nesta tese, aborda-se o desafio de descarregar o canal visual recorrendo a outros sentidos humanos para fornecer uma informação multimodal durante a teleoperação. Para atingir este objetivo, apresentamos uma arquitetura de teleoperação integrando (1) um módulo detector de tração, para discriminar percas de tração, e (2) uma interface háptica para transmitir o estado de tração do robô ao operador humano através de diferentes tipos de estímulo táctil, recorrendo a três dispositivos hápticos (E-Vita, Cilindro Rotacional e Luva Vibrotáctil). Também são relatados os resultados experimentais de um estudo com utilizadores para avaliar até que ponto esta nova modalidade melhora a compreensão dos participantes em relação ao estado de Tração do robô. Foram encontrados resultados estatisticamente significantes para afirmar que dois dos dispositivos hápticos melhoraram a compreensão do estado de tração do robô.

Palavras-chave: Novas Interfaces e Modalidades de Interação; Compreensão Multimodal da Situação; Design de Robôs Centrado no Utilizador; Interação Homem-Máquina Háptica; Fatores Humanos; Teleoperação de Veículos Terrestres não Tripulados.

ABSTRACT

TELEOPERATION of Unmanned Ground Vehicles (UGVs) is dependent on several factors as the human operator is physically detached from the UGV. This thesis focuses on situations where the UGV loses traction, thus becoming unable to comply with the operator's commands. In such situations, the lack of Situation Awareness (SA) may lead to an incorrect and inefficient response to the current UGV state usually confusing and frustrating the human operator. The exclusive use of visual information to simultaneously perform the main task (e.g. Search and Rescue) and to be aware of possible impediments to UGV operation, such as loss of traction, can become a very demanding task for a single human operator. The challenge of unburdening the visual channel is addressed by using other human senses to provide multi-modal feedback in UGV teleoperation. To achieve this goal is present a teleoperation architecture comprising (1) a laser-based traction detector module, to discriminate between traction losses (stuck and sliding), and (2) an haptic interface to convey the detected traction state to the human operator through different types of tactile stimuli provided by three haptic devices (E-Vita, Traction Cylinder and Vibrotactile Glove). It is also reported the experimental results of a User Study to evaluate to what extent this new feedback modality improves the user SA regarding the UGV traction state. Statistically significant results were found supporting the hypothesis that two of the haptic devices improved the comprehension of the traction state of the UGV.

CONTENTS

x

LIST OF FIGURES

LIST OF TABLES

GLOSSARY

ANOVA Analysis of variance. 59, 60

DoF Degree of Freedom. 21, 30

GPS Global Positioning System. 25

GUI Graphical User Interface. 6

IDE Integrated Development Environment. 34, 44

IMU Inertial Measurement Unit. 5

LIDAR Light Detection And Ranging. 5

PWM Pulse-width modulation. 35, 44

ROS Robot Operating System. 34, 39, 44

SA Situation Awareness. 1, 7, 49, 50

SAGAT Situation Awareness Global Assessment Technique. 9, 50, 51

SAR Search and Rescue. 1, 5

SLAM Simultaneous Localization and Mapping. 6

SMA Simple Moving Average. 17, 18

UGV Unmanned Ground Vehicle. 1, 5, 27, 49

USAR Urban Search and Rescue. 1, 7, 13

1| Introduction

Contents

1.1 Motivation

Teleoperation of Unnamed Ground Vehicles (UGVs) allows the human operator to explore and act on remote environments. However, the fact that the human operator is physically detached from the UGV raises several challenges. One particular challenge consists in providing an effective awareness of the robot situation, known as Situation Awareness. This thesis focuses on the problem of dealing with situations where the UGV loses traction and is unable to comply with a human operator's commands. In these situations, awareness of traction loss is compromised by the physical detachment of the operator with respect to the UGV.

The concept of Situation Awareness (SA) was formally defined by Endsley [1] as "a person's perception of the elements of the environment within a volume of time and space, the comprehension of their meaning and the projection of their status in the near future". This definition of SA, characterizes an understanding of the environment's state and its parameters, that can be divided into three levels of SA. Perception (Level 1 SA), is the first and lowest level of SA, in which a person is capable of perceiving the relevant information provided by the system. Comprehension (Level 2 SA), is the second and middle level of SA, in which a person is capable of understanding the perceived information and integrate it with the operation goals. Projection (Level 3 SA), is the last and top level of SA, in which a person is capable of predicting future events and system states, based on the previous comprehension of the system and its environment, "...allowing for timely and effective decision making" [1].

In situations where the UGV loses traction, the lack of SA can lead to an incorrect and inefficient response to the current UGV state, usually confusing and frustrating the human operator [2]. In these circumstances, it is fundamental to have interfaces that can provide the relevant SA information when needed, without distracting the operator from its main task (e.g. Search and Rescue). Interfaces that exclusively use visual information can become challenging to human operators in situations where the robot is unable to comply with the given commands, such as loss of traction, as it requires the extraction of information based on subtle visual cues to estimate the current situation. Furthermore, only having a visual interface may hinder the perception of relevant information, and clutter the image provided by the on-board cameras, which is needed to search for victims. One way of reducing the burden on the visual channel is to use other human senses and provide multi-modal feedback in UGV teleoperation. In this thesis visual and tactile modalities have been used.

Teleoperation of mobile vehicles extends the human cognition to remote and hazardous environments. These environments can include Urban Search and Rescue (USAR) scenarios, in the case of RAPOSA-NG [3], but also the Moon, Mars, and other orbiting bodies, as a future application. Provid-

ing an effective Situation Awareness in these conditions is crucial for on-orbit human teleoperators to be able to drive the UGV and perform tasks, such as remote assembly on planetary surfaces. In these environments, the locomotion of the robot serves as a base element for exploration and manipulation tasks, thus, is essential to ensure full mobility of vehicle at all times, including in situations were it loses traction and it is unable to comply with the given commands. The addition of human cognition to the usual autonomous approach in this kind hazardous and unpredictable environments is a valuable asset to ensure the success of task completion. Therefore, ensuring the Situation Awareness of the human operator concerning the robot's situation is a fundamental factor toward task completion. In this thesis, RAPOSA-NG was the used research platform and the extension of the developed work goes beyond the use of teleoperation for the search of victims.
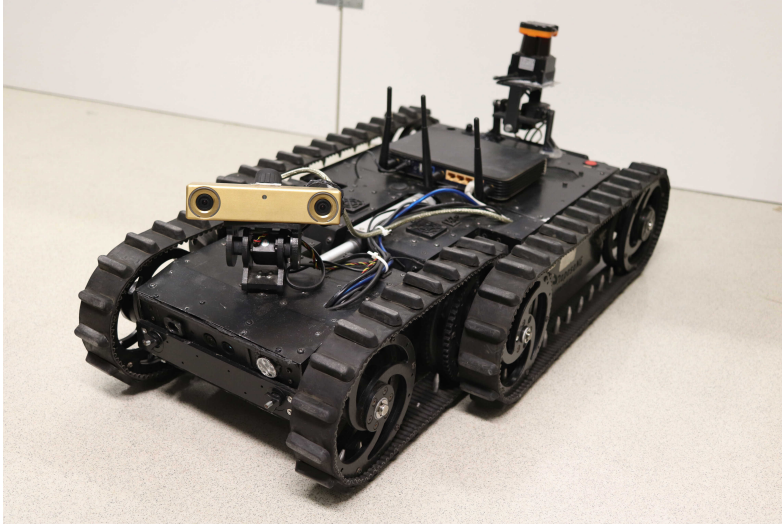
Figure 1.1: RAPOSA-NG, a tracked wheel search and rescue UGV prototype.

1.2   Thesis Objectives

The Objectives to be achieved with thesis were:

Objective 1: Develop a detection algorithm capable of detecting losses of traction and discriminate the corresponding traction states using the given tracked wheel odometry and laser-based odometry.

Objective 2: Iteratively develop different haptic devices capable of providing the traction state of the UGV to the human operator, exploring different types of tactile stimuli in each device and providing different patterns for each detected state.

Objective 3: Perform a user study to quantitatively evaluate the Situation Awareness (SA) of the users, regarding the traction state of the robot with and without the haptic devices and quantitatively compare those.

1.3   Major Contributions

The major contributions of this thesis are:

1. The development of a traction detection module capable of detecting traction loss regarding position and orientation, and classified the detected traction state as normal, stuck or sliding. The traction detection and classification is based on determining whether there is a mismatch between the expected motion, given tracked wheel odometry, and the actual motion, given laser-based odometry. Whenever a significant mismatch is found, the traction situation of the robot is computed, following the situation classification;

2. The development of three haptic devices to convey the estimated traction state to the human operator resorting to tactile stimuli. These devices are capable of providing different haptic patterns according to the detected state. In particular, it is explored three types of tactile stimuli: (1) *friction*, using a rotating cylinder in contact with the operator's hand, (2) *vibration*, using a vibrotactile glove, and (3) *texture*, using a texture rendering device. The integration of the haptic devices on the teleoperation system of RAPOSA-NG (Figure 1.1), a tracked wheel search and rescue UGV prototype, which included the physical construction of the above-mentioned friction and vibration devices;

3. The description of a detailed user study to evaluate the three haptic devices, in comparison with the exclusive use of the visual channel, involving the teleoperation of RAPOSA-NG on locomotion challenging scenarios. The presented user study intends to answer two research questions:

   Q1 "Does the addition of haptic feedback to the exclusively visual interface improves the user SA regarding the UGV traction state?";

   Q2 "Which of the presented haptic devices can better convey to the operator the traction state of RAPOSA-NG?".

   The experimental results allowed to answer the first research question. An improvement was found when using the Vibrotactile Glove and the Traction Cylinder regarding comprehension of the UGV's traction state, with respect to the exclusively visual modality. Regarding the second research question, no supported answer was obtained. Although it was found a statistically significant improvement of SA, regarding traction state, using the Traction Cylinder (*VC*) and the Vibrotactile Glove (*VB*) when comparing to E-Vita (*VE*), no statistically significant difference was found between *VC* and *VB*.

As far as it is known, this is the first work that tackles traction loss in teleoperated UGVs, by providing tactile feedback to human operators.

1.4   Thesis Outline

This thesis is structured as follows:

Chapter 2 Background and State of the Art presents a brief description of the background and a succinct summary of the state of the art. The described background compromises a description of RAPOSA-NG, the UGV utilized during the development of this thesis, a description of the concept of Situation Awareness, and an introduction to the field of human-machine interaction. Finally, a brief introduction and description of teleoperation of mobile robots is presented, its applications, challenges and previously proposed approaches;

Chapter 3 Traction State Detection presents two different methods to detect traction loss and its classification. The first method resorts to the calculation of velocity values to compare the mismatch between the expected motion and the actual motion of the UGV, while the second Method resorts to the calculation of displacement vectors;

Chapter 4 Haptic Devices presents the project requirements, a brief description of the proposed concepts of haptic devices and its implementation. It is also described in detail the development of three haptic devices capable of providing different types of stimuli to human operator accordingly to the detected traction state of the UGV. Two of the presented devices (Traction Cylinder and Vibrotactile Glove) were implemented and integrated by the author while the third device (E-Vita) solely the integration with RAPOSA-NG system was performed;

Chapter 5 User Study describes in detail the design of the user study, its implementation, apparatus, and method, including a description of the population, the implemented procedure, and the obtained measures. The performed user study intends to evaluate the three haptic devices, in comparison with the exclusive use of the visual channel and answer two research Questions: (*Q1*) *Does the addition of haptic feedback to the exclusively visual interface improves the user SA regarding the UGV's traction state?* and (*Q2*) *Which of the presented haptic devices can better convey to the operator the traction state of RAPOSA-NG?*;

Chapter 6 Results and Discussion reports the Results of the performed user study and its Discussion. The obtained results include a statistical analysis of the SAGAT data. This analysis compares the use of haptic feedback with the exclusive use of visual feedback. It is also reported the results of a statistical analysis concerning the obtained qualitative data from the post-trial questionnaires. Finally, the results of the statistical analyses are interpreted and discussed. Furthermore, it is presented a brief compilation of the comments made by the participants during the user study, concerning the different haptic devices.

Chapter 7 Conclusions presents the conclusions of this thesis and a few suggestions for future work.

2| Background and State of the Art

Contents

THIS Chapter presents a brief description of the Background, in Sections 2.1, 2.2 and 2.3, and a succinct summary of the State of the Art is performed , in Section 2.4. In Section 2.1 it is described RAPOSA-NG, the UGV explored during the development of this thesis, its current features, and limitations. In Section 2.2 is presented the concept of Situation Awareness, its assessment and the used technique during the user study. In Section 2.3 is performed an introduction to the field of human-machine interaction, a brief description of the cognitive senses intrinsic to the human haptic channel and possible applications of haptic interfaces. Finally, in Section 2.4, it is presented a brief introduction and description of teleoperation of mobile robots, its applications, challenges and previously proposed approaches.

2.1   RAPOSA-NG, a Search and Rescue UGV prototype
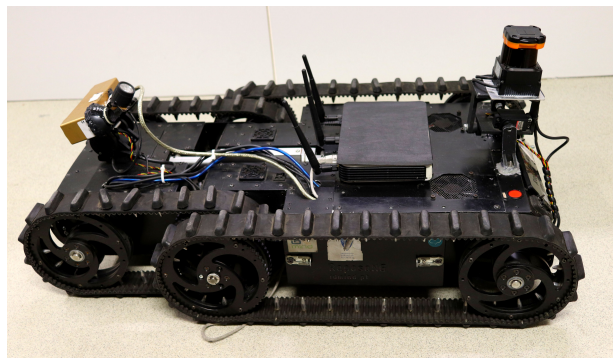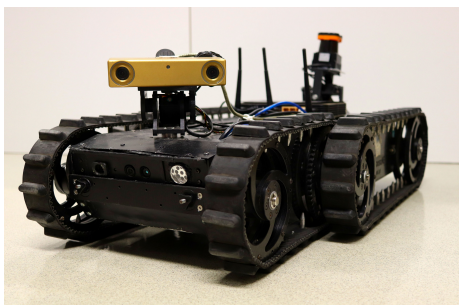
Figure 2.1: RAPOSA-NG, a tracked wheel Search and Rescue UGV prototype.

RAPOSA-NG is a tracked wheel Search and Rescue UGV prototype, designed to operate in outdoors hazardous environments. This UGV was also designed to perform a teleoperated detection of possible victims. The robot is equipped with two cameras, a LIDAR, and IMU sensor. These sensors provide information regarding the robot status, including robot and stereo camera attitude, battery level, and network latency. The LIDAR is installed on top of a tilt & roll structure acting as gimbal stabilizer to maintain the laser scans in a horizontal plane and increase the robustness of the mapping while traveling in irregular terrain.

Figure 2.2: RAPOSA-NG during an on-field exercise. On the bottom, and teleoperation team, on the top-right, using the Oculus Rift and the teleoperation console [4].

The status of the robot is conveyed to the user using a visual augmented reality GUI. This teleoperation GUI is composed of two components: (1) the teleoperation console (Figure 2.3), displayed on the teleoperation PC, and (2) the Oculus Rift Head Mounted Display (Figure 2.4), worn by the teleoperator (Figure 2.2), displaying a stereo image of the remote environment. The visual interface displayed on the Oculus Rift was designed to provide an immersive navigation resorting to augmented reality. The Oculus Rift Glasses provide to the user a depth perception of the environment and allows to mark points of interest (yellow markers shown in Figures 2.3 and 2.4). The stereo camera, on-board the robot, is installed on top of a tilt & pan structure acting as gimbal stabilizer to follow the direction that the operator is facing with the Oculus Rift, as shown in Figure 2.3. Having this feature allows the teleoperator to "look around" in an intuitive way, without needing to control the tilt and pan of the camera with the joypad.

Figure 2.3: GUI of the Teleoperation Console of RAPOSA-NG with the Operator View. On top, the interactive 3D Virtual Mode, on bottom-left, and Real Time 2D Map (Hector SLAM), on bottom-right [4].
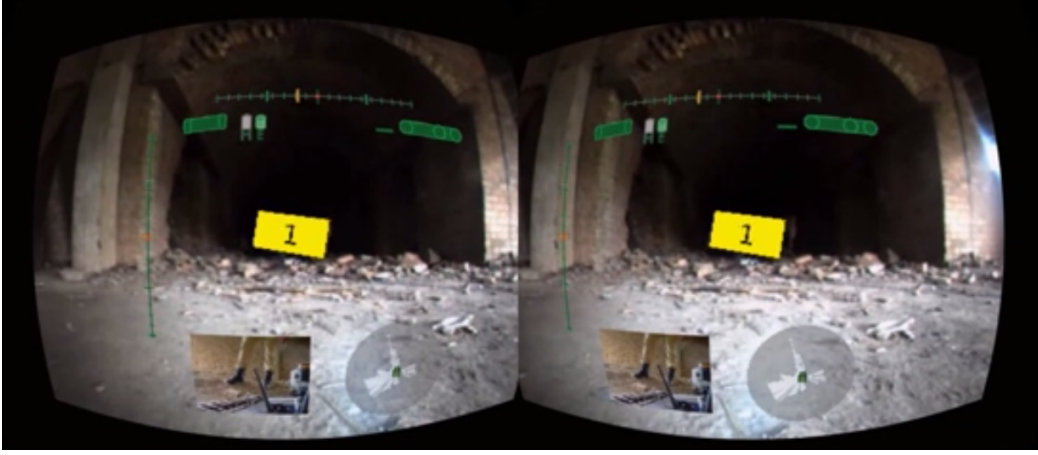
Figure 2.4: Stereo view on the Head Mounted Display (Oculus Rift) including stereo and rearview images from the on-board cameras, robot status, map and a label, marked on the map and displayed using augmented reality.[4].

The teleoperation of RAPOSA-NG requires three team members: one operator to navigate and control RAPOSA-NG while using the Oculus Rift, one co-member to assist using the information in the teleoperation console, on the teleoperation PC, and one specialized member of the Urban Search and Rescue (USAR) Response Team.

Although research has been developed to create an immersive teleoperation of RAPOSA-NG [3], [5], [6], [7], still, there are situations where the lack of Situation Awareness leads to the inability to control the robot's movement. These situations include the loss of traction due to the irregularity of the terrain and unpredictability of the obstacles. Scholtz [2] reports many instances of robots getting stuck or entangled with obstacles, while the operators lacked sufficient Situation Awareness to understand the cause of the entanglement. Operators inferred that something was wrong whenever the image received from the on-board cameras doesn't change even though they are commanding the robot to move. In these situations, it is necessary to have as much information as possible without hindering the search for the needed information and clutter the visual information provided by the on-board cameras, needed for the main task. One way of reducing the burden on the visual channel is resorting to other human senses and provide multi-modal feedback in UGV teleoperation as presented in this thesis.

2.2 Situation Awareness

The concept of Situation Awareness (SA) was formally defined by Endsley [1] as "a person's perception of the elements of the environment within a volume of time and space, the comprehension of their meaning and the projection of their status in the near future". This definition of SA characterizes an understanding of the environment's state and its parameters, that can be divided into three levels of SA:

1. **Perception** is the first and lowest level of SA in which a person is capable of perceiving the relevant information provided by the system (Level 1 SA).

2. **Comprehension** is the second and middle level of SA in which a person is capable of understanding the meaning of the perceived information and integrate it with the operation goals (Level 2 SA).

3. **Projection** is the last and top level of SA in which a person is capable of predicting future events and system states based on the previous comprehension of the system and its environment. This projection of events and states will allow "timely and effective decision making" [1] (Level 3 SA).

2.2.1 Assessment of Situation Awareness

To assess the Situation Awareness of the participants during the several trials of the user study, it is necessary to query them on their understanding of the system and its environment. This queries can be administered to the participants using different methods. Each of these methods queries the participants in different moments of the trials as described below:

- **Post-test:**

  When using a Post-test method an extent and detailed questionnaire is administered to the user <u>after</u> each trial. This questionnaire includes a list of questions concerning the Situation Awareness of the users during the trial.

  This method allows the user to perform the given task as naturally and close to the real situation as possible. In this method, it is given plenty of time to the participant to answer the extent questionnaire. The main disadvantage of this method is the fact that users are not good at reporting detailed information about past mental events. Such information tends to be overgeneralized and over-rationalized [1]. The ability to recall relevant past events is affected by the amount of time occurred until the administration of the questionnaire. Earlier misperceptions can be quickly forgotten as the real situation of the environment becomes clear during the course of the following events. Such misperceptions are important to the SA assessment.

  Therefore, a Post-test questionnaire will reliably capture the participant's SA only at the very end of the trial [1].

- **On-line:**

  Using an On-line method to administrate the questionnaires will overcome the limitations of the Post-test. Using this method the queries are administrated to the users <u>while</u> they are performing the requested tasks. This allows to assess the user's SA during the trial and not only at the very end. This method has two main drawbacks. First, answering questions while performing the tasks constitutes a form of ongoing **secondary task loading**, which may alter their performance [1]. Second, the administrated query can cue the participant to attend to the requested information on the displays, thus modifying the operator's true SA [1].

  Overall, this method will be able to assess the users SA during the performance of the task. However, it will be highly intrusive on the primary task of system operation [1].

- **Freeze Technique:**

  Using a Freeze Technique will allow reaching a compromise between the Post-test and On-line methods. In this technique, the system is frozen at randomly selected times, <u>while</u> the user is performing the task. At that moment the system displays are blanked, the task is suspended and the users quickly answer the queries. These queries inquire the users about their understanding of the system and environment at the moment of the interruption.

  This technique has one main drawback. When the task is frozen, it is created a **disruptive halt**, causing an interruption of the natural flow of the task execution. For that reason, the task completion time cannot be used as a measurement of the user study.

  Hence, using a Freeze technique will allow assessing the users SA during the task without overloading them with a secondary task (answering the questionnaires). However, it might be intrusive to the primary task (system operation) due to interruption of the natural task flow.

During the user study reported in this thesis, the participants had to go through various and intricate situations. Thus, assessing the SA of the participants, while performing the task, was an important requirement for the designed user study. Therefore, a Post-test questionnaire will not be

employed. Concerning the On-line administration method, the fact that this one constitutes a form of an ongoing secondary task was the main reason to discard this method. Using a Freeze technique, it is reached a compromise between Post-test and On-line methods. The participant answers the queries during the course of the task while having a specific period of time to do so.

For the user study reported in this thesis, it was selected the Situation Awareness Global Assessment Technique (SAGAT), a freeze on-line probe technique developed by Endsley and one of the best publicized and most widely known measures of SA [8]. Studies have been conducted with SAGAT over a wide range of application including aviation and Air Traffic Management.

2.2.2   Situation Awareness Global Assessment Technique (SAGAT)

The Situation Awareness Global Assessment Technique (SAGAT) is a global tool developed to assess SA across all of its elements based on a comprehensive assessment of operator SA requirements [9]. When using SAGAT, the teleoperation task is frozen at randomly selected times and, at that moment, a set of queries is provided to the participants. These queries assess the participant's perceptions of the situation at the interruption time. SAGAT queries allow obtaining detailed information concerning the subject's SA. This information is collected on an element by element basis.

This type of assessment is a direct measure of SA. It assesses the operator's perceptions rather than inferring them from behaviors that may be influenced by other factors besides SA. Using this approach to collect SA data, the users' perception is assessed while the events are still fresh in their minds. Thus, reducing multiple problems incurred when collecting data on mental situations after the event, while avoiding the addition of a secondary task loading. This way, individual "snapshots" of operators' SA can be acquired, producing an SA quality index of a particular design [9].

Because SAGAT is a global technique, it comprises queries concerning all levels of SA. These queries include the status of the system and relevant environment features. The inclusion of queries across the complete spectrum of an operator's SA requirements minimizes possible biasing of attention. This way, the subjects cannot prepare for the queries in advance.

This method is not without some detriments. It might be intrusive to the primary task due to interruption of the natural task flow. Therefore, a detailed analysis of SA requirements is necessary to ensure the correct development of the administered queries.

2.3   Haptic Human-Machine Interaction

Haptics refers to the human capability to sense and manipulate a natural or synthetic mechanical environment through touch [10]. Furthermore, it concerns to the part of the human physiology and encompasses a broad range of sensations resulting from mechanical deformation of the skin. The field of haptic human-machine interaction is inherently multidisciplinary, utilizing knowledge from many other fields including robotics, experimental psychology, biology and computer science, systems and control. This field refers to the study of human touch as a modern human-machine interaction paradigm [11].

Haptic human-machine interaction relies on the exploration of three cognitive senses, intrinsic to the human haptic channel [12]:

Kinesthetic Sense that provides information regarding the movement of the body [10].

Proprioceptive Sense that provides information regarding the limbs position, weight and applied forces through a variety of receptors located in the skin, joints, skeletal muscles, and tendons [10].

Tactile Sense that provides an awareness to stimuli on the surface of the body through a range of different receptors located in the skin, such as mechanoreceptors that detect skin deformation [10].

The stimulation of the receptors in the skin and consequent transmission of information can be accomplished by resorting to, for example, a force-feedback type of interfaces. The high density of fast conducting mechanoreceptors makes the fingers and hands ideal for discriminative touch and allows the fingers to, for example, detect the textures of an object [13]. Tactile sensations include pressure, texture, puncture, thermal properties, softness, wetness, friction-induced phenomena such as slip, adhesion, and micro failures, as well as local features of objects such as shape, edges and embossings [10].

Together, the kinesthetic, proprioceptive and tactile senses are fundamental components of human manipulation and locomotion [10]. The exploitation of these senses makes it possible to enhance the current exclusively visual interfaces and achieve richer and more immersive interactions by providing a multi-modal interaction to the user. Here, multi-modal refers to visual, kinesthetic and tactile modalities.

Although the neurophysiologic study of discriminative touch is relatively well matured in terms of receptors, pathways to the brain and perception, some challenges still remain regarding the use of haptic displays [13]. One of those challenges is determining what information can be conveyed and what parameters of the stimuli should be used in order to provide an effective message to the user [14]. The psychophysical study of capabilities of different sensory modalities, e.g. vibration, textures, friction, pressure or curvature display, provided a better comprehension of the underlying biological mechanisms that account for these sensory abilities and allow to understand the processes involved in human decision making [15].

Once the physiologic mechanisms inherent to the haptic channel are well understood, haptic interfaces can be developed to provide information through the user's haptic channel. Such information can include, for example, the state of a system, which will allow the user to make decisions based on conveyed information [14]. Haptic interfaces are mainly characterized by their capability of generating mechanical signals that stimulate the kinesthetic, proprioceptive and/or tactile senses. The process by which the users perceive the haptic stimuli can be either passive or active. Both passive and active types of haptic devices share the characteristic of being programmable, but differ in the way that the information is extracted by the user:

Passive Haptic Devices display tactile cues to the user, whose stationary hand makes contact with a surface or object, that may or may not be moving [15]. This type of haptic device is usually designed to have programmable dissipation, as a function of position and/or time [10]. In this case, the exchange of energy is performed in a single direction: machine to human.

Active Haptic Devices allow the user to actively explore and sense a surface or object where it is displayed both tactile and kinesthetic cues regarding the object being explored [15]. This type of haptic device allows a two-way exchange of energy between the user and machine based on a closed-loop function of the feedback control [10].

Possible applications of haptic interfaces are: Telerobotics and Teleoperation [16], Rehabilitation [17], Medical Training Simulators [18], Exploration of Virtual Environments [19], Gaming [20] and Immersive Entertainment [21].

In this thesis, the addition of haptic feedback to the human-machine interaction emerges as a way to display a greater amount of information during the teleoperation of RAPOSA-NG, without overloading the visual channel. To accomplish that, it is used the haptic channel to provide intuitive feedback regarding the traction state of the robot. Thus, it is used a passive haptic device that actuates on the hand of the user. Using a passive type of haptic device allows creating an alternative modality display of information without requiring the user to explore the device during teleoperation, which could represent an additional task to the user.

(a) Shared autonomy control strategy [26].   (b) Absolute teleoperator control [26].
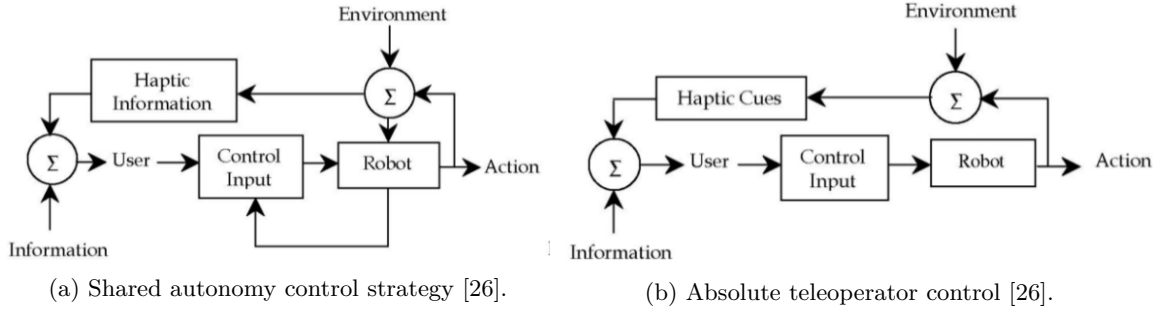
Figure 2.5: Different autonomy levels in Teleoperation control systems.

2.4   Haptics Applied to Teleoperation of UGVs

Teleoperation is the extension of a person's sensing, decision making, and manipulation capability in a remote location [12]. In particular, the teleoperation of Unnamed Ground Vehicles (UGVs) allows the human operator to explore and act on remote environments. However, the fact that the human operator is physically detached from the UGV raises several challenges.

Teleoperated robotic systems have been used in many real-world applications, such as Urban Search and Rescue (USAR) [22], Explosive Ordnance Disposal [23], Hazardous Material Handling [24] and Surveillance and Target Acquisition [25].

In these dynamic, unpredictable and chaotic environments having a human in the control loop, through teleoperation, yields the capability to overcome cognitive limitations of the robotic system by introducing many human desirable attributes. Such attributes include the ability to adapt to a variety of conditions, a relatively high-level of intelligence, advanced sensory capabilities and human-level judgment and intuition. Many real-world applications, such as USR, require such attributes in order to achieve successful task completion. Yet, the human in the loop strategy in robotic systems can have two possible autonomy levels [26]:

Shared Autonomy Control: the human operator is able to control the robot, located in a remote environment, in a shared autonomy control architecture, as represented in Figure 2.5a. Therefore, in some cases, the robot has the capability to override the teleoperator commands and control its own actions. In this scenario, the teleoperator does not have absolute control of the robotic system, which might result in conflict between the intention of the human operator and that of the robot.

Absolute Teleoperator Control: The capabilities of the human operator are acknowledged as superior and this one holds the ultimate decision-making authority. In this scenario, the robot's cognitive capabilities may be used to augment the teleoperator's control process, as represented in Figure 2.5b. Hence, an indication of the robot's intent may provide suggestions or cues to the operator rather than directly intervening in the control process. This scenario excludes the ambivalence of control decisions as the teleoperator has total control of all of the robot's actions.

In the particular case of RAPOSA-NG platform, the robotic system is equipped with an absolute teleoperator control. The current teleoperation interface currently provides visual information to the teleoperator. Now, this visual information is coupled with haptic cues to improve the human decision making and teleoperation control of RAPOSA-NG.

Before starting the enhancement of the RAPOSA-NG interface a review of the literature was performed. This one was conducted to obtain a better understanding of the mainly explored challenges in teleoperation of a mobile robot. In particular, the ones that resort to haptic interfaces. The performed review revealed three mainly investigated challenges: (1) Low wireless signal, (2) Collision avoidance,

and (3) Goal and trajectory task following. Below, it is briefly described those three challenges and some of the developed approaches tackling them:

1. **Low Wireless Signal:**

   Search and rescue scenarios often exhibit characteristics that hinder wireless communication. Additionally, teleoperation requires a high bandwidth to provide continuous feedback to the user, which can be difficult in areas with a low wireless signal.

   One of the developed approaches to tackle the challenge of low wireless signal was proposed by Owen-Hill [27]. The developed approach demonstrated, with simulated experiments, the feasibility of using haptic feedback to perceive wireless signal strength. During the experiments, the users drove a field robot in search and rescue environment and mission. Resorting to the haptic feedback, the users were able to perceive the wireless signal strength and to avoid regions with a low wireless signal. Information regarding the signal strength was provided to users using force feedback conveyed by the PHANToM OMNI device. This haptic device was also used to control the robot.

   The intent of the provided force feedback was to guide the teleoperator towards areas with higher signal strength. The teleoperator control was only restricted when the robot was in areas where the signal was too low to operate the robot. With this approach, the teleoperator of the robot was allowed to intuitively perceive the wireless signal while exploring a remote environment.

   The proposed method allows the operator to make better decisions and avoid communication issues. This approach is an example of a human-in-the-loop control model using a shared autonomy.

2. **Collision Avoidance:**
   During navigation of a mobile robot, a fundamental task of the teleoperator is ensuring the physical integrity of the robot. Therefore, the teleoperator should be aware of the environment and existing obstacles in order to accomplish a safe navigation. However, preventing the robot from colliding with obstacles can become a difficult task. Particularly, if this one is not their primary task, e.g. search of victims. This is primarily due to (a) limited information from the robot's sensors, such as a limited image from the on-board cameras, and (b) the delay in the communication between the teleoperator and the mobile robot [28].

   To undertake the challenge of collision avoidance, Lee [28] presented a force feedback approach. In this strategy, it was used SensAble PHANToM 1.5 device to control the robot while receiving force feedback. The force felt by the user was computed from the position of the obstacles surrounding the robot. Considering two types of forces, environmental and collision-preventing, significantly improved the overall navigational safety and performance. The experiments were conducted in both virtual and real environments. The added haptic feedback also improved the user's awareness of the environment in several ways. These ways include a reduction in the number of collisions and an increase in the minimum distance between the robot and obstacles. This was accomplished without degradation in other aspects of performance such as navigation time.

   A different approach, for collision avoidance, was proposed by Corujeira [29]. The introduced method used Xbox One S Wireless Controller to both control the robot and convey vibrotactile cues. The vibrotactile feedback informed the user of the obstacle's proximity and direction. These cues were provided to the teleoperator using directional haptic feedback and depended on the zone of proximity to the obstacle. The zones of proximity to the obstacle were also utilized to constrain the velocity of the robot. The conducted experiments were performed in a simulated static environment, in a dual-task teleoperation scenario. The haptic feedback improved the human operator's navigational performance, both in completion time and in collision duration.

Both approaches, proposed by Lee and Corujeira, employed a shared autonomy control in the teleoperation of a mobile robot, limiting the mobility of the robot near the obstacles for safety reasons.

3. **Goal and Trajectory Task Following:**

   In scenarios such as Urban Search and Rescue, it is fundamental to reach the goal location as fast as possible, especially if human lives are at risk. Moreover, the teleoperator needs to ensure the safety of the remote mobile robot during navigation by following safe trajectories.
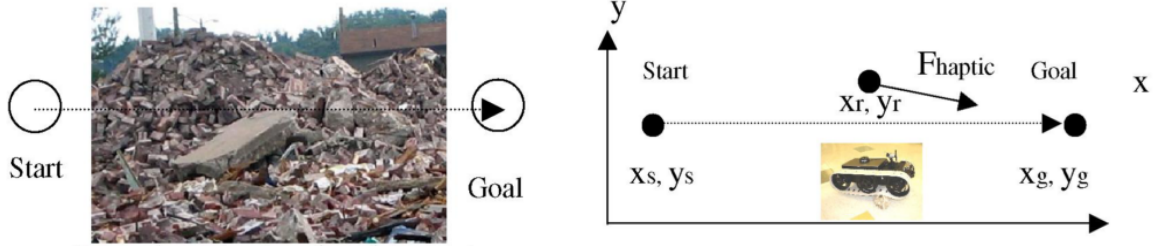
(a) Example of a Urban Search and Rescue (USAR) environment [26].

(b) Haptic augmentation methodology using force feedback [26].

Figure 2.6: Haptic augmentation for goal and trajectory task following in teleoperation of a UGV proposed by Horan [26].

Horan [26] and Fielding [30] presented two similar approaches to tackle the challenge of path and goal following. Both approaches provide force feedback to augment the teleoperated navigation of a mobile robot in a USAR scenario. By exploring a multi-modal feedback of the interfaces, the teleoperator can focus their visual sense in the main task while relying on haptic cues for a safe navigation. The multi-modal nature of the interfaces provides haptic augmentation to aid the teleoperator during goal and/or trajectory following. Using haptic cues, it is provided, to the teleoperator, indications regarding direction and distance to the goal location, as represented in Figure 2.6.

The proposed methods aid the teleoperator during navigation of the mobile robot. The provided haptic information is exclusively an augmentation of the visual interface that does not limit the robot's movement. Thus, these approaches are examples of absolute teleoperator autonomy.

Additionally, there was one more challenge that has not been so widely investigated but fundamental for this thesis: traction loss during teleoperation of a mobile robot. Below, it is described this challenge and the only found approach that tackles it by resorting to a haptic device:

4. **Traction Loss:**

   Loss of traction in teleoperated mobile robots requires the extraction of information based on subtle visual cues to estimate the current situation. In this situation, the lack of SA can lead to an incorrect and inefficient response to the current robot state, usually confusing and frustrating the human operator [2].

   Researchers have addressed the problem of traction loss in [31], however, applied to autonomous operation, while the concept of friction rendering was explored using haptic devices such as E-Vita [32]. Still remained the need to integrate all these concepts in a single teleoperation interface.

   Weihua [33] presents a teleoperation scheme that takes into account the existence of longitudinal slippage in the teleoperation of a mobile vehicle (ROSTDyn). The designed teleoperation controller compensates for the existence of longitudinal slippage by limiting the velocity values of the robot. The velocity control of a simulated robot is performed using a Phantom Premium 1.5A haptic device, where the linear velocity of the robot is mapped from the position of the haptic interface.

The user receives force feedback if the desired velocity, provided by the user using the haptic device, is different from the robot's actual velocity. In such situations, the user feels a pushing or pulling force whenever the robot is unable to move as much as desired or more than desired, respectively.

The presented architecture has the disadvantage of being quite complex since it requires the definition of the robot's and haptic device's kinematic model to predict and control the movement of the robot. Therefore, the architecture proposed by Weihua lacks the ability to easily adapt to different mobile robots while the detection of traction loss is limited to longitudinal slippage, which might be very limited in a real scenario such as USAR.

The teleoperation of mobile vehicles allows humans to extend their sensing, decision making, and manipulation capability into a remote location. Still, the lack of situation awareness in a teleoperation scenario can lead to the inability to control the robot's movement [2]. In particular, situations were the UGV loses traction requires the human operator to extract this information based on subtle visual cues. By adding haptic feedback to the human-machine interaction it can be displayed a greater amount of information during the teleoperation of RAPOSA-NG, without overloading the visual channel.

In this thesis, it is presented a novel method to detect traction loss. The developed method represents a simpler and more adaptable approach than one presented in [33]. This new method is capable of detecting traction loses regarding position and orientation and classify different traction states. Additionally, it is developed three haptic devices capable of conveying the detected traction states of the mobile robot to the human operator through tactile stimuli.

3| Traction State Detection

Contents

Iɴ this Chapter is presented the traction state detection divided in three Sections: Section 3.1 states the odometric measurements and respective sources, Sections 3.2 and 3.3 present two different methods to detect traction loss and its classification. The first method, presented in Section 3.2, resorts to the calculation of velocity values to compare the mismatch between the expected motion and the actual motion of the UGV, while the second method, presented in Section 3.3, resorts to the calculation of displacement vectors. Once the Traction States have been detected and classified, these ones can be then conveyed to the human operator through tactile stimuli using the different develop devices described in Chapter 4.

Typical situations causing loss of traction are obstacles that either block the motion of the robot or raise the body of the robot in such a way the tracks lose contact with the ground. Another, less common, situation is the robot sliding down a smooth ramp. In this Chapter, it is presented two methods to detect these situations that are based on determining whether there is a mismatch between the expected motion, given tracked wheel odometry, and the actual motion, given laser-based odometry. Whenever a significant mismatch is found (defined below), it is estimated the traction situation of the robot, following the situation classification being shown in Table 3.1.

Traction State	Tracks (odometry)	UGV (laser)	Traction Situation
Normal	Moving	Moving in the same direction	*With*
	Stopped	Stopped	*With*
Stuck	Moving	Stopped	*Without*
Sliding	Moving	Moving in a different direction	*Without*
	Stopped	Moving	*Without*

Table 3.1: Classification of UGV traction states, where same/different direction refers to the movement given by the odometry.

The mismatch-based detection was performed using two different methods. The first method (Velocity Method) calculates and compares velocity values, while the second method (Displacement Method) calculates and compares displacements vectors and its respective values. Finally, the detection of the traction state of the robot, in both methods, is based on the comparison of the mismatch values with a decision threshold.

3.1 Odometry Measurements

Let the pose of the robot $\mathbf{Z}(t)$ be defined by three coordinates, two for position and one for orientation (we use boldface to denote vectors),

$$\mathbf{Z}(t) = \begin{bmatrix} x(t) & y(t) & \theta(t) \end{bmatrix}^\top = \begin{bmatrix} \mathbf{p}(t) & \theta(t) \end{bmatrix}^\top \tag{3.1}$$

The tracked wheel odometry is obtained directly from the ROS drivers of the robot, in the form of a coordinate transformation between two frames denominated "/odom" and "/base_link". The frame coordinate "/odom" corresponds to the world frame of the wheel odometry component while "/base_link" corresponds to the robot's body frame, attached to the base of the mobile robot. The transformation between these two frames corresponds to the integration of the robot differential kinematic model starting when the drivers were initialized.

The laser-based odometry results from the integration of a scan matching algorithm, implemented by the *laser_scan_matcher* ROS package [34] (Canonical Scan Matcher - CSM). This package allows to scan match between consecutive "sensor_msgs/LaserScan" messages, and publish the estimated position of the laser as a "geometry_msgs/Pose2D" or a coordinate transformation between two frames denominated "/world" and "base_link". The frame "/world" corresponds to the world frame of the laser-based odometry component. The relationship between all the mentioned coordinate frames can be visualized in the tree structure (transform tree) represented in Figure 3.1. Conceptually, each node in the transform tree corresponds to a coordinate frame and each edge corresponds to the transform that needs to be applied to move from the current node to its child.
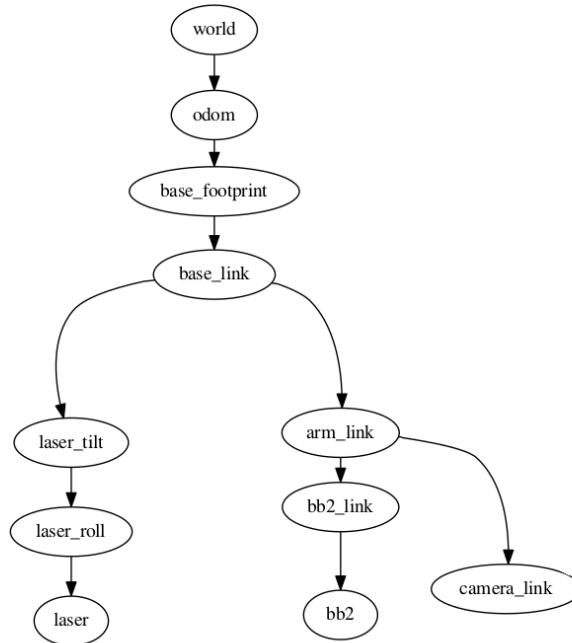
Figure 3.1: Transform tree of RAPOSA-NG system during Traction Detection.

From both odometry sources, it is obtained the pose of the UGV given by $Z_{tracks}(t)$, Eq. (3.2), and $Z_{laser}(t)$, Eq. (3.3), regarding tracked wheel odometry and laser-based odometry respectively.

$$\mathbf{Z}_{tracks}(t) = \begin{bmatrix} \mathbf{p}_{tracks}(t) & \theta_{tracks}(t) \end{bmatrix}^{\top} \tag{3.2}$$

$$\mathbf{Z}_{laser}(t) = \begin{bmatrix} \mathbf{p}_{laser}(t) & \theta_{laser}(t) \end{bmatrix}^{\top} \tag{3.3}$$

where the indices *tracks* and *laser* denote odometric measurements coming from the tracked wheel odometry and laser odometry.

3.2 Velocity Method

3.2.1 Method Formulation

The motion of the robot, and consequent mismatch, are quantified resorting to the velocity values $v(t_k)$ and $\omega(t_k)$ at a given instant t_k, yielding position and orientation respectively. These values are calculated resorting the measured current pose $\mathbf{Z}(t_k)$ and previous pose $\mathbf{Z}(t_{k-1})$.

$$v(t_k) = \sqrt{v_x^2(t_k) + v_y^2(t_k)} \tag{3.4}$$

$$\omega(t_k) = \|\theta(t_k) - \theta(t_{k-1})\| \ / \ \Delta t \tag{3.5}$$

where $v_x(t_k)$ and $v_y(t_k)$ stand for velocity values regarding position in x and y axes respectively and Δt stand for sampling period such that,

$$\Delta t = t_k - t_{k-1} \tag{3.6}$$

$$v_x(t_k) = (x(t_k) - x(t_{k-1})) \ / \ \Delta t \tag{3.7}$$

$$v_y(t_k) = (y(t_k) - y(t_{k-1})) \ / \ \Delta t \tag{3.8}$$

From the computed velocities $v(t_k)$ and $\omega(t_k)$, the mismatch between the two odometry measures is quantified resorting to $\delta_p(t_k)$ (3.9) and $\delta_\theta(t_k)$ (3.10), concerning position and orientation respectively at a given time instant t_k,

$$\delta_p(t_k) = \|v_{tracks}(t_k) - v_{laser}(t_k)\| \tag{3.9}$$

$$\delta_\theta(t_k) = \|\omega_{tracks}(t_k) - \omega_{laser}(t_k)\| \tag{3.10}$$

Finally, the traction situation of the robot can be accessed by comparing $\delta_p(t_k)$ and $\delta_\omega(t_k)$ with a corresponding decision threshold for both position and orientation. Whenever the obtained value of $\delta(t_k)$ is above the defined threshold it is considered that traction has been lost and the traction state should be classified as *Stuck* or *Sliding*. Otherwise, it is considered that the robot has traction and the traction state is classified as *Normal*. The filtering of the velocity values is performed using a Simple Moving Average (SMA) as explained in detail in Section 3.2.2, the definition of the decision threshold is detailed in Section 3.2.3 and the state classification in Section 3.2.4.

3.2.2 Data Filtering

The calculation of velocity values is performed by comparing two consecutive samples, the current and previous pose, $\mathbf{Z}(t_k)$ and $\mathbf{Z}(t_{k-1})$ respectively. The obtained data revealed to be very noisy, especially when the sampling frequency was increased to obtain a faster detection. Increasing the frequency led to the comparison of very close samples resulting in computational errors (subtractive cancellation), that
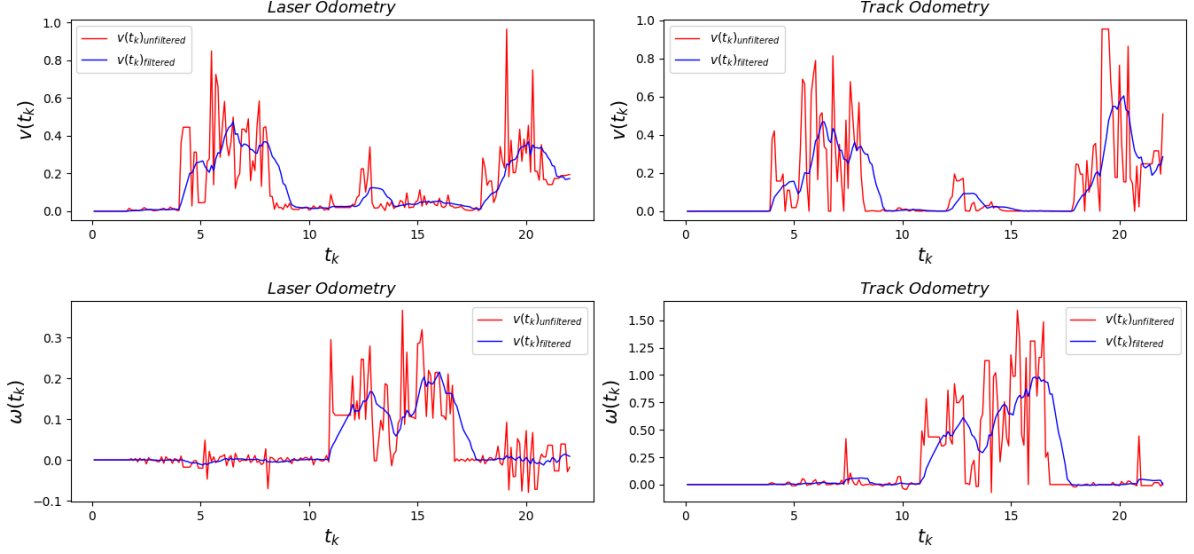
Figure 3.2: SMA filtering of $v(t_k)$ and $\omega(t_k)$ with a sampling frequency of 10Hz and a moving window of 5 samples (0.5 seconds, $n = 5$): Red curves represent the unfiltered measured velocity (red) and the blue curves represent the filtered velocity (blue) from both odometry sources (laser and tracks).

are amplified by the direct proportionality of the obtained values with the high sampling frequency f_s,

$$f_s = \Delta t \tag{3.11}$$

Because the detection of the traction state depends on the comparison of the noisy velocity values, filtering became fundamental in order to avoid false detections due to the existence of excessive noise. The noise was mainly due to a slight shaking of the LIDAR platform on-board the robotics system and also due to the environment. In the case where the was straight walls, the noise would decrease in comparison with environments with small or curved surroundings or people moving.

The filtering of the computed velocity values $v(t_k)$ and $\omega(t_k)$ is performed using a Simple Moving Average (SMA). The mean of the velocity values is calculate for a moving window of n samples of the most recent velocity values. Here, the filtered velocity is denominated as $v_{filtered}(t_k)$ (3.12) and $\omega_{filtered}(t_k)$ (3.13), regarding position and orientation respectively, and are represented in Figure 3.2 with a blue curve.

$$v_{filtered}(t_k) = \sum_{i=0}^{n-1} v(t_{k-i})/n \tag{3.12}$$

$$\omega_{filtered}(t_k) = \sum_{i=0}^{n-1} \omega(t_{k-i})/n \tag{3.13}$$

The defined window size n influences the sensitivity to noise (greater n means smaller sensitivity) and the detection latency (smaller n means faster detection). The use a moving window allowed to significantly reduce the noise of the computed velocity values, as shown in Figure 3.2 and to compare the mismatch between the expected and the actual motion, $\delta(t_k)$, with a decision threshold.

The filtered velocities obtained from the tracks and laser-based odometry are represented in Figure 3.3, with a blue and red lines respectively, concerning both position and orientation. For abbreviation purposes, from now on, the notation $v(t_k)$ and $w(t_k)$ stands for the the filtered velocity values.

The selection of window size n was performed experimentally. During the teleoperation of the robot we chose a n value that could reach an acceptable compromise between having a fast detection of

traction loss (small n) and avoid false detections (big n) due to the noisy data. This value needed to be adjusted depending on the operation environment. Environments with straight walls require smaller n values and environments with curved, small or moving elements require greater n values.
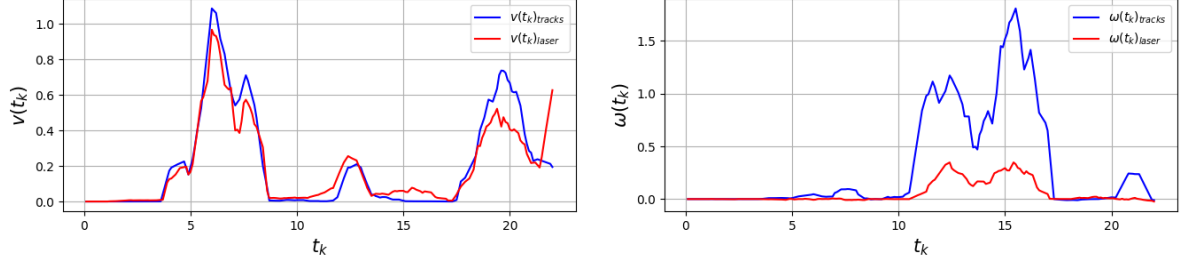
Figure 3.3: Filtered velocity values regarding track odometry (blue) and laser-based odometry (red), where, concerning orientation, the robot was stuck.

3.2.3   Threshold Definition

The first approach to define a decision threshold consisted in formulating $\eta_p^1(t_k)$ (3.14) and $\eta_\theta^1(t_k)$ (3.15),

$$\eta_p^1(t_k) = \eta_{p,min} \tag{3.14}$$

$$\eta_\theta^1(t_k) = \eta_{\theta,min} \tag{3.15}$$

two constant thresholds regarding position and orientation respectively, to evaluate if the computed values of δ_p and δ_θ represent a significant mismatch and consider that the traction as been lost.

However, a constant threshold failed to adapt to different situations where traction was lost. In certain situations it was obtained false positives and in others false negatives, as different values of threshold were necessary to detect different traction states. To address that limitation, it was explored variable thresholds $\eta_p^2(t_k)$ (3.16) and $\eta_\theta^2(t_k)$ (3.17), proportional to the previously computed velocity values as follow:

$$\eta_p^2(t_k) = \max\left(v_{tracks}(t_k), v_{laser}(t_k)\right) \cdot \beta \quad , \quad \beta \in]0{,}1[\tag{3.16}$$

$$\eta_\theta^2(t_k) = \max\left(\omega_{tracks}(t_k), \omega_{laser}(t_k)\right) \cdot \beta \quad , \quad \beta \in]0{,}1[\tag{3.17}$$

where β stands for the threshold proportional factor, here dominated as *threshold sensitivity factor*, that influences the sensitivity to the noise.

The defined thresholds $\eta_p^2(t_k)$ and $\eta_\theta^2(t_k)$ use the velocity values, obtained from track and laser-based odometry, to be able to deal with situations where the robot gets stuck ($v_{tracks}(t_k) \approx 0$ and/or $\omega_{tracks}(t_k) \approx 0$) or slides ($v_{laser}(t_k) \approx 0$ and/or $\omega_{laser}(t_k) \approx 0$). However, the threshold $\eta^2(t_k)$ still failed to correctly detect loss of traction in situations where the both velocities $v(t_k)$ and $\omega(t_k)$ were close to zero, making the slightest noise to be wrongly detected as a traction loss.

Finally, it was reached a compromise between the two previously defined thresholds, $\eta^1(t_k)$ and $\eta^2(t_k)$, by combining those two into $\eta(t_k)$,

$$\eta_p(t_k) = \max(\eta_p^1(t_k), \eta_p^2(t_k)) \tag{3.18}$$

$$\eta_\theta(t_k) = \max(\eta_\theta^1(t_k), \eta_\theta^2(t_k)) \tag{3.19}$$

yielding position and orientation respectively, and represented in Figure 3.4 (yellow curve).

From the comparison of thresholds, $\eta_p(t_k)$ and $\eta_\theta(t_k)$, with the mismatches, $\delta_p(t_k)$ and $\delta_\theta(t_k)$, it can be obtained the traction situation of the robot (*With* or *Without* traction). It is considered that

traction has been lost in the following cases:

$$\delta_p(t_k) \geq \eta_p(t_k) \tag{3.20}$$

$$\delta_\theta(t_k) \geq \eta_\theta(t_k) \tag{3.21}$$
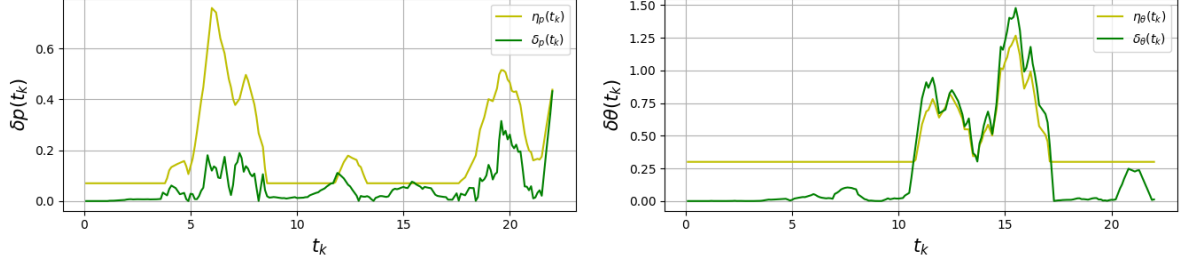
Figure 3.4: Traction detection using a decision variable threshold $\eta(t_k)$ (yellow curve), regarding position (left) and orientation (right), in comparison with $\delta(t_k)$ (green curve).

In Figure 3.4 it is represented a situation where traction was lost in orientation but not in position. In terms of position, using $\eta_p(t_k)$ allowed to ignore values of $\delta_p(t_k)$ greater than $\eta_{p,min}$ but that did not represent a traction loss. Regarding orientation, it was detected traction loss when $\delta_\theta(t_k) \geq \eta(t_k)$ (green curve $\geq$ yellow curve).

The formulated threshold can be adjusted using the two previously defined parameters *minimum threshold*, η_{min}, and *threshold sensitivity factor*, β. Increasing η_{min} will decrease the sensitivity to the noise, while the increase of β will increase the sensitivity to the noise. In Figure 3.4 it was used the parameters $\beta = 0.7$, $\eta_{p,min} = 0.07$ and $\eta_{\theta,min} = 0.266$. These were obtained similarly to moving average window size n. By performing some experimental tests in the operating environment of the robot, the threshold values were adjusted. By passing through all possible traction states these parameters can be iteratively adjusted before the SAR operations.

3.2.4 Traction State Classification

Once the traction situation of the robot has been obtained, resorting to the defined decision threshold, the traction state is classified as *Normal*, *Stuck* or *Sliding*.

If the traction situation was previously consider as *With* traction, the traction state of the robot should be classified as *Normal*. Otherwise, a traction loss has been detected and it is necessary to classify the traction state as: *Stuck* or *Sliding*. To discern between these two traction states, the earlier computed velocities $v(t_k)$ and $\omega(t_k)$ are compared. This comparison will allow to ascertain if either the tracks or the UGV is moving and classify the state as shown in Table 3.1. From the verification of the comparison (3.22), regarding position, or the comparison (3.23), regarding orientation,

$$\|v_{laser}(t_k)\| > \|v_{tracks}(t_k)\| \tag{3.22}$$

$$\|\omega_{laser}(t_k)\| > \|\omega_{tracks}(t_k)\| \tag{3.23}$$

it can be inferred that the UGV is moving while the tracks are stopped, or moving significantly less. In such case, the traction state is classified as *Sliding*, Otherwise, it is classified as *Stuck*.

A generic decision tree for traction state classification is shown in Figure 3.5, where $\delta(t_k)$ stands for the mismatch quantification, $\eta(t_k)$ the defined threshold and $X(t_k)$ the physical quantity used to obtain the mismatch $\delta(t_k)$. Regarding position and orientation the evaluated physical quantities are different and are summarized in Table 3.2.

	$\delta(t_k)$	$\eta(t_k)$	$X(t_k)$
Position	$\delta_p(t_k)$	$\eta_p(t_k)$	$v(t_k)$
Orientation	$\delta_\theta(t_k)$	$\eta_\theta(t_k)$	$\omega(t_k)$

Table 3.2: Physical quantities used in the decision tree regarding position and orientation, for the velocity method.
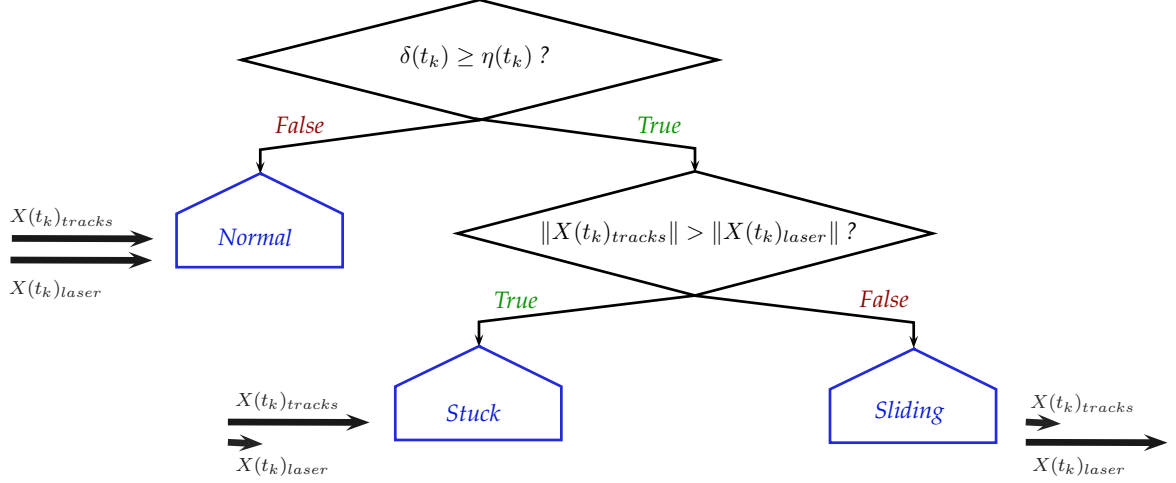
Figure 3.5: Generic Decision tree for traction state classification.

The Velocity Method for traction detection successfully detects traction loss, and its respective traction state, in situations where the tracks of the robot are moving while the robot is stopped (*Stuck*) and when the robot is moving while the tracks are stopped (*Sliding*). However, using the velocity values to obtain the traction state of the robot revealed to be limited. This method is unable to detect situations where the tracks are moving in one direction and the robot is actually moving in a different direction. This deficit occurs because the computed values of the velocities don't allow to have information regarding the direction of the motion. Therefore, emerged the need to develop a new detection method capable of detecting this situation.

3.3 Displacement Method

3.3.1 Method Formulation

In the Displacement Method, the mismatch detection between two odometry measures is based on the comparison of the displacement vectors, according to each measure, along a moving window of $(n+1)$ samples. By comparing displacement vectors instead of velocities values, it can be achieved two goals: (1) compare the motion direction of the robot, given by the two odometry sources, and (2) reduce the noise of the measurements, as the evaluated physical quantity used in this method (displacement) represents an integration of the quantity used in the previous method (velocity).

The filtering of the measurements is done by comparing the measurements $\mathbf{Z}(t)$ at the start (t_{k-n}) and end (t_k) of the window, yielding the displacement $\Delta\theta(t_k)$ and $\Delta p(t_k)$ regarding orientation and position respectively.

In what concerns orientation, there is only 1 DoF which simplifies the equations: the displacement $\Delta\theta(t_k)$ (3.24) can be obtained using the scalar difference of the orientation at the beginning (t_{k-n}) and

end (t_k) of the moving window, modulo π,

$$\Delta\theta(t_k) = [\theta(t_k) - \theta(t_{k-n})], \quad \theta(t) \in [-\pi, \pi] \tag{3.24}$$

To obtain the position displacement vector $\Delta\mathbf{p}(t_k)$ (3.25), with respect to a frame attached to $\mathbf{p}(t_{k-n})$, the following expression is used:

$$\Delta\mathbf{p}(t_k) = R^\top \left(\theta(t_{k-n})\right) [\mathbf{p}(t_k) - \mathbf{p}(t_{k-n})] \tag{3.25}$$

where $R(\theta)$ stands for the usual rotation matrix in $SO(2)$,

$$R(\theta) = \begin{bmatrix} \cos(\theta) & -\sin(\theta) \\ \sin(\theta) & \cos(\theta) \end{bmatrix} \tag{3.26}$$

From the computed displacements $\Delta\theta(t_k)$ and $\Delta\mathbf{p}(t_k)$, the mismatch between the two odometry measures is quantified resorting to $\delta_p(t_k)$ (3.27) and $\delta_\theta(t_k)$ (3.28), concerning position and orientation respectively,

$$\delta_p(t_k) = \|\Delta\mathbf{p}_{tracks}(t_k) - \Delta\mathbf{p}_{laser}(t_k)\| \tag{3.27}$$
$$\delta_\theta(t_k) = \|\Delta\theta_{tracks}(t_k) - \Delta\theta_{laser}(t_k)\| \tag{3.28}$$

where the indices *tracks* and *laser* denote odometric measurements coming from the tracked wheel odometry and laser odometry. The representation of the displacement vectors of both odometry sources and the corresponding mismatch vector are exemplified in Figure 3.6, regarding position.
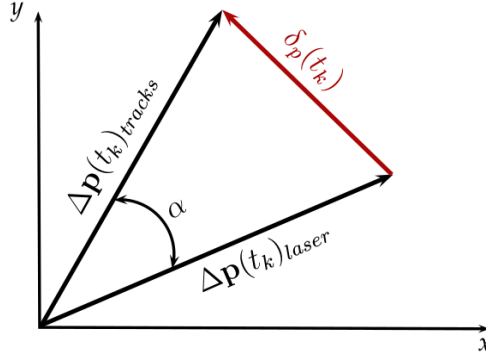
Figure 3.6: Representation of the displacement vectors obtained from track and laser-based odometry and consequent mismatch

Finally, the traction situation of the robot can be accessed using $\delta_p(t_k)$ and $\delta_\theta(t_k)$ and a corresponding decision threshold for both position and orientation, $\eta_p(t_k)$ and $\eta_\theta(t_k)$ respectively. Whenever the obtained value of $\delta(t_k)$ is above the defined threshold $\eta(t_k)$ it is considered that traction has been Lost and the current traction state should be classified as *Stuck* or *Sliding*. Otherwise, it is considered that the robot has traction and the current traction state is classified as *Normal*. The thresholds used in the Displacement Method are defined in the same way as it was previously done for the Velocity Method and presented in Section 3.2.3.

3.3.2 State Classification

By comparing the previously defined mismatch values, $\delta_p(t_k)$ (3.27) and $\delta_\theta(t_k)$ (3.28) with the corresponding decision thresholds, $\eta_p(t_k)$ and $\eta_\theta(t_k)$, the traction situation of the robot can be obtained.

In case the comparisons (3.29), regarding position, and (3.30), regarding orientation, are verified,

$$\delta_p(t_k) \geq \eta_p(t_k) \tag{3.29}$$

$$\delta_\theta(t_k) \geq \eta_\theta(t_k) \tag{3.30}$$

the traction situation of the robot is classified as *Without* traction and the traction state should be classified as *Stuck* or *Sliding*. Otherwise, the traction situation is classified as *With* traction and the traction state is classified as *Normal*, as shown in Figure 3.7.
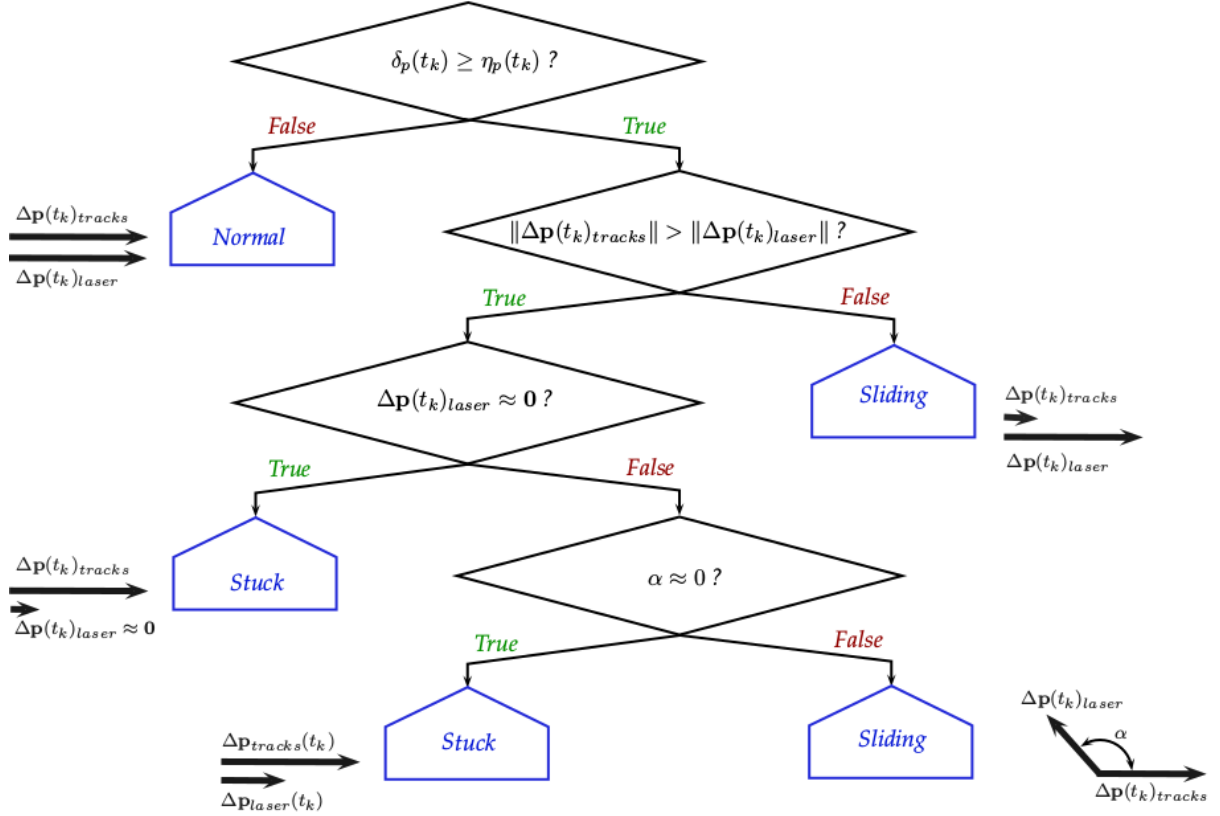
Figure 3.7: Decision tree for traction state classification, regarding position, when using the displacement method.

To discern between the *Stuck* and *Sliding* traction states, the earlier computed displacements $\Delta\mathbf{p}(t_k)$ and $\Delta\theta(t_k)$ are compared between odometry sources. This comparison will allow to ascertain if either the tracks or the UGV are moving and classify the traction state as shown in Table 3.1. From the verification of the comparison (3.31), regarding position, or the comparison (3.32), regarding orientation,

$$\|\Delta\mathbf{p}(t_k)_{laser}\| > \|\Delta\mathbf{p}(t_k)_{tracks}\| \tag{3.31}$$

$$\|\Delta\theta(t_k)_{laser}\| > \|\Delta\theta(t_k)_{tracks}\| \tag{3.32}$$

it can be inferred that the UGV is moving while the tracks are stopped, or moving significantly less and the traction state is classified as *Sliding*. Otherwise the traction state is classified as *Stuck* regarding orientation. Calculating α,

$$\alpha = \angle(\Delta\mathbf{p}(t_k)_{laser}, \Delta\mathbf{p}(t_k)_{tracks}) \tag{3.33}$$

allows to investigate the possibility that both the tracks and the UGV are moving, however, in different directions. In such situation, the value of α is greater than a small threshold value and the traction state is classified as *Sliding*. Otherwise, the traction state is classified as *Stuck* regarding position.

In the particular situation where $\Delta\mathbf{p}(t_k)_{laser} \approx \mathbf{0}$, meaning that the UGV is stopped, the obtained vector $\Delta\mathbf{p}(t_k)_{laser}$ is mostly noise, making the calculated value of α a random number. To address this issue, it was added one more query to the decision tree (Figure 3.7) to verify if the module of $\Delta\mathbf{p}(t_k)_{laser}$ is greater than a small threshold and, only than, the value of α can be calculated. In the case that the module of $\Delta\mathbf{p}(t_k)_{laser}$ is smaller than a small threshold ($\Delta\mathbf{p}(t_k)_{laser} \approx \mathbf{0}$) the traction state is classified as *Stuck*.

Respecting to orientation, it is used the generic decision tree represented in Figure 3.5 with the calculated quantities presented in Table 3.3.

	$\delta(t_k)$	$\eta(t_k)$	$X(t_k)$
Orientation	$\delta_\theta(t_k)$	$\eta_\theta(t_k)$	$\Delta\theta(t_k)$

Table 3.3: Physical quantities used in the decision tree regarding orientation, for the displacement method.

Using the Displacement Method it is possible to detect the situation where both the tracks and the UGV are moving, but in different directions that could not be done using the Velocity Method. For that reason, the detection of the traction state of RAPOSA-NG during its teleoperation is performed using the Displacement Method.

3.4   Limitations and Future Work

The developed traction detection methods require two independent sources of the robot's position. One of them to provide the motion of the robot according to the tracks' movement (expected motion) and another one to provide the real movement of the robot (actual motion).

In the particular case of RAPOSA-NG, its operation consists in exploring the inside of a building for the search of victims. Therefore, to obtain the expected motion it was used the given tracked wheel odometry, and to obtain the actual motion it was used the given laser-based odometry. However, in open-field operations, the lack of obstacles, such as walls, would not allow obtaining the given laser-based odometry. Alternatively to the laser, the GPS could be used as the position source to provide the actual motion of the robot.

As possible future work, it is suggested the possibility of detecting the source of traction loss, additionally to the traction state. For example, when the robot is *Stuck*, it would be interesting to know if there is an obstacle under the body of the robot or if its dimensions are preventing its movement.

4| Haptic Devices

Contents

T HIS Chapter is divided in two Sections: 4.1 Conceptual Discussion and 4.2 Devices Development. In Section 4.1 Conceptual Discussion, is presented the project requirements, a brief description of the proposed concepts of haptic devices and respective advantages and disadvantages and, finally, is presented the selection of the concepts to be implemented. In Section 4.2 Devices Development, is described the development of three haptic devices capable of providing different types of stimuli to human operator accordingly to the detected traction state of the UGV. Two of the presented devices (Traction Cylinder and Vibrotactile Glove) were implemented and integrated by the author while the third device (E-Vita) solely the integration with RAPOSA-NG system was performed.

4.1 Conceptual Discussion

4.1.1 Project Requirements

One of the goals of this thesis is to improve the human operator's situation awareness regarding the traction state of RAPOSA-NG, during its teleoperation, by adding haptic feedback to the current exclusively visual interface. In Figure 4.1 is provided an overall view of the teleoperation architecture envisioned for RAPOSA-NG. The intent of this new teleoperation architecture is to compromise haptic feedback as an addition to the current exclusively visual interface. This will be accomplished by developing two new haptic devices to provide feedback regarding the attitude and traction state of the UGV.

This thesis focus only on the development of the haptic device that will provide feedback regarding the traction state of the UGV, symbolized with a red rectangle in the Figure 4.1. The haptic device
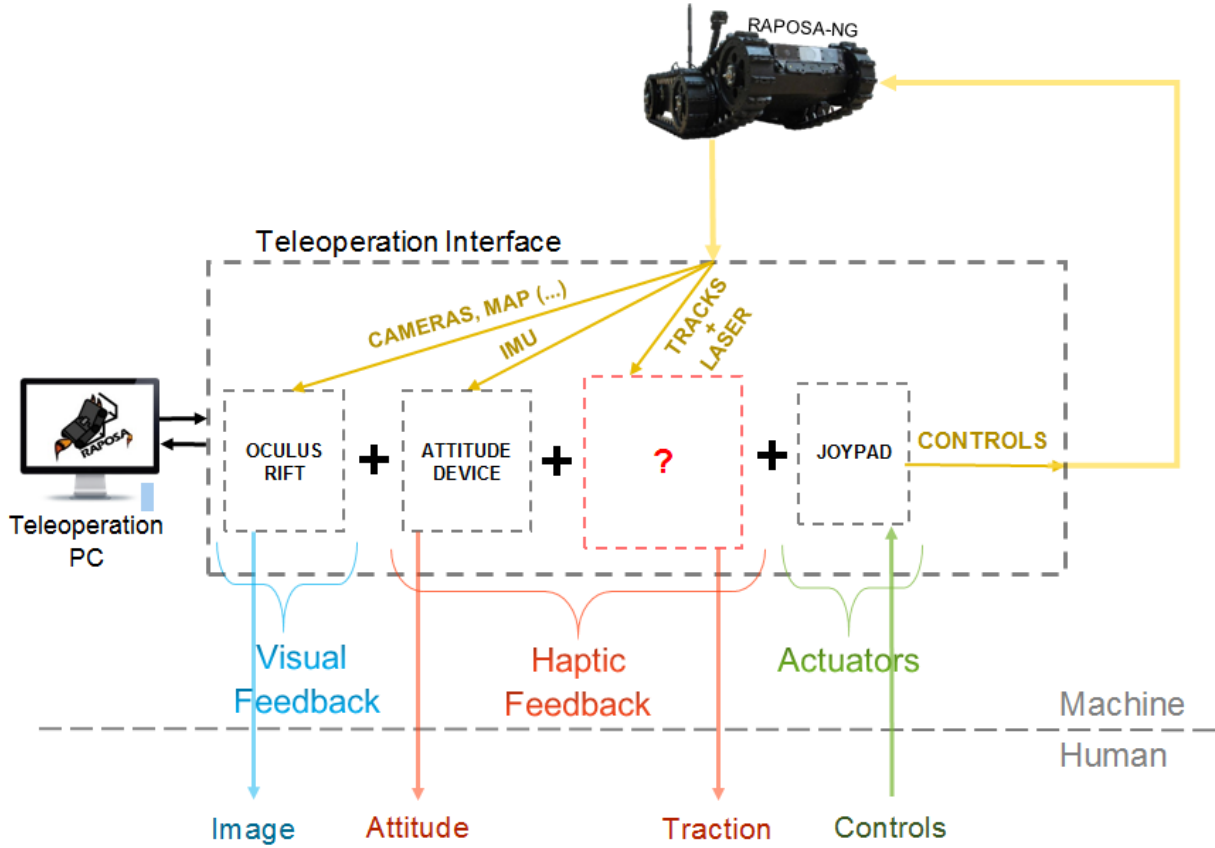
Figure 4.1: Envisioned Teleoperation Architecture of RAPOSA-NG comprising Visual and Haptic Feedback.

that provides feedback regarding attitude of the UGV is currently being developed by José Corujeira, a PhD student at ISR-Lisboa / IST. The goal is to integrate one of the three developed traction devices, presented in this Chapter, in the attitude device. The requirements of the traction devices to be developed are enumerated below:

1) The developed traction devices should be able to provide different tactile patterns, corresponding to all possible traction states of the UGV defined in Chapter 3 (*Normal*, *Stuck* and *Sliding*);

2) The created haptic patterns should be as simple and intuitive as possible to avoid increasing the mental workload during teleoperation to understand the patterns' meaning;

3) Future integration with the attitude device should be possible, without needing drastic changes to its design.

4.1.2 Concept Development

The development of the haptic devices started with a conceptual discussion. This discussion intended to investigate what kind of devices could be developed to better fulfill the design requirements. In this Section, it is briefly presented four different concepts, its characteristics and operation. The presented concepts endeavor to explore different types of tactile stimuli and actuation points to provide the traction state to the human operator.

Rotating Cylinder

The first proposed device is a Rotating Cylinder that actuates on the palm of the hand as represented in Figure 4.2. This device would have a very simple operation: the cylinder would revolve

Figure 4.2: Concept Development: Rotating Cylinder (blue), where the green arrow represents the motion of the cylinder.
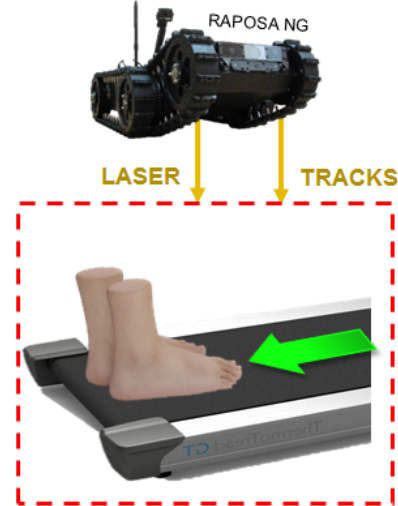
Figure 4.3: Concept Development: Feet Platform, where the green arrow represents the motion of the treadmill mat.

whenever traction was lost and provide different revolving patterns, accordingly to the traction state of the robot. If traction has not been lost, the cylinder would remain stopped, as the robot is moving as intended and no attention is required for this item of the interface. The manufacturing of the Rotating Cylinder would require the design of the 3D model of its structure (3D printed), the addition of a motor and some electronic components for the motion control and integration with RAPOSA-NG system.

Feet Platform

The second proposed device is a Feet Platform that actuates on the palm of the feet of the human operator as represented in Figure 4.3. This feet platform would transmit the perception of traction, and lack of it, resorting to a sliding mat of a treadmill. Similarly to the cylinder device for the hand, this feet platform would remain stopped if the robot had traction and would start rotating otherwise, giving a slippage sensation on the feet when traction was lost. This concept arises from the question: *how can the actuation point influence the perception of the traction state of the robot?* as a complement to the Rotating Cylinder. The manufacturing of this device would require the purchase, or development, of a treadmill and some electronic components for the motion control and integration with RAPOSA-NG system.

Vibrotactile Glove

The third proposed device is a Vibrotactile Glove that actuates on the hand or arm of the human operator as represented in Figure 4.4. To transmit the traction state, several vibration actuators are displayed along the hand or arm of the operator. The position, frequency, amplitude, and sequence of actuation of which of the actuators would be controlled to provide different tactile sensations, accordingly to the traction state of the robot. The vibrotactile sensations would be provided to the teleoperator when traction was lost. This device would distinguish itself from the other devices because it allows creating more diverse tactile patterns and explores more complex rendering algorithms. The manufacturing of this device would require the purchase of vibrotactile motors and some electronic components for the pattern rendering and integration with RAPOSA-NG system.

Flexible Pressure Chamber

The fourth, and last, proposed device is a Flexible Pressure Chamber, resembling a balloon shape, that actuates on the hand of the human operator as represented in Figure 4.5. This device would consist of a pneumatic system controlled by a motor and a pressure sensor. The motor would control the pressure inside the balloon-shaped chamber while the pressure sensor would allow measure it. The measured

Figure 4.4: Concept Development: Vibrotactile Glove, where the yellow circles represent vibration actuators.
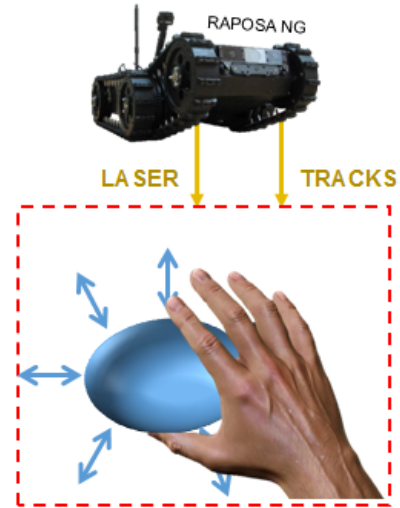
Figure 4.5: Concept Development: Flexible Pressure Chamber (blue), where the arrows represent the inflating and deflating of the chamber.

pressure values could then be used to control the speed of the robot proportionally to the obtained value. To provide the traction state of the robot the chamber would inflate and deflate accordingly to the detected state. If the traction has traction the chamber would be inflated allowing the speed control by "squeezing" the device. Otherwise, the chamber would be deflated, not allowing the user to increase the speed, and provide the notion of an undesired situation.

4.1.3 Concept Selection

From the proposed devices it was necessary to select the concepts to be developed. To support that decision, it was elaborated a comparative analysis of the proposed concepts that include the following steps:

1. Creation of a table listing the actuation point, advantages and disadvantages of which concept;

2. Creation of a hierarchy of factors and respective weights to quantify their impact on the overall design. This factors and weights allowed to attribute a final score to each concept and reach a decision regarding the concept implementation and respective order.

3. Decision making regarding the selection of the concept to be implemented, based on the obtained scores from the hierarchical analysis and advantages/disadvantages Table.

1. Advantages and Disadvantages of the Proposed Concepts

In Table 4.1, it is presented a summary of the actuation areas and main advantages and disadvantages of the four proposed concepts. Both the Rotating Cylinder and Vibrotactile concepts had a great advantage regarding the small size and manufacturing simplicity. Both the Rotating Cylinder and Feet Platform concepts would provide a very limited quantity and/or richness of tactile patterns, due to its simplicity of motion. The Vibrotactile Glove would allow providing richer tactile patterns when using a matrix of actuators (2 DoF, regarding actuation point), although the control of a matrix of actuators would increase the complexity of the rendering algorithm comparatively to a single line of actuators (1 DoF). The feet platform could allow studying the impact of the actuation point on the information acquired by the user but didn't bring a lot of other advantages compared to the cylinder concept, especially due to the large size and manufacturing complexity. Regarding the Flexible Pressure Chamber

concept, on the one hand, it would be interesting to develop an active haptic device, allowing the user to receive feedback and provide an input control, on the other hand, it's implementation, manufacturing and size represent a big challenge.

Device	Actuation Area	Advantages	Disadvantages
Rotating Cylinder	Palm of the hand	Small size; Relatively easy development.	Might require the redesign of the attitude device; Only 1 DoF limiting the tactile richness of the patterns.
Vibrotactile Glove	Hand or arm	Small size; Accessible/cheap material; Applicability to several actuation points and other functionality.	Complexity of the vibration control algorithm.
Feet Platform	Palm of the feet	More intuitive feeling of slippage; Independent of the attitude platform.	Relatively big device: difficult transport and manufacturing; Necessity to maintain the feet static while the mat rotates.
Pressure Chamber	Palm of the hand	Might allow to control the robot; Notion of traction directly associated with the control of velocity (active device).	Difficulty to implement both pressure feedback and velocity input; Complexity of the mechanical components

Table 4.1: Advantages and disadvantages of the proposed device concepts.

2. Creation of a Hierarchy of Factors and Ranking Table

The creation of the hierarchy of factors and respective weights to the overall design, Figure 4.6, intended to attribute a final score to each of the devices to be used during the decision making. Although the attribution of weights and scores was a subjective process, this analysis only intended to obtain an indication of the most promising concepts through the discussion of the characteristics of each design. The final decision included the concept implementation and order of device implementation. With that in mind, it was established two main decision factors:

- **Difficulty/Complexity** of development and implementation, comprising: Existing Technology that could be used during the development of the device; Cost and Accessibility to the Components/Materials; Development Complexity, including hardware and software; Development Time; Size.

- **Potential/Interest** of the concepts, comprising: Innovation of the device; Future Applicability to different situations; Feeling of Immersion provided to the operator during teleoperation; sensitivity of Actuation Point.

For each device, it was attributed a rating from 0 to 10 in each of defined factors. Here, a higher rating represents the most desirable characteristic, in such a way that a greater score corresponds to a more promising device. E.g: regarding the difficulty/complexity factor, the smaller is the complexity of the design, the greater is the given rating, as this one is the most desirable characteristic. Contrarily, regarding potential/interest factor, the greater the score, the greater is the potential/interest, as this one is the most desirable characteristic. Once all the concepts have been rated in all factors, it was performed a weighted average of the rates and calculated the final scores of each device. The obtained results are presented in Table 4.2, where the Rotating Cylinder got the highest score followed by the Vi-

brotactile Glove and Feet Platform respectively while the Flexible Pressure Chamber got the lowest score.
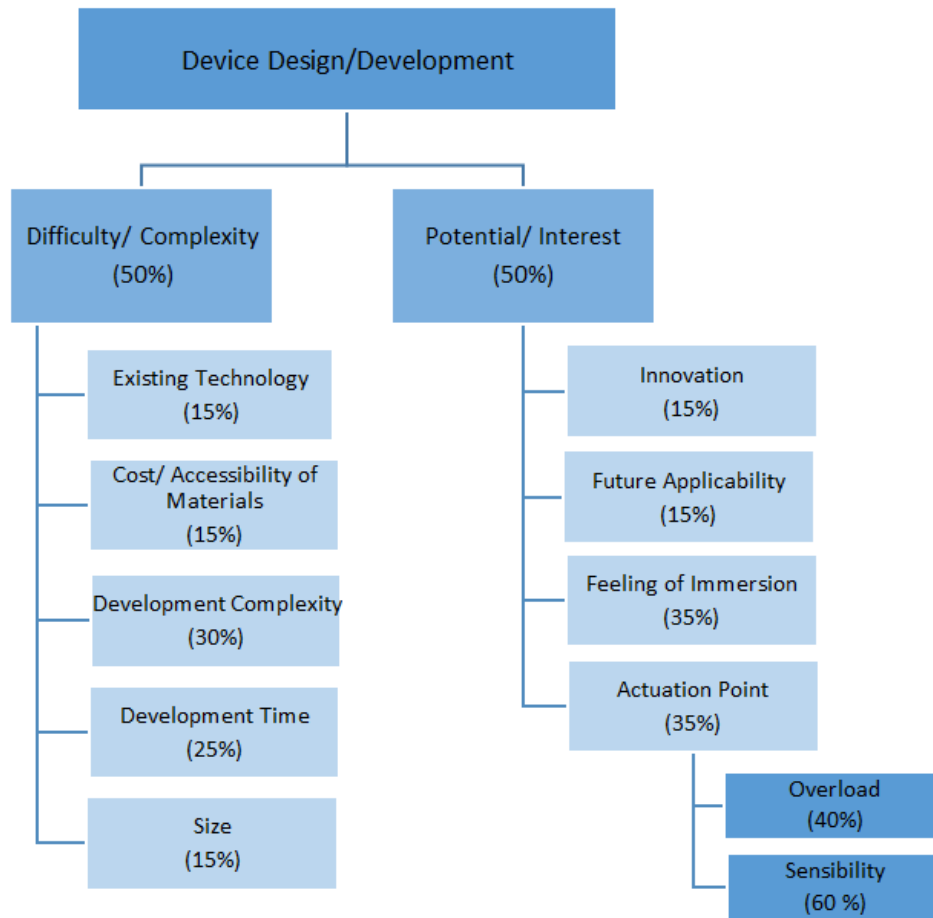
Figure 4.6: Comparative Analysis Hierarchy.

	Weight (%)	Vibrotactile Glove	Rotating Cylinder	Feet Platform	Pressure Chamber
Existing Technology	15	7	9	8	7
Cost/ Accessibility of Materials	15	9	8	7	6
Development Complexity	30	5	9	7	7
Size	15	9	9	5	7
Development Time	25	6	9	7	7
Difficulty/ Complexity	**50**	**6,75**	**8,85**	**6,85**	**6,85**
Innovation	15	9	7	8	8
Future Applicability	15	9	7	7	8
Feeling of Immersion	35	8	8	9	7
Overload of Information	*40*	*8*	*7*	*10*	*9*
Sensibility	*60*	*8*	*9*	*10*	*9*
Actuation Point	35	8	8,2	10	9
Potential/ Interest	**50**	**8,3**	**7,77**	**8,9**	**8**
Total		7,53	**8,31**	7,88	*7,43*

Table 4.2: Comparative analysis: ranking scores of the several concepts.

3. Decision making

Based on the results presented in Table 4.2 and the advantages/disadvantages presented in Table 4.1 it was reached the decision of implementing the Rotating Cylinder, from now on denominated as "Traction Cylinder". The second device to be implemented was chosen out of the devices with second and third best scores in Comparative analysis: the Vibrotactile Glove and Feet Platform. In order to have greater diversity of types of tactile stimulus while maintaining the actuation region for future comparison during the user study, the second device to be implemented was the Vibrotactile Glove.

4.2 Devices Development

One way of reducing the burden on the visual channel during the teleoperation of RAPOSA-NG is to use other human senses and provide multi-modal feedback in UGV teleoperation. In this thesis it is used visual and tactile modalities. The tactile component of the provided multi-modal feedback was conveyed through three haptic devices: Traction Cylinder (Figure 4.9), Vibrotactile Glove (Figure 4.24), and E-Vita (Figure 4.17). Both the Traction Cylinder and Vibrotactile Glove were constructed and integrated by the author, while E-Vita, solely the integration with RAPOSA-NG system was performed. The complete development of E-Vita was performed by the MINT research team, from Inria Lille - Nord Europe, France.

4.2.1 Traction Cylinder

The Traction Cylinder uses ***friction***, provided by a cutaneous tangential motion stimuli, as the tactile feedback modality to convey the traction state of the UGV. The tangential motion is accomplished resorting to a dynamic cylinder present on the device that rotates accordingly to the traction state of the UGV. During the operation of this device, different motion stimulus are applied to the skin, on the palm of the hand, while the user is holding the device, as shown in Figure 4.8.

This device aims to explore the use of friction to convey the idea of existence or nonexistence of Traction as an intuitive feedback modality. By creating a tactile stimuli resembling the occurrence in the UGV, the loss of traction, this devices intends to provide to the users an intuitive mental mapping between the perceived haptic sensation and the real movement of the robot.
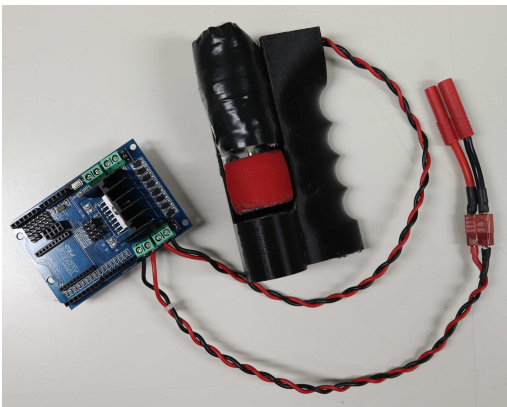
Figure 4.7: Photo of the Traction Cylinder.
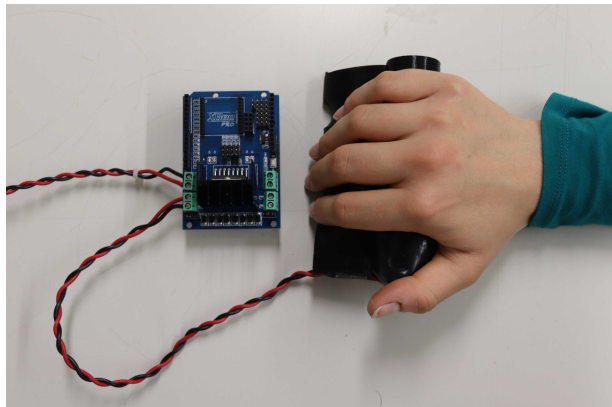
Figure 4.8: Interaction mode with the Traction Cylinder.

Tactile Patterns

To convey the traction state of the UGV using the Traction Cylinder it was designed three different t actile patterns to be provided by the Traction Cylinder as illustrated in Figure 4.9 and explained below:

(a) *Normal State*: As illustrated in Figure 4.9a, no rotation is displayed by the cylinder, to convey the idea that the UGV has traction and it is moving accordingly to the movement of the tracks.

(b) *Stuck State:* As illustrated in Figure 4.9b, the cylinder rotates back and forward providing a change of direction of the tangential motion applied to the skin. This pattern intends to convey the idea of moving tracks while the UGV is unable to move and provide a stuckness sensation on the palm of the hand.

(c) *Sliding State*: As illustrated in Figure 4.9c, the cylinder rotates constantly in one single direction providing a constant tangential motion applied to the skin. This pattern intends to convey the idea that, although the UGV is moving, the tracks are stopped or moving in a different direction by providing a sliding sensation on the palm of the hand.

(a) Normal State.   (b) Stuck State.   (c) Sliding State.
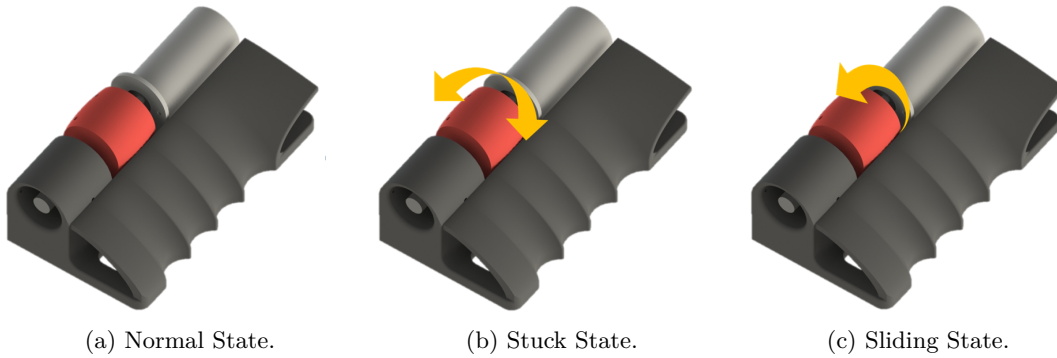
Figure 4.9: Tactile Patterns provided by the Traction Cylinder, where the yellow arrows represent the motion direction of the cylinder).

Device Implementation and Integration

The flow chart of the Implementation of the Traction Cylinder and its Integration with RAPOSA-NG system is represented in Figure 4.10. The Integration of the device with RAPOSA-NG system is accomplished using *rosserial_arduino* ROS package [35], which allows using ROS directly with Arduino IDE by providing a ROS communication protocol that works over Arduino's serial port. Using *rosserial_arduino* ROS package, a node is launched to perform the control of the rotation speed and direction of the motor depending on the received messages through the rostopic containing current traction state of the UGV. All the control was programmed using the Arduino IDE and the integration with ROS performed by including the *ros.h* library in the *.ino* file.

To implement the described device, it was necessary the following components:

- 3D printed cylinder and device structure. The 3D model of the Traction Cylinder, shown in Figure 4.11, was developed using *SolidEdge®*. The shape of the device intends to fit the morphology of the human hand in a resting position by creating a curve shaped structure with a specifically shaped location to rest the fingers;

- 1 gear motor (jm100-2530, DC 12 V, 60 *rpm*), to rotate the 3D printed cylinder;

- 1 MotoMama L298N H-Bridge DC Motor Stepper Driver, to drive the motor;
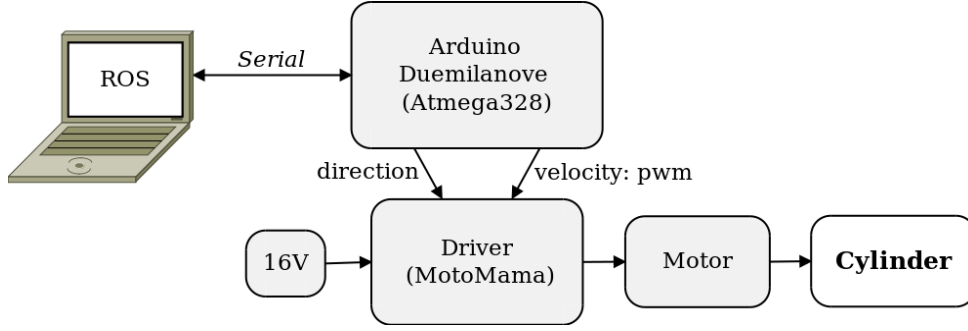
Figure 4.10: Flow chart of the Traction Cylinder.

- 1 bearing, to attach the axle of the cylinder to the device structure;

- 1 Arduino Duemilanove Atmega328, to control the rotation of the cylinder accordingly to the detected traction state. The control of the cylinder patterns is performed using a PWM signal, to control the speed of the motor, and two logic signals, to control the direction of rotation;

- 1 4S Lipo battery (16 V power source), to provide power to the motor;

- 1 Arduino USB cable, to perform serial communication between the Arduino and the PC running the ROS platform;

- 4 flexible connection wires, to connect the Motor to the driver and the driver to the battery.
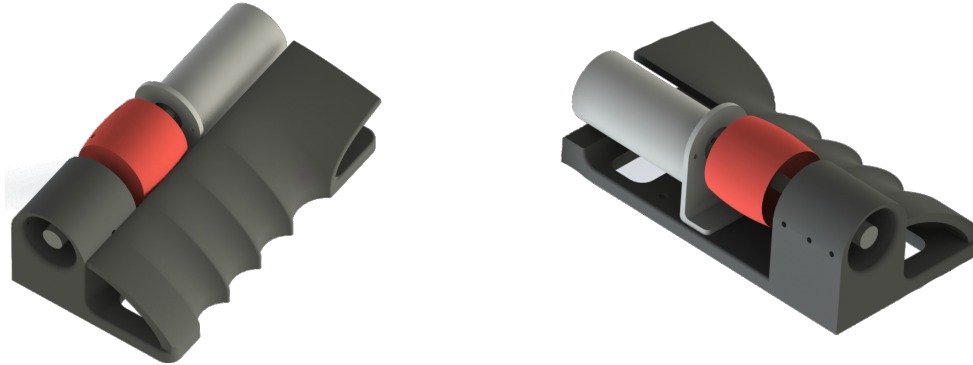
Figure 4.11: 3D model of the Traction Cylinder, where the black area is the structure of the device, the red area is the rotating cylinder and in grey is the gear motor.

Using the Arduino and driver setup shown in Figure 4.12, the tactile patterns are created by controlling the speed and direction of the DC Motor, connected to the pins $OUT3/OUT4$ of the Driver. The speed of the motor is controlled using a PWM signal as the input of the pin EnB of the driver, where the speed of the motor changes proportionally to the duty cycle of the PWM signal. The rotation direction is controlled through the combination of two Logic Signals, pins $In3$ and $I4$ of the Driver, as presented in [36] and summarized in Table 4.3. The pins EnB, $In3$ and $In4$ of the Driver are respectively connected to the following pins of the Arduino: 11 (analog pin), 13 (digital pin) and 12 (digital pin).

The implementation of the rotation control, including speed and direction, was performed using the Arduino to render the tactile patterns that convey the detected traction state of the UGV to the user and is summarized in the Algorithm 1 and Figure 4.13. Setting the analog pin (EnB) to a certain value is accomplished resorting the the function *analogWrite(pin_number, w_{pwm})*, where *pin_number* stands for the defined Arduino pin to perform the velocity control (pin 11) and w_{pwm} stands for the rotation speed of the motor such that $w_{pwm} \in [0, 255]$ and is proportional to the duty cycle of the PWM signal,

EnB	$In3$	$In4$	Rotation
1	1	0	Forward
1	0	1	Reverse
0	-	-	Stop

Table 4.3: Direction control of the motor in the drivers pins, where $EnB = 1$ represents a duty cycle of 100% corresponding to the maximum speed of the Motor.
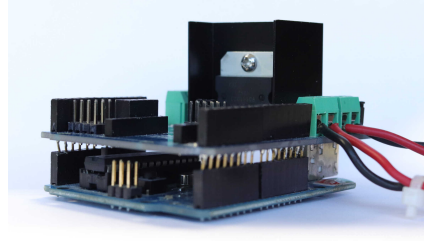
Figure 4.12: Photo of the connection mode between the Arduino and the motor driver.

where the value 0 stands for a duty cycle of 0% and 255 a duty cycle of 100%. Setting the digital pin ($In3$ or $In4$) to a certain value (0 or 1) is accomplished resorting to the function *digitalWrite(pin_number, digital_value)*, where *pin_number* stands for defined Arduino pin to perform the direction control (pins 12 and 13) and *digital_value* stands for the intended output of the digital pin such that *digital_value* $\in \{0,1\}$.

Algorithm 1 Traction Cylinder: Rendering the Tactile Patterns
___
 1: Get *Rotation Mode* through the traction rostopic
 2: **switch** *Rotation Mode* **do**
 3:     **case** *Normal*:
 4:         Stop rotation:
 5:         $EnB = 0$, $In3 = 0$, $In4 = 0$
 6:     **case** *Stuck*:
 7:         **if** $\Delta t_{forward} < \Delta tmax$ **then**
 8:             Rotate forward:
 9:             $EnB = w_{pwm}$, $In3 = 1$, $In4 = 0$
10:         **else if** $\Delta t_{back} < \Delta tmax$ **then**
11:             Rotate backward:
12:             $EnB = w_{pwm}$, $In3 = 0$, $In4 = 1$
13:     **case** *Sliding*:
14:         Constant Rotation backwards:
15:         $EnB = w_{pwm}$, $In3 = 0$, $In4 = 1$

The ***Normal*** *Rotation Mode* consists in setting the rotation speed (w_{pwm}) of the motor to zero, i.e. no rotation is displayed by the Traction Cylinder.

The ***Stuck*** *Rotation Mode* consists in alternatively changing the direction of rotation of the motor during equal amounts time, Δt_{max}, starting always with a forward rotation, while the rotation speed w_{pwm} is maintained constant.

The value of Δt_{max} can be changed to obtain a shorter or longer pattern, increasing Δt_{max} creates a longer pattern as the cylinder will be rotating one single direction during greater periods of time causing a greater rotation. The value of w_{pwm} can also be changed to create faster or slower patterns, increasing
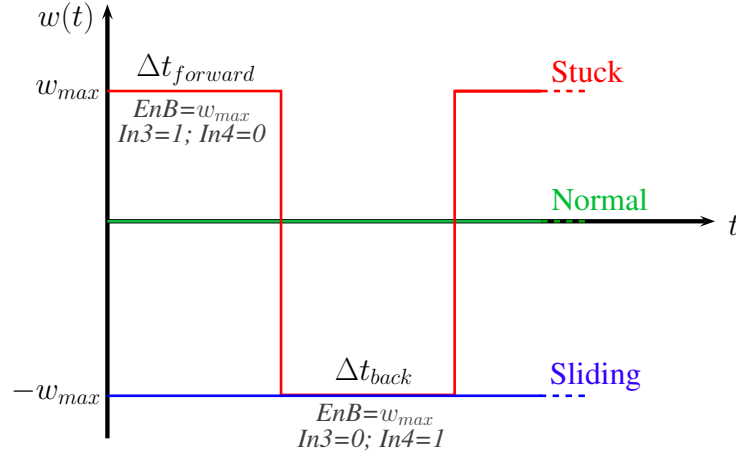
Figure 4.13: Speed and direction of the cylinder regarding all rotation modes, where $w(t)$ stands for the rotation speed of the cylinder and its negative values represent a backward rotation.

the value of w_{pwm} will make the cylinder rotate faster and, consequently, obtain a faster pattern.

The values of Δt_{max} and w_{pwm} were iterated to find a fast and short pattern, while making sure that the cylinder rotates enough for it to noticeable by the users. The iterated speed value took into account the fact that the speed needed to big enough so the users were unable to stop the rotation of the cylinder when holding it too tightly. However, the speed value could not be so large that it would cause fatigue to the user due to transmission of friction during long periods of rotation.

In conclusion, in this *rotation mode* a back and forward tangential motion is displayed by the Traction Cylinder.

The **Sliding** *Rotation Mode* consists in rotating the cylinder at a constant speed in a single direction. This is accomplish by defining the following pin outputs: $EnB = w_{pwm}$, $In3 = 0$ and $In4 = 1$, where w_{pwm} stands for the previously defined value of rotation speed. The backward direction of rotation was chosen to differentiate this rotation mode from the beginning of the *stuck rotation mode*. It was possible that the the UGV lost traction in such a small time period that the *stuck rotation mode* rotates only in one direction and be misinterpreted as the *sliding rotation mode*. To avoid such situations the sliding sensation always rotates backwards while the *stuck rotation mode* always starts with a forward rotation.

In conclusion, in this *rotation mode* a constant backward rotation of the cylinder is displayed by the Traction Cylinder.

Limitations and Future Work

The main limitations of the Traction Cylinder are: (1) the slight noise produced while the cylinder is rotating and (2) the size of the device. Regarding the noise, this one could influence the perception of the patterns, as the users might associate the created sound with the traction loss and respective traction state. To address this problem, a future version of the cylinder could use different material to avoid amplifying the noise. During the user study the participants used headphones to deal with this current limitation of the device. Regarding the size of the device, given its current dimensions, this one could not be directly integrated in the attitude device and would required a downsizing of the device by changing to a smaller motor and consequent size of the cylinder.

4.2.2 E-Vita

E-Vita is a tactile tablet presented by Frédéric Giraud in [32]. Its operation consists of modifying the perception of *texture* on the screen of the device. This *texture* perception is accomplished through the generation of ultrasonic vibrations of a plate as described in [37], and the rendered **texture** corresponds to the tactile feedback modality used to convey the traction state of the UGV.
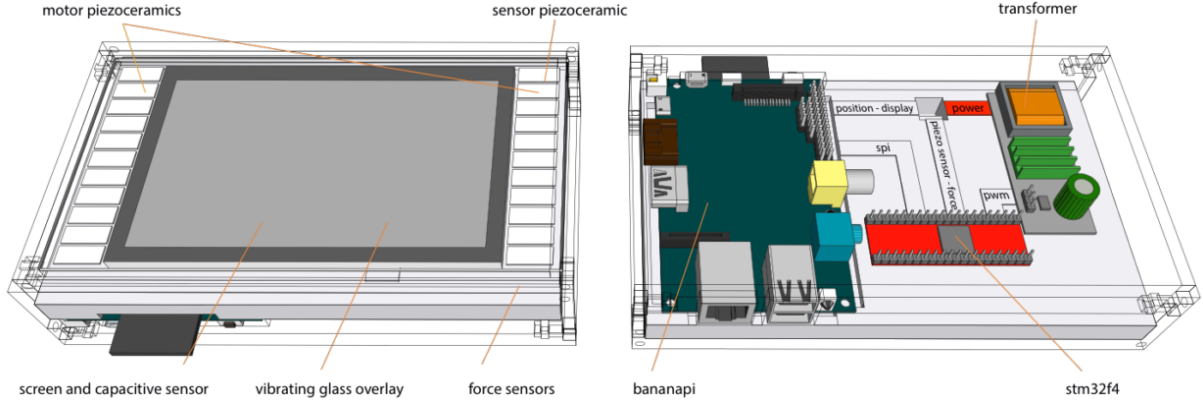
Figure 4.14: E-Vita Structure and Components [38].

This device consists of a vibrating glass overlay and several sensors and motors, as shown in Figure 4.14. These sensors and actuators allow obtaining the position of the finger on the screen and vibrate the glass overlay in such way that the user's perception of friction will change when sliding the finger along the screen. By using both input (finger position) and output (friction) it can be created a closed loop that allows providing both control and feedback of RAPOSA-NG. However, in order to be able to compare all the devices in the performed user study it was developed an open loop system that provides only feedback regarding the traction state of the UGV. The development of the control of RAPOSA-NG using E-Vita will be set for future work.

The use of this device in the teleoperation of RAPOSA-NG intends to create a direct map between the existence of friction in the pulp of the finger with the adhesive friction between the tracks and the floor: Traction.

Figure 4.15: Photo of E-Vita.

Figure 4.16: Interaction mode of E-Vita.

Tactile Patterns

In order to convey the traction state of the UGV to the human operator, three distinct tactile patterns were designed to be provided by the E-Vita as illustrated in Figure 4.17 and explained below:

(a) *Normal State*: As illustrated in Figure 4.17a, a rough texture (yellow area) is rendered with the goal of creating a high friction texture between the finger and the moving device's screen and convey the idea of existence of traction between the tracks of the UGV and floor.

(b) *Stuck State:* As illustrated in Figure 4.17b, to provide feedback regarding the stuck state, a split screen with both rough (yellow area) and smooth (white area) textures was rendered. To convey the sensation of loss of traction the frictionless area of the screen (smooth texture) was generated and to transmit the information that the UGV is unable to move the remaining area of the screen was rendered with high friction (rough texture).

(c) *Sliding State*: As illustrated in Figure 4.17c, a smooth texture (white area) was rendered to convey the idea of traction loss while the finger slides along a complete low friction screen.

(a) Normal State.   (b) Stuck State.   (c) Sliding State.
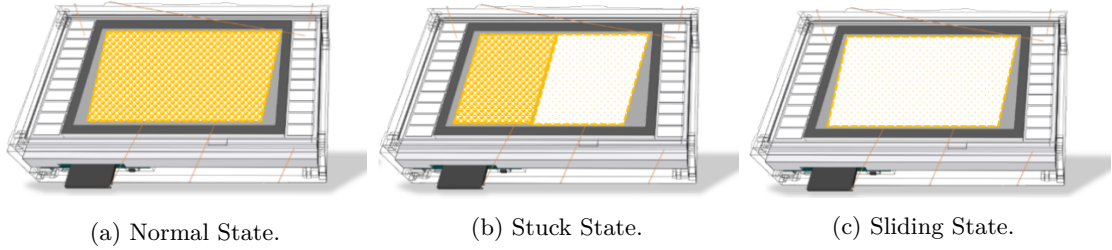
Figure 4.17: Tactile Patterns provided by E-Vita.

Device Integration

The integration of E-Vita on RAPOSA-NG's system was performed using the ROS platform, where the communication with E-Vita was accomplished using a WebSocket communication protocol. The flow chart of the performed Integration of E-Vita with RAPOSA-NG system is represented Figure 4.18. This integration was accomplished using *Python* to perform the communication between E-Vita (WebSocket) and RAPOSA-NG teleoperation system (ROS) and required the following components:

- E-Vita, to render the screen textures;

- PC running the ROS platform, to perform the communication between E-Vita and the RAPOSA-NG;

- Ethernet cable, to connect E-Vita to the PC;

- 5V 2A ITE power supply AC adaptor charger (wallet power), to provide power to E-Vita.
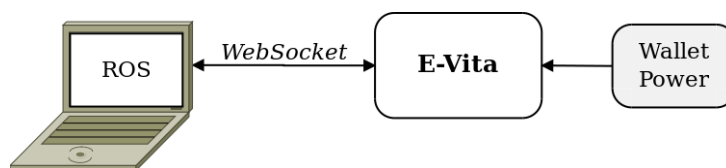
Figure 4.18: Flow chart of the system of E-Vita.

The generation of textures on E-Vita's screen is performed on a layer-on-layer basis, i.e. by creating several layers on top of other layers, also denominated as *taxtels*, and defining a certain *texture* to each of them, as summarized in Algorithm 2. This textures are rendered by sending string messages to E-Vita via WebSocket with the following formats:

- **/taxtel**;<id_taxtTel>;<id_texture>;**rect**;<x1>;<y1>;<x2>;<y2>
  To create a rectangular layer with the id *id_taxtTel*, where the ($x1$, $y1$) is the top left vertex, ($x2$, $y2$) the bottom right vertex and *id_texture* the texture id to be attributed to this layer.

- **/taxtel**;<id_taxtTel>
  To eliminate the layer with the id *id_taxtTel*

- **/texture**;<id_texture>;**rect**;<offset>;<amplitude>;<period>;<ratio>;<speedFunc>
  To attribute a texture with the id *id_texture* to the layers that used that *id_texture* by creating a rectangular wave with an certain *offset*, *amplitude*, *period*, high/low *ratio* and direction of the intended texture *speedFunc* (horizontal/vertical/diagonal).

- **/texture**;<id_texture>;**cos**;<offset>;<amplitude>;<period>;<speedFunc>
  To attribute a texture with the id *id_texture* to the layers that used that *id_texture* by creating a sinusoidal wave (cosine) with an certain *offset*, *amplitude*, *period* and direction of the intended texture *speedFunc* (horizontal/vertical/diagonal).

- **/disableAllTaxtels**;<nb_taxtels>
  To eliminate all the layers with id in the interval [1 , *nb_taxtels*]

Algorithm 2 E-Vita Device: Rendering Textures

1: Rendering Rate = 10 Hz
2: Get *Texture Mode* through the traction rostopic
3: **switch** *Texture Mode* **do**
4:   **case** *Normal*:
5:     Set the complete screen to Rough Texture
6:   **case** *Stuck*:
7:     Set the complete screen to Smooth Texture
8:     Set one half of the screen to Rough Texture
9:   **case** *Sliding*:
10:     Set the complete screen to Smooth Texture

The ***Normal*** *Texture Mode* consists in defining a new layer along the complete screen with a rough texture. This texture is rendered using the following sequence of messages, sent via WebSocket:

1. *"/disableAllTaxtels;20"*, to eliminate all previously created layers;

2. *"/taxtel;1;1;rect;0;0;1024;501"*, to create a layer that occupies the complete screen;

3. *"/texture;1;rect;60;50;3000;1.5;diagonal"*, to attribute a rough texture to the layer defined in message 2.

The ***Stuck*** *Texture Mode* consists in defining two new layers in each half of the screen, one with a rough texture and the other one with a smooth texture. This texture is rendered using the following sequence of messages, sent via WebSocket:

1. *"/disableAllTaxtels;20"*, to eliminate all previously created layers;

2. *"/taxtel;1;1;rect;0;0;1024;501"*, to create a layer that occupies the complete screen;

3. *"/texture;1;rect;60;50;3000;1.5;diagonal"*, to attribute a rough texture to the layer defined in message 2;

4. *"/taxtel;2;2;rect;0;0;400;501"*, to create a layer that occupies half of the screen on top of the previously defined layer using message 2;

5. *"/texture;2;cos;100;0;3000;horizontal"*, to attribute a smooth texture to the layer defined in the message 4.

The **Sliding** *Texture Mode* consists in defining a new layer along the complete screen with a smooth texture. This texture is rendered using the following sequence of messages, sent via WebSocket:

1. *"/disableAllTaxtels;20"*, to eliminate all previously created layers;

2. *"/taxtel;1;1;rect;0;0;1024;501"*, to create a layer that occupies the complete screen;

3. *"/texture;1;cos;100;0;3000;horizontal"*, to attribute a smooth texture to the layer defined in message 2.

Development of a Translating Mechanism to Move E-Vita

An additional mechanism was developed with the purpose of translating E-Vita side to side at a constant frequency while the participant maintains the finger motionless. This added mechanism was designed because the perception of the different textures requires a sliding finger along the screen. However, asking the participants of the user study to move the finger during teleoperation could represent a difficult task, as well as prone to forgetfulness.
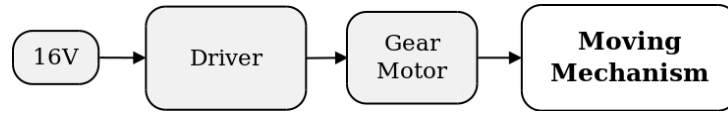
Figure 4.19: Flow chart of the translating mechanism built for E-Vita.

This device uses a slider-crank mechanism that allows to convert the rotational motion, performed by the motor on one axle, into reciprocating translating motion of the sliding platform along a single direction, using a connecting rod between these two. The structure of this device, shown in Figure 4.20, contains three main components: (1) a fixed part containing two rails, (2) a moving structure that slides along the rails of the fix part and (3) two rods that connect to each other and each of them connect to the axle of the motor or to the sliding part. All of the structure was designed using *SolidEdge®* and printed using a 3D printer. To the printed structure it was added the components listed below and shown in Figure 4.21:
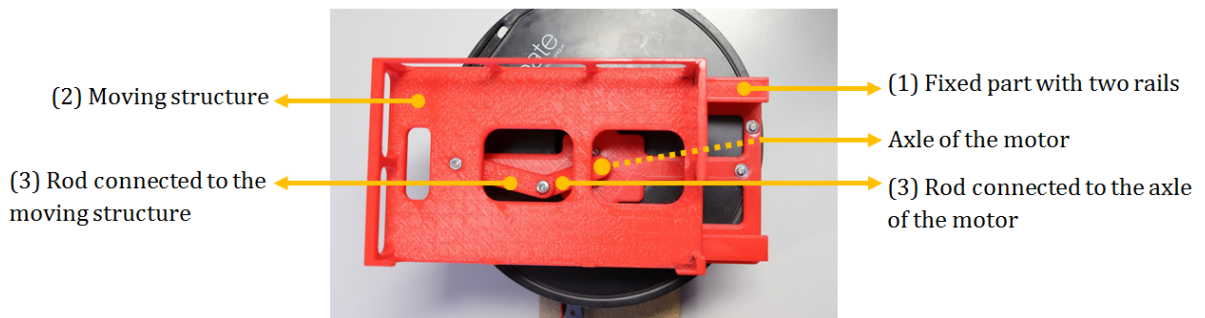
Figure 4.20: E-Vita translating mechanism.
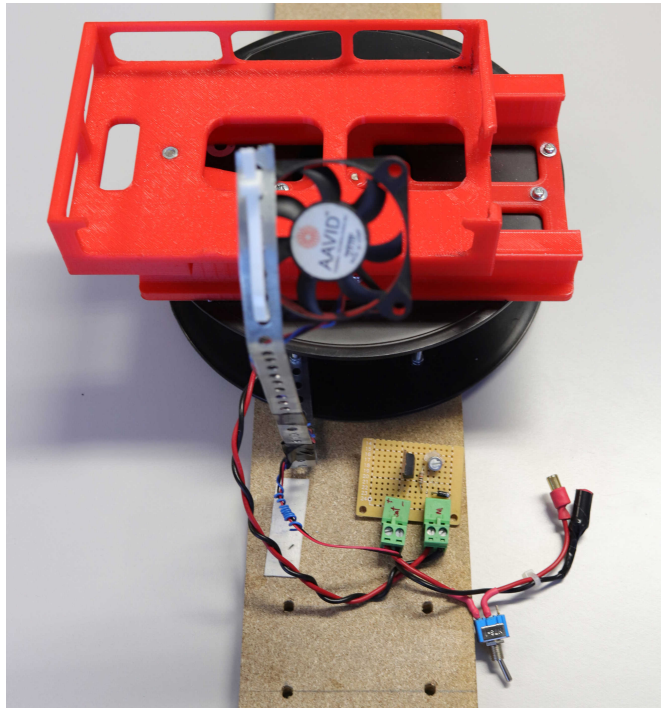
Figure 4.21: E-Vita translating mechanism: photo of the device with electric components.

- 1 gear motor (jm100-2530, DC 12 V, 60 rpm), to rotate the axle of the structure and translate E-Vita side to side. The Motor is placed vertically, rotating around vertical axle, while the sliding part is placed and translates in a horizontal plane;

- 1 costum made motor drive containing a switch, to turn on and off, and a potentiometer to control manually the translation speed of the mechanism;

- 1 4S Lipo battery (16 V power source), to provide power to the motor;

- 1 small fan, to cool down E-Vita during its operation;

- Several connection wires, to connect the battery to the driver and the driver to the motor.

The E-Vita device will then be placed in the sliding part of the mechanism that, after turning on the switch, will make E-Vita move side to side at a constant frequency. By maintaining the E-Vita device moving, the user can simply rest the finger motionless on the screen to receive feedback regarding the traction state of the UGV while teleoperating. This translating mechanism allows to avoid creating a secondary task, and increase the workload and fatigue of the human operator.

Limitations and Future Work

The main limitation of the E-Vita device is requiring the movement of the finger to receive feedback. Although it was developed a translating mechanism to move E-Vita, this solution was very noisy and, due to the movement of the device, some undesired vibration. This added motion of the device might have interfered with the perception of texture. A possible solution would be to design a closed loop system where the user could both receive feedback regarding the traction state of the UGV and perform the control of the robot. The control using E-Vita would require a design that would depend upon constant movement of the finger for the robot to move.

4.2.3 Vibrotactile Glove

The Vibrotactile Glove relies on ***vibration*** as the tactile feedback modality to convey the traction state of RAPOSA-NG. The interest of the researchers on this type of tactile feedback has been growing due to the small size and lightweight of the vibrotactile actuators, allowing to develop highly-wearable devices [39].

The presented device consists of a glove, worn by the human operator, as show in Figure 4.23, with 3 vibrotactile actuators placed on the palm of the hand, in the area under the little finger. The actuators were displayed along a single direction with a constant distance between each consecutive motor, as shown in Figures 4.22 and 4.27. The actuation region was chosen to achieve a compromise between a high sensitivity hand area while being as planar as possible. Choosing that actuation area allows the user to move the hand freely while the contact of the actuators with the skin is not compromised.

This device takes advantage of the sensory funneling illusion presented by Lederman in [40] where, by providing a stimuli in two discrete sites (two actuators) at the same instant, the resulting actuation point is perceived between these two. By creating a sequence of illusory perceived actuation points, it can be created a dynamic sensation along the hand, such as a sliding sensation.

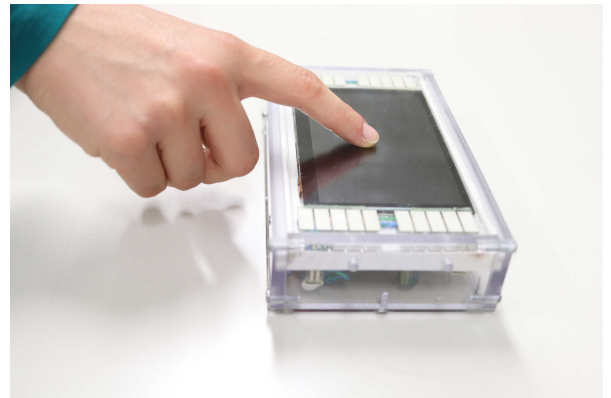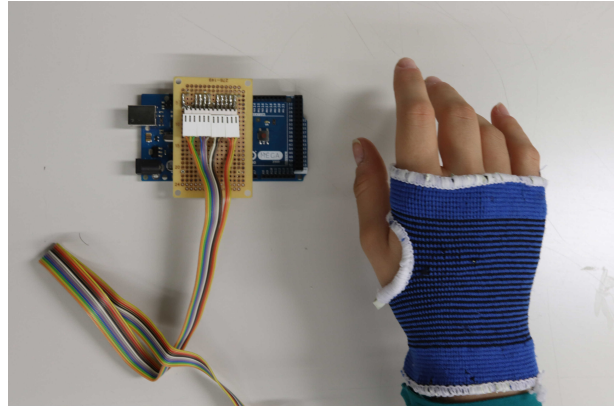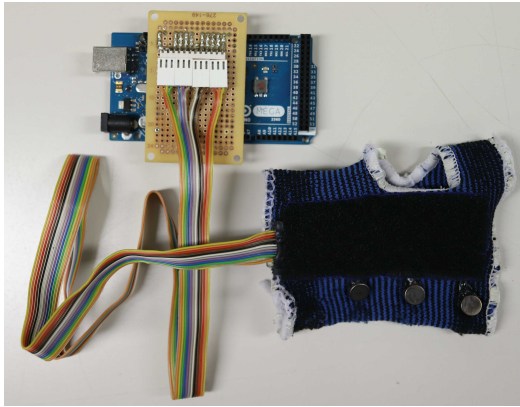Figure 4.22: Photo of the Vibrotactile Glove. Figure 4.23: Interaction mode of the Vibrotactile Glove.

Tactile Patterns

In order to convey the traction state of the UGV to the human operator, three distinct tactile patterns were designed to be provided by the Vibrotactile Glove as illustrated in Figure 4.24 and explained below:

(a) *Normal State*: As illustrated in Figure 4.24a, no vibrotactile cues are displayed by the device, as the UGV has traction and no attention from the user is required to this component of the system.

(b) *Stuck State:* As illustrated in Figure 4.24b, one of the vibrotactile actuators provides a start and stop cue pattern with constant frequency. This pattern intends to transmit the idea of attention being needed to the movement of the UGV as it is trying to move and it is unable to do so.

(c) *Sliding State*: As illustrated in Figure 4.24c, the three vibrotactile actuators (activated two by two) are used to provide a pattern based on the sensory funneling illusion. By taking advantage of this illusory tactile sensation it was rendered an "apparent movement" [41] by changing the perceived actuation point sequentially along the palm of the hand to simulate a sliding sensation and resemble the current traction state of the UGV.

(a) Normal State.

(b) Stuck State.

(c) Sliding State.
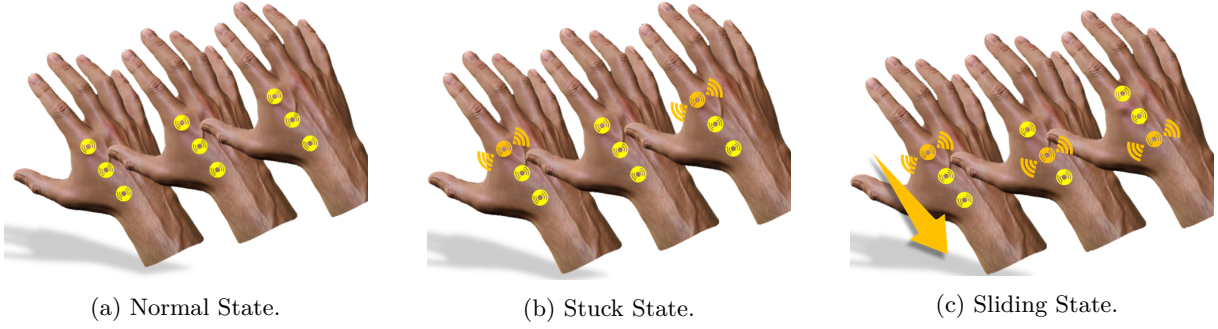
Figure 4.24: Tactile Patterns provided by the Vibrotactile Glove, where the side by side hands represent the patterns along time.

Device Implementation and Integration

The flow chart of the implementation of the Vibrotactile Glove and its integration with RAPOSA-NG system is represented Figure 4.25. The Integration of the this device with RAPOSA-NG system is accomplished using *rosserial_arduino* ROS package [35], which allows using ROS directly with Arduino IDE by providing a ROS communication protocol that works over Arduino's serial port. Using *rosserial_arduino* ROS package, it is launched a node that will perform the control of the actuation of the motors depending on the messages being published to the rostopic containing a message with the current traction state of the UGV. All the control was programmed using the Arduino IDE and the integration with ROS performed by including the *ros.h* library in the *.ino* file.
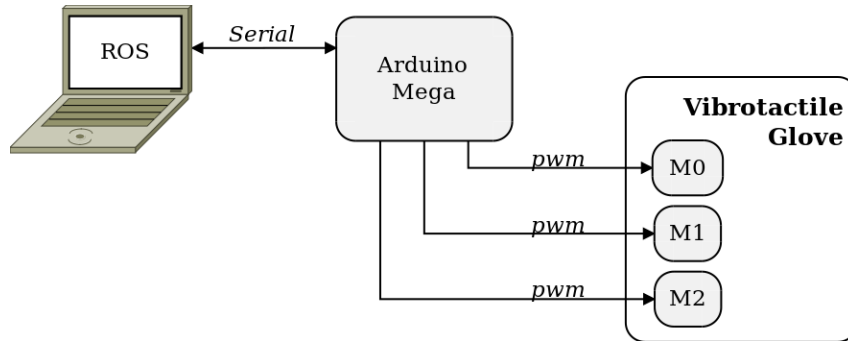
Figure 4.25: Flow chart of the system of the Vibrotactile Glove.

To implement the described device was necessary the following components:

- 1 Elastic glove, to adapt to different hand sizes while maintaining the actuators in contact with the skin;

- 3 Mini Vibrating Disk Motors (10 mm diameter, 2.7 mm thick), attached to the glove and displayed in a single line on the area under the little finger, on the palm of the hand, to provided the different vibrotactile patterns. The vibration amplitude of these motors can be controlled with a PWM signal, where greater duty cycle of the PWM signal means greater vibration amplitude of the motors;

- 1 Arduino Mega 2560, to control the three motors accordingly to the detected traction state, using a PWM signal to control the amplitude of vibration of each motor independently;

- 1 Arduino USB cable, to perform Serial communication between the Arduino and the PC running the ROS platform;

- Several flexible jumper wires, to connect each motors to the Arduino PWM pins and provide the control signal.

Using the Arduino, the Vibrotactile Patterns are sequentially rendered, on a frame-by-frame basis, depending on the detected traction state of the UGV (*Vibration Mode*), summarily described in Algorithm 3.

Algorithm 3 Vibrotactile Glove: Rendering one Vibration Frame
---
 1: Rendering Rate = 15 Hz
 2: Get *Vibration Mode* through the traction rostopic
 3: **switch** *Vibration Mode* **do**
 4:     **case** *Normal*:
 5:         $A_0 = 0$ and $A_1 = 0$ and $A_2 = 0$
 6:     **case** *Stuck*:
 7:         **if** $\Delta t_{vibrating} < \Delta t_{start/stop}$ **then**
 8:             $A_0 = A_{max}$
 9:         **else if** $\Delta t_{stopped} < \Delta t_{start/stop}$ **then**
10:             $A_0 = 0$
11:     **case** *Sliding*:
12:         M_k, M_{k+1}, M_{stop} = Get Active Motors (current x_n)
13:         A_k, A_{k+1} = Get Motors Amplitude (current x_n)
14:         Generate next x_n

The ***Normal** Vibration Mode* consists in setting the Amplitude of Vibration (A) of all motors (M_0, M_1 and M_2) to zero, i.e. no vibration is displayed by the Vibrotactile Glove.

The ***Stuck** Vibration Mode* consists in alternatively changing the vibration amplitude of the motor M_0 to zero (0) or to the maximum vibration amplitude (A_{max}), as represented in Figure 4.26. In this *Vibration Mode* an intermittent vibration is displayed by the Vibrotactile Glove. The time intervals where the motor is vibrating or stopped are constant and have a maximum value of $\Delta t_{start/stop}$, as presented in the Algorithm 3, that can be changed to obtain a faster or slower pattern (increasing $\Delta t_{start/stop}$ creates a slower pattern).
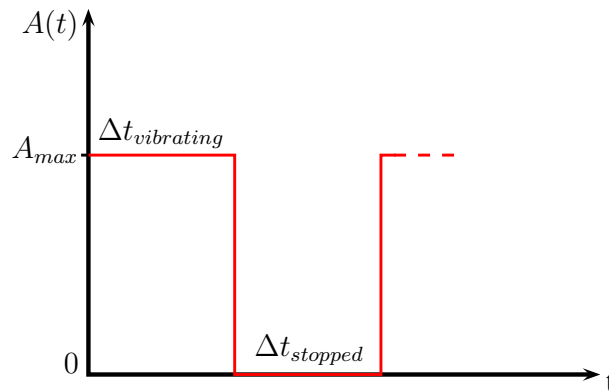
Figure 4.26: Amplitude Rendering, $A(t)$, of one motor (M_0) of the Vibrotactile Glove along the time t in *Stuck Vibration Mode*.

Finally, the PWM signal is sent to the motors resorting to the function *analogWrite(Motor, Amplitude)*, where *Motor* corresponds to the number of the PWM pin to each the Motor M_0 is connected to and the *Amplitude* is the amplitude value of $A(t) \in \{0, A_{max}\} = \{0, 255\}$, proportional to the duty cycle of the PWM signal. A value $A(t) = 0$ corresponds to a duty cycle of 0%, making the motors to stop vibrating, and the value $A(t) = 255$ corresponds to a duty cycle of 100%, making the motors vibrate
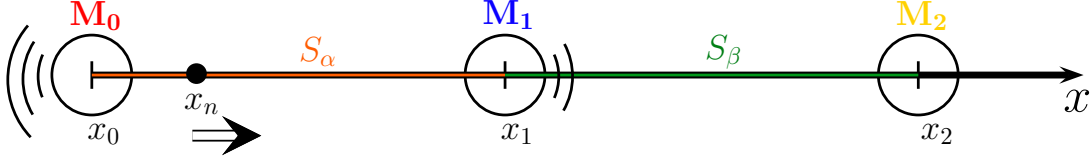
Figure 4.27: Configuration of the three motors (actuators) of the Vibrotactile Glove.
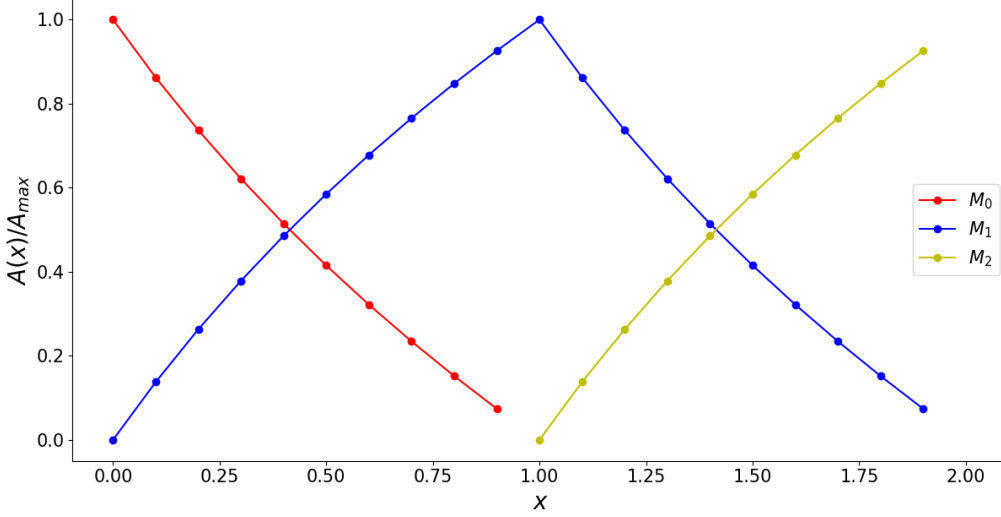
Figure 4.28: Logarithmic amplitude rendering, $A(x)/A_{max}$ (normalized), of the three motors (actuators) of the Vibrotactile Glove depending on the intended actuation point x_n (*Sliding Mode*).

with maximum amplitude.

The **Sliding** *Vibration Mode* consists in generating a tactile sensation based on the sensory funneling illusion. To obtain such tactile sensation the vibration amplitude, A_k and A_{k+1}, of two consecutive motors, M_k and M_{k+1}, are manipulated in such a way that the perceive actuation point, x_n, is placed between these two, as represented in Figure 4.27. The sensations are created sequentially on a frame-by-frame basis, where which frame correspond to the generation of one perceived point x_n between two consecutive motors (M_k and M_{k+1}) in one of the possible Sections (S_α or S_β). In this *Vibration Mode* a sliding sensation along the hand is displayed by the Vibrotactile Glove.

During the implementation of the Vibrotactile Glove, it was tested two different interpolation methods to obtain the amplitude of vibration of a pair of consecutive motors [41]: Linear and Logarithmic Interpolation.

First, it was implemented the linear interpolation, where the vibration amplitude of each motor is linearly proportional to its distance to the intended actuation point x_n. When subjected to this first prototype, several members of the laboratory reported, through qualitative comments, that the sensation created using a linear interpolation was perceived as very discrete, instead of the intended continuous and smooth actuation along the hand.

Second, the linear interpolation was replaced by a logarithmic interpolation, where the vibration amplitude of each motor is logarithmically proportional to its distance to the intended actuation point x_n, as shown in Figure 4.28. When subjected this second prototype, the members of the laboratory noticed an improvement and showed preference in this second prototype over the first one. Using a logarithmic interpolation, it is provided a smother and a more realistic sensation to convey a motion along the hand comparatively to the linear approach.

The implemented functions to obtain the amplitude, A_k and A_{k+1}, of two consecutive motors M_k

and M_{k+1} are presented in Equations (4.1) and (4.2),

$$\frac{A_k(x_{norm})}{A_{max}} = \frac{\log(x_{norm}+1)}{\log(\Delta x_{section}+1)} = \frac{\log(x_{norm}+1)}{\log(2)} \tag{4.1}$$

$$\frac{A_{k+1}(x_{norm})}{A_{max}} = 1 - \frac{\log(x_{norm}+1)}{\log(\Delta x_{section}+1)} = 1 - \frac{\log(x_{norm}+1)}{\log(2)} \tag{4.2}$$

where x_{norm} stands for normalized position of the intended actuation point in a Section, such that $x_{norm} \in [0,1[$ when $x_n \in [0,2[$, and $\Delta x_{section}$ stands for the length of the Section between the two motors M_k and M_{k+1} that, for simplicity purposes, was defined: $\Delta x_{section} = 1$.

To render the sliding sensation along the hand it was discretely incremented the intended actuation point x_n and obtained the corresponding vibration amplitude of each motor, as represented in Figure 4.28. The rendered sliding sensation, conveys sequentially the intended actuation points, were the distance between each point is the defined parameter $\Delta x_{min} = 0.1$, and the rendering frequency is defined by the parameter $f_{rendering} = 25\,Hz$.

The two parameters Δx_{min} and $f_{rendering}$ can be changed to obtain a smoother sensation, by decreasing Δx_{min} and increasing $f_{rendering}$, or to obtain a faster sensation, by increasing Δx_{min} and/or increasing $f_{rendering}$. The used values of Δx_{min} and $f_{rendering}$ were obtained iteratively to reach a compromise between a smooth and a fast sensation while taking into account the physical limitations of the devices. These limitations include the existence of a maximum $f_{rendering}$ allowed by the motors. When the rendering frequency was too high the motors would malfunction by either stopping or displaying random behaviors of the motors, as these ones were unable to generate the vibration amplitude at such high frequency. The motor limitations also include the existence of a minimum value of duty cycle of the PWM signal that causes the motors to vibrate. This minimum value of duty cycle of the PWM signal was experimentally determined and later used to transform the calculated $A_M/A_{max} \in [0,1]$ into the $A_{min_{PWM}} \in [A_{min}, A_{max}]$,

$$A_{min_{PWM}}(A_M) = \frac{A_M}{A_{max}}(A_{max} - A_{min}) \tag{4.3}$$

Finally, the PWM signal is sent to the motors resorting to the function *analogWrite(Motor, Amplitude)*, where *Motor* corresponds to the number of the PWM pin to each the active Motor is connected to and the *Amplitude* is the obtained value of $A_{min_{PWM}} \in [A_{min}, A_{max}] = [40, 255]$ which is proportional to the PWM duty cycle. The value $A = 40$ corresponds to the minimum duty cycle of $\approx 2\%$ and the value $A = 255$ corresponds to a duty cycle of 100%.

Limitations and Future Work

The main limitation of the Vibrotactile Glove is that in larger hands the glove can become too tight, making it uncomfortable to wear it during long periods of time. To address this issue it was created a second version of the Vibrotactile Glove that would close with velcro and be adjusted to all hand sizes. However, this second version used a more rigid material than the elastic glove causing the vibration to spread along the glove, losing the richness of the sliding sensation, and, when flexing the hand, the contact between actuators and the skin was compromised. A better choice of material would be necessary to address this issue.

Future work could include the development of a matrix of vibrotactile actuators that could transmit a greater amount of information, such as knowing the source of traction. This new version of Vibrotactile Glove would require both the development of new hardware for the glove and software for the source detection.

5| User Study

Contents

THIS thesis focuses on the problem of dealing with situations where the UGV loses traction and is unable to comply with a human operator's commands. In these situations, awareness of traction loss is compromised by the physical detachment of the operator with respect to the UGV. In order to overcome such limitations it a novel teleoperation was developed and a user study was conducted to assess the Situation Awareness (SA) of the users with and without haptic feedback. This user study is described in detail in this Chapter. This Chapter is divided into three Sections: Section 5.1 discusses the design of the user study, Section 5.2 describes its implemented apparatus and Section 5.3 reports its method, including a description of the population, the implemented procedure and the performed measures.

5.1 Design

One of the main contributions of this thesis is the report of the user study presented in this Chapter. This one intends to evaluate the three haptic devices, in comparison with the exclusive use of the visual channel. It should be noted that this study proposes to investigate the viability of adding haptic feedback to the interface, as an alternative sensory modality, and do not investigate if this new modality can replace the same information to be provided visually.

The set of research questions and hypothesis of this user study are established below:

Research Questions:

Q1 Does the addition of haptic feedback to the exclusively visual interface improves the user SA regarding the UGV traction state?

Q2 Which of the presented haptic devices can better convey to the operator the traction state of RAPOSA-NG?

Hypothesis:

H1 Having haptic feedback, regarding the traction state, will improve the user Situation Awareness regarding this item.

This study involves the teleoperation of RAPOSA-NG on locomotion challenging scenarios. In these scenarios, the participants went through all possible traction states: *Normal*, *Stuck* and *Sliding*. To accomplish that, the constructed scenarios had elements, such as ramps, to make the robot slide, and small blocks and small navigation spaces, to make the robot stuck. To ensure that all participants passed through all traction states, sometimes, these ones were imposed artificially. This artificiality was accomplished using a rope attached to the robot and used as a last resource.

During this study were provided to the participant three haptic devices. These devices transmitted information about the robot traction state through the sense of touch as an addition the visual feedback from the cameras. The participants used the haptic devices during three of the four possible trials:

V: Exclusively Visual

VC: Visual & Traction Cylinder

VB: Visual & Vibrotactile Glove

VE: Visual & E-Vita

In this user study, it was used a within subject-design, meaning that all participants went through all four trials. This design was chosen to reduce the number of needed users, however, it was necessary taking into account the carry-over effect, where the participation in one condition can impact the performance or behavior on all other conditions.

The most robust design to ensure that there is no carry-over effect would be a complete counter balance design, resulting in 24 possible trial orders ($4! = 24$). However, this design would require a high number of participants to obtain a reasonable number of samples per condition. Another possibility is using a balanced latin square design, resulting in four possible trial orders. Even though this design is not so robust, when ensuring no carry-over effect, it represents the most feasible option. Hence, each participant completed the four trials in one of the following trial orders:

Trial Order 1: *V*, *VC*, *VE*, *VB*;

Trial Order 2: *VC*, *VB*, *V*, *VE*;

Trial Order 3: *VB*, *VE*, *VC*, *V*;

Trial Order 4: *VE*, *V*, *VB*, *VC*.

Using a balanced latin square design, the minimum of participants was initially defined as 24. This amount was established to collect a minimum of six samples per trial order. Because there are four possible trial orders, increasing the number of participants would require securing a number of participants multiple of 4, such as 24, 28, 32, 36 and so on. By the end of the study, it was possible to obtain 32 participants, reaching a total of eight samples per trial order.

During each trial, the participants were probed on their SA. This was achieved by administrating, at randomly selected times (different across trials and participants), a subset of the SAGAT questionnaire. The questionnaire was designed accordingly to the guidelines presented in Subsection 5.1.1 and the complete SAGAT questionnaire is available in Annex D.

Additionally, a set of qualitative questionnaires were conveyed to the participants to evaluate their overall perception of the traction states, several metrics of the haptic devices and their preference on the devices, available in Annexes E.1, E.2, and E.3 respectively.

Finally, a set of five pilot tests were performed. The first test was conducted with an expert on the project and the remaining four tests with inexperienced participants. These pilot tests allowed to hone the developed interface, questionnaires, teleoperation station and devices' arrangement. Concerning the

interface, a few flaws and instructions were amended. Regarding the questionnaires, some of the queries were reformulated, for better understanding, and the number of questions was reduced, to decrease the duration of the user study. Concerning the teleoperation station, it was added a partition and partial noise-canceling headphones to adequately isolate the participants. Regarding the Devices, the Traction Cylinder was secured to the table, to guarantee the same hand position across participants, and to E-Vita, it was annexed a small fan to decrease its temperature during operation.

5.1.1 SAGAT Implementation Guidelines

Based on previous experience using the SAGAT technique, a set of recommendations have been proposed by Endsley [9] for the development and administration of SAGAT queries:

- **Training:** Before the teleoperation tasks, the participant must receive an explanation of the SAGAT procedures and detailed instructions for answering each query.

- **Test Design:** Tests using SAGAT do not require any special test considerations. The same principles of experimental design and administration apply to SAGAT as to any other dependent measure [9].

- **Procedures:** Users should be instructed to perform the tasks as normally as possible and consider the SAGAT queries merely as secondary. While the users are answering the queries no display or visual aids should be visible. The users should be encourage to make their best guess in case of uncertainty in the answer as there is no penalty for guessing. In case the users do not feel comfortable enough to make a guess, they may continue to the next question.

- **Developing of SAGAT Queries:** In order to successfully develop SAGAT queries these should include all levels of SA in the task domain (perception, comprehension, and projection). Special attention should be taken during the development and selection of the SAGAT queries not to focus excessively on the item of interest (traction state) and avoid shifting the attention of the participants to this factor and affect SA artificially. Furthermore, previous investigation revealed that implementing changes to a part of the system may inadvertently affect SA on other issues [9]. Having a broader range of queries allows to investigate if adding this new component to the system could cause these changes. Finally, the terminology used should be both understandable by the participant and appropriated to the domain language and concepts.

- **Selecting SAGAT Queries:** At each SAGAT stop, a set of queries are administrated to the participant. The complete SAGAT questionnaire can be administrated or solely a randomly selected subset. Using a random subset allows dealing with possible time limitations. Furthermore, selecting a random subset of queries prevents the participants from preparing to specific questions. Care should be taken to avoid narrowing the questionnaire subset excessively. Asking only questions that are of high priority at a particular point of the task should also be avoided so as not to cue operators to specific events and, thus, alter SA and performance.

- **Administrating and Collecting SAGAT Data:** Regarding the administration of the SAGAT queries, the following guidelines should be taken into account [42]:

  1. the duration between SAGAT stops should be randomly determined and not occur only at times of increased activity;
  2. a SAGAT stop should not occur within the first three minutes of an experimental trial. This will enable the participant to develop a thorough understanding of what is going on in the scenario prior to being quizzed;
  3. two consecutive stops should not occur within one minute of each other;

    4. which stop should not exceed a duration of six minutes and should have an ideal duration of two minutes.

Over the course of a user study, a total of 30 to 60 samples should be collected per SA query (across subjects and trials in a within-subjects experimental design) for each experimental condition [42].

- **Analyzing SAGAT Data:** The participants' answers to the SAGAT queries are scored as either correct or incorrect. Queries asked the participant but not answered should be considered incorrect. Queries not asked during a given stop should not be evaluated. This classification is performed by comparing the participants' answers with the actual status, obtained from the recorded data and expert judgment. The SAGAT data is binomial and can be analyzed employing methods appropriate for binomial data, depending on the test design. That method can then be used to assess the statistical significance of differences in SA between test conditions.

    The SAGAT employed in the present user study followed all the guidelines mentioned above. These guidelines were taken into consideration during the design of the user study, the development of the user study's Interface and design of the SAGAT questionnaire and its subsets.

    The SAGAT questionnaire were obtained through several iterations, including a final one performed after five pilot tests. The complete Questionnaire is available in Annex D. A subset of the SAGAT questionnaire was administered at each interruption. This subset contained 11 out of 16 possible queries, randomly selected. To provide queries regarding all levels of SA, at each stop, was administrated six queries regarding perception, five regarding comprehension and five regarding projection. The amount of queries was iteratively obtained during the pilot tests to comply with the SAGAT implementation guidelines and avoid reaching a stop duration greater than six minutes. Additionally, the generation of the subset of SAGAT queries was performed in such a way that every participant answered every query at least once per setup conditions.

    All questionnaires were implemented and administrated resorting to Google Forms tool. This approach was adopted to facilitate the implementation of the questionnaires and future collection and processing of the collected data.

5.2 Apparatus

5.2.1 Teleoperation Station

    During each of the different trials, the participants sat in front of the teleoperation interface, shown in Figure 5.1. The participants could visualize the image received from the on-board camera (Visual Feedback) while using a 3Dconnexion SpaceNavigator 6DoF joystick to control RAPOSA-NG

Figure 5.1: Teleoperation Station: participant using the joystick and the Traction Cylinder while receiving Visual feedback.
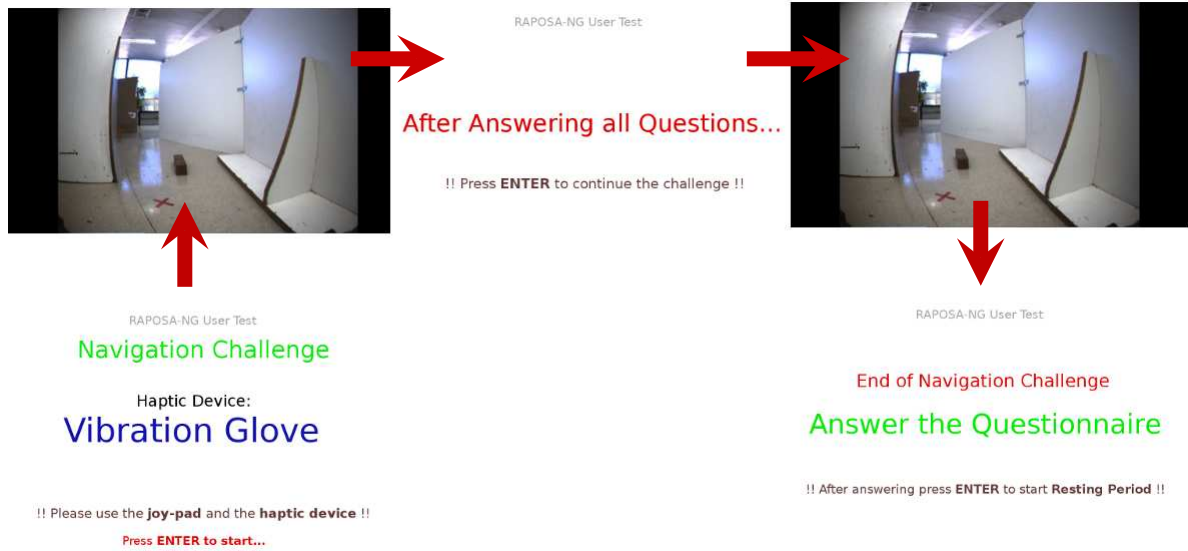
Figure 5.2: Operation flow of the interface used during the user study.

and the three haptic devices to receive the tactile feedback regarding the traction state of the robot. During the trials, the participants wore headphones with partial noise cancellation to ensure that the surrounding sounds would not interfere with the tests.

All participants used the left hand to handle the joystick and control the UGV and the right hand to receive the tactile feedback through the haptic devices that were not visible during the trials. In standard systems (gamepad) the user controls the robot's movement using the left hand (left joystick of the gamepad). As a design choice, this configuration was maintained.

The haptic devices were not visible by the participants during the trials. This way, it was ensured that the movement of the devices did not affect the participants' tactile perception. For this user study, the control of the RAPOSA-NG was changed to from the gamepad to the joystick to ensure that the participants used only one hand to teleoperate the robot across all trials. This feature of the teleoperation architecture was modified because, during the pilot tests, most of the participants used both hands to teleoperate during the Trials *V* and *VB*. To ensure homogeneity between trials, it was used the 3Dconnexion SpaceNavigator 6DoF joystick to control RAPOSA-NG.

As shown in Figure 5.1, during the trials it was used two different PCs. The Questionnaire PC was connected to the internet and was used to administrate the questionnaires (Google Forms) to the participants and record the image stream from the scenarios. The teleoperation PC was connected to RAPOSA-NG and was used to teleoperate the robot and provide instructions to the participants.

For the administration of user study, an application-specific Interface was developed. This interface was displayed in the teleoperation PC and was used to: (1) provide instructions to participants, (2) convey the image from the on-board camera, used during teleoperation, and (3) ensure the SAGAT interruptions.

The user study Interface was implemented using both Python and Bash scripts. These were used to launch all the needed elements for each trial and change the trial order based on the participant number. In Figure 5.2 is represented, in a simplistic way, the flow of the interface during each of the trials. At the beginning of the trial instructions regarding what device to use were provided. To continue, the participant pressed "Enter" prompting the image from the on-board camera, on the PC screen. After a random amount of time, the screen would become suddenly black and instructions to answer the SAGAT questionnaire were provided, repeating this process a maximum of two times. After the two interruptions, or the maximum trial time, new instructions prompted and the participant answered the post-trial questionnaires.

5.2.2 Navigation Scenarios

While the participant sat in front of the Teleoperation Station the UGV crossed four different exploratory maps: *M1*, *M2*, *M3* and *M4* created in two different scenarios. In this thesis, the term map is used to denominate the path that UGV needs to cross inside a specific scenario. The created maps intended to resemble a search and rescue environment and were explored by the participant while teleoperating RAPOSA-NG.

Due to the existence of space limitations in the lab, it was only possible to create two asymmetric scenarios which were traversed in two different directions, providing a total of 4 different Maps, as shown in Figures 5.3 and 5.4. These maps were built in such way that along the path the UGV would go through all of the possible traction states (*Normal*, *Stuck* and *Sliding*). The maps had elements that caused the possible traction states. Ramps to make it slid and small blocks and small navigation spaces to make it stuck.
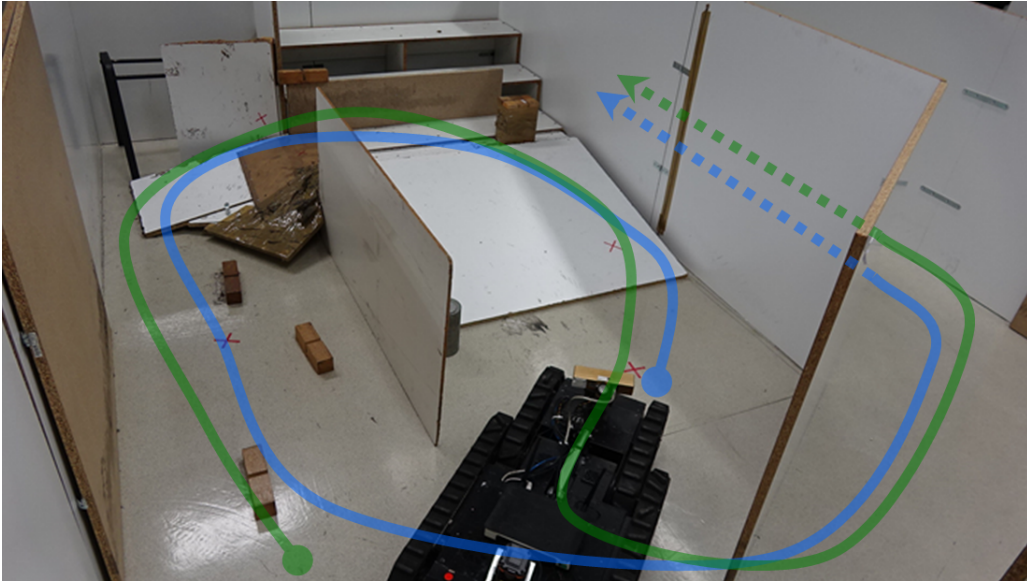
Figure 5.3: Navigation scenario 1 containing the map *M1* (blue) and map *M2* (green).
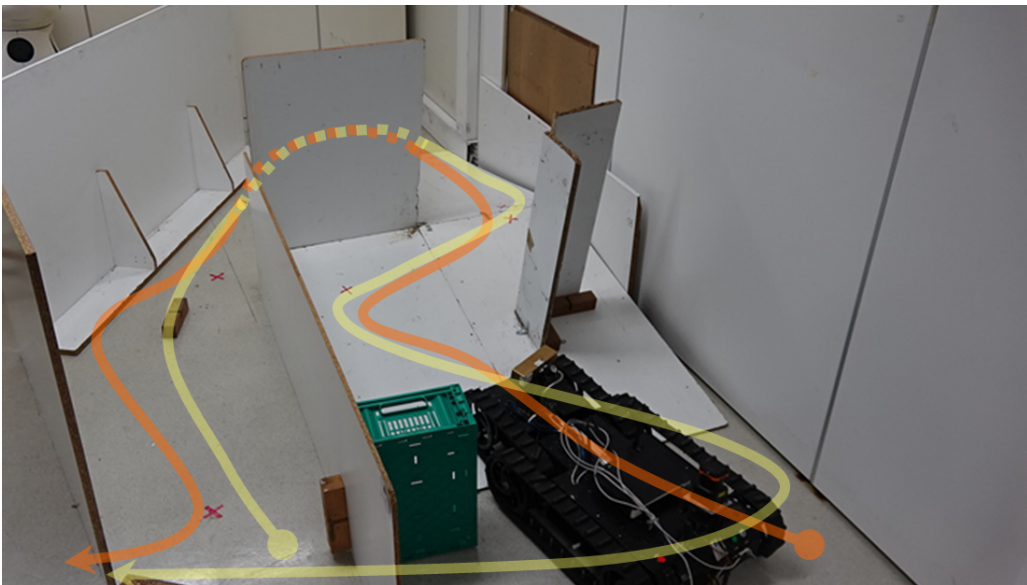
Figure 5.4: Navigation scenario 2 containing the map *M3* (orange) and map *M4* (yellow).

In the scenarios was marked several red "X" to provide guidance to the participants regarding the path to take. The marked "X" intended to make sure that the participants took the path that would maximize the traction loss occurrences.

5.3 Method

5.3.1 Participants

Thirty-two unpaid subjects aged between 18 and 27 years voluntarily participated in the user study where they were provided written instructions and consent, available in Annexes A and B respectively. The participants had neither prior experience teleoperating RAPOSA-NG or prior knowledge regarding the maps to be explored during the several trials. The population of the user study was inquired regarding their gender, nationality, dominant hand and English level. The following demographic data were collected:

- *Gender*: 20 male and 12 female.

- *Nationality*: 28 Portuguese, 1 Italian, 1 German, 1 Cape Verdean and 1 Brazilian.

- *Dominant Hand*: 26 right and 6 left.

- *English Level*: 5 English basic users, 10 English independent users, 15 proficient English users and 2 mother tongue.

When the participants were inquired on their everyday navigation, travels to unknown routes and use of teleoperation, the data represented in Figures 5.5, 5.6 and 5.7 was obtained.
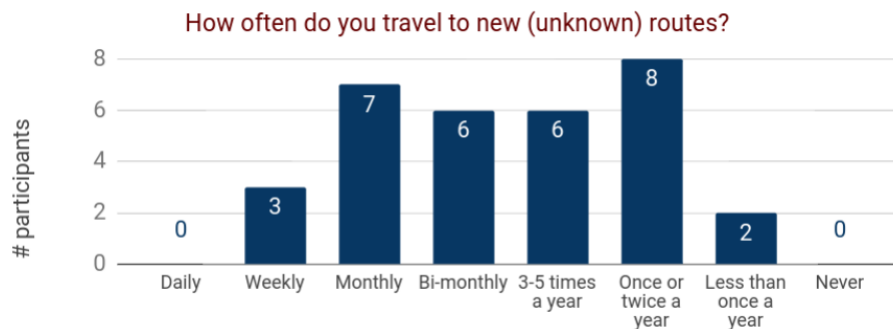
Figure 5.5: Demographic data of the participants: data from the query *How often do you travel to new (unknow) routes?*
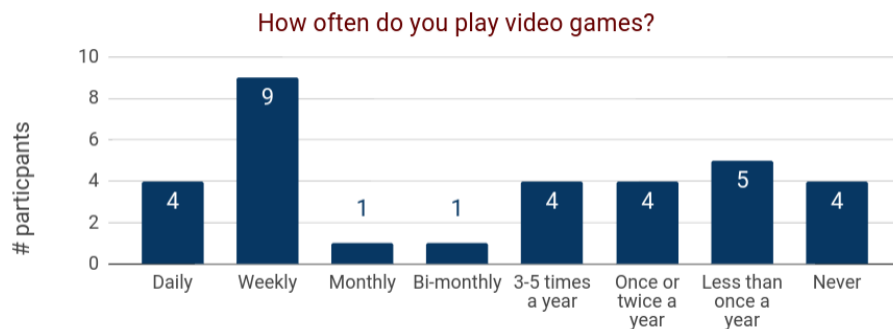
Figure 5.6: Demographic data of the participants: data from the query *How often do you play video games?*
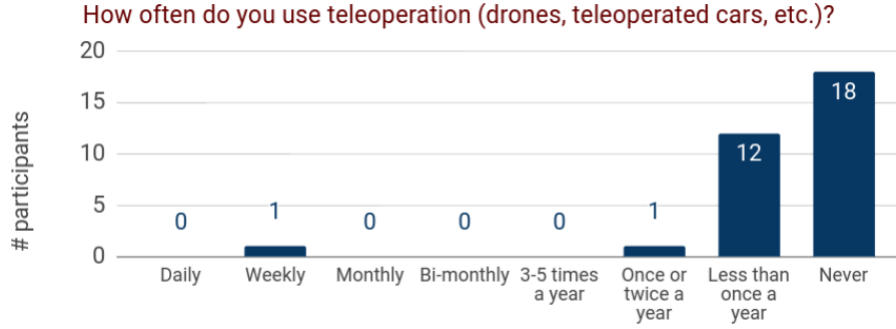
Figure 5.7: Demographic data of the participants: data from the query *How often do you use teleoperation (drones, teleoperated cars, etc.)?*

5.3.2 Procedure

- **Instructions and Demographic Questionnaire:**

  Written instructions regarding the apparatus and procedure of the user study were provided to the participants. After reading the provided instructions (Annex A) and signing the consent form (Annex B), participants answered to a demographic questionnaire (Annex C).

- **Training Session:**

  Each participant completed a training session where they got familiarized with the teleoperation interface, the robot operation, and the haptic devices. The participants also received instructions on how to answer each of the SAGAT queries (Annex D). During this period the participants could see the robot and were free to control it while having access to the visual feedback from the on-board cameras and the different haptic devices. The participants were shown the different possible traction states of the robot, their implications for the robot's movement and possible actions that would allow the robot to overcome such states. In particular, the participants practiced overcoming a small block, shown in Figure 5.1, which allowed them to get familiar with the teleoperation interface and controls. This training session had a minimum of fifteen minutes.

- **Navigation Challenges:**

  After the training period, each participant completed four trials: Exclusively Visual (*V*), Visual & Cylinder (*VC*), Visual & Vibrotactile Glove (*VB*) and Visual & E-Vita (*VE*) in one of the four trial orders: (*V, VC, VE, VB*); (*VC, VE, V, VB*); (*VE, VB, VC, V*); (*VB, V, VE, VC*). These possible orders where defined using a balanced latin square design with the intent of reducing the risk of carry-over effect between trials. At the beginning of the trials *VC*, *VB* and *VE* the participants had a brief training period to review the patterns of the haptic devices until they felt confident and ready to start. To start the trial, they would press the key "Enter", marked in red on the keyboard, prompting the image from the on-board camera on the screen and enabling the control the robot.

  During all trials, the participants had to follow multiple red "X" placed on the walls and floor of the scenarios with the goal of finding the "Stop" sign. After crossing the "Stop" sign the trial would be terminated. Each trial was performed in a different Map and add a maximum duration of 8 minutes. During the trials, the teleoperation would be paused with a black screen and the participants were subject to the **SAGAT questionnaires**. Once the participants finished answering all SAGAT questions they could press "Enter" and resume the teleoperation of the robot. These interruptions would occur at random moments, a maximum of two times per trial.

- **Post-Trial Questionnaires:**

  After each trial, the participants answered two post-trial questionnaires: (1) NASA-TLX to evaluate workload and (2) a qualitative questionnaire (Annex E.1) to assess overall perception of the traction states during that trial. After the trials *VC, VB* and *VE*, an extra set of questions were given to evaluate several metrics of the haptic devices (Annex E.2).

- **Resting Period:**

  Following each trial, the participants would have a resting period (minimum 2 minutes) where the participants were free to move around the room until they felt relaxed and ready to start the next trial.

- **Questionnaire Regarding Device Preference:**

  Once all 4 trials were complete, the participants were inquired regarding their preference and comments on the haptic devices (Annex E.3).

The complete procedure of the user study took, in average, one hour and half. This duration depended on how fast the participants answered the questions, how fast they could reach the stop sign and how much time they needed to rest between trials.

5.3.3 Measures

The primary measure is SAGAT data. The secondary measures are: (1) Qualitative evaluation on the difficulty to perceive the traction states and (2) Qualitative evaluation of several metrics of the haptic devices (discomfort, fatigue, distinguishability of the haptic patterns, usefulness, importance for the decision making and number of felt sensations). The tertiary measures are (1) NASA TLX questionnaire and (2) Video recordings of the participants during trials. Because the tasks were interrupted to answer the SAGAT questionnaires, task time could not be used as a measure of the study.

The conducted user study had a total duration of five weeks and required the maintenance of RAPOSA-NG and the scenarios to obtain homogeneity of operation across participants. During each session of the user study, it was necessary two members of the research team. One of the members sat near the participants (teleoperation station) to aid in case of existing doubts or problems along the experiment. The other member, responsible for the study, was next to the robot (navigation scenarios) to accomplish the following tasks:

- ensure that all participants went through all traction states during each of the four trials;

- answer the SAGAT questionnaires at the same time as the participants to obtain the actual status of the robot at the interruption time. This information was later double-checked with the recorded data during the trials;

- ensure the safety of the robot. The user study was performed with inexperienced participants that lacked awareness regarding dangers to the integrity of the robot. These dangers included mainly two different situations. First, the tracks became constantly stuck, putting a greater effort in the motors and track belts. Second, many participants caused the robot to reach a dangerous attitude or even surpass the turning point.

After conducting the user study, it was necessary to score the participants' answers to the SAGAT queries as correct or incorrect and perform the appropriated statistical analysis. The collected data from the SAGAT and qualitative questionnaires are available in Annexes F and G. Its analysis and discussion are presented in Chapter 6.

6| Results and Discussion

Contents

IN this chapter it is presented the Results of the performed user study and its Discussion. In Section 6.1 it is reported the results of a statistical analysis of the SAGAT data including a two-way repeated measures ANOVA to evaluate the interaction between Maps and Devices and between SA Levels and the Devices, and a Wilcoxon signed-ranks test to compare the use of haptic feedback with the exclusive use of visual feedback. In section 6.2 the results obtained in the previous section are interpreted and discussed. In section 6.3 it is reported the results of a statistical analysis of the data obtained from the qualitative questionnaires regarding the participants' ability and difficulty to notice the stuck and sliding states and regarding several metrics of the haptic devices. Finally, in Section 6.4, the results obtained in the previous section are interpreted and discussed and it is presented a brief collection of the comments made by the participants during the user study, concerning the different Haptic Devices.

6.1 Quantitative Results: SAGAT

The collected data from the SAGAT questionnaires is available in Annex F.

Interaction between Maps (*M1*, *M2*, *M3*, *M4*) and Devices (*V*, *VC*, *VB*, *VE*):

This data was first analyzed using a two-way repeated measures ANOVA on *% of SAGAT Correct Answers*. The *% of SAGAT Correct Answers* data was obtained from the weighted average of the correct answers of the participants on the several queries in each of the *SA levels*, *Maps* and *Devices*. The way this averages were obtained is explained with greater detail in Table F.2 in Annex F. A parametric test was used because the range of values of the dependent variable (*% of SAGAT Correct Answers*) can be considered continuous (0% to 100%) and its distribution close to a normal distribution.

A two-way repeated measures ANOVA on *% of SAGAT Correct Answers* data with factors of *Maps*(4 levels) and *Devices*(4 levels) as within-subject variables was performed. No interaction between factors *Maps* and *Devices* was found in the two-way repeated measures ANOVA for *% of SAGAT Correct Answers*.

Interaction between SA Levels (Perception, Comprehension, Projection) and Devices (*V*, *VC*, *VB*, *VE*):

A two-way repeated measures ANOVA on % *of SAGAT Correct Answers* data with factors of *SA Levels* (3 levels) and *Devices* (4 levels) as within-subject variables. No interaction between factors *SA Levels* and *Devices* was found in the two-way repeated measures ANOVA for % *of SAGAT Correct Answers*. No statistically significant difference was found across the different levels of the factors *SA Levels* and *Devices*. All subsequent statistical analyses are done on the factor *Devices* and performed with a confidence level of 95%.

SAGAT query-by-query Analysis:

To assess the participant's SA regarding the traction state of the UGV, a query-by-query analysis. This query-by-query analysis required a non-parametric test. In this analysis the % *of SAGAT Correct Answers* of each participant, in each query and *Device*, was analyzed. The way this data was obtained is explained with greater detail in Table F.1 in Annex F. In each trial, there were a maximum of two SAGAT stops during the task. Therefore, % *of SAGAT Correct Answers* could only take three possible values: 0%, 50% or 100% (non-parametric data). For this analyzes, a Wilcoxon signed-ranks test was performed to analyze the % *of SAGAT Correct Answers* on a query-by-query basis.

For the SAGAT results of the query *"What is the state of the robot?"*, a Wilcoxon signed-ranks test showed that *Devices VB* ($Z = -3.00$, exact $p = 0.002$, one-tailed) and *VC* ($Z = -2.00$, exact $p = 0.038$, one-tailed) were statistically significantly higher than only visual feedback, where higher represents a greater amount of correct answers. No statistically significant difference was found for the remaining queries of the SAGAT questionnaire.

6.2 Quantitative Discussion: SAGAT

6.2.1 Maps, SA Levels and Devices:

No interaction was found between the *Maps* and *Devices* factors, whereby it was verified that having only two scenarios did not influence the % *of SAGAT Correct Answers* and subsequent statistical analysis did not require taking into account the *Maps* factor.

When investigating the interaction between *SA Levels* and *Devices*, no interaction was found between these two factors. From the obtained result, one can conclude that adding haptic devices to exclusively visual interface did not influence SA of the participants in any of the SA Levels (perception, comprehension, projection). Therefore, it can be stated that the SA, regarding all levels, provided by the complete interface was not affected by the addition of the haptic devices to the RAPOSA-NG system. The obtained results regarding the frequency of correct answers to queries of all SA levels across the Devices are represented in Figure 6.1.

It is interesting to notice the results shown in Figure 6.2. These results, concerning % *of SAGAT Correct Answers* across *SA Levels*, show two expected tendencies:

1. Greater % *of SAGAT Correct Answers* in the first and lowest level of SA (perception), followed by the second and middle level of SA (comprehension) which was followed by the last and top level of SA (projection). This tendency was expected as the difficulty to understand the provided information increases as the SA level increases.

   In the lowest level of SA, the participant only needed to report direct information conveyed by the teleoperation interface. In the middle level of SA, the participant had to develop a comprehension of all the perceived information. In the top level of SA, the participants not only needed to have a
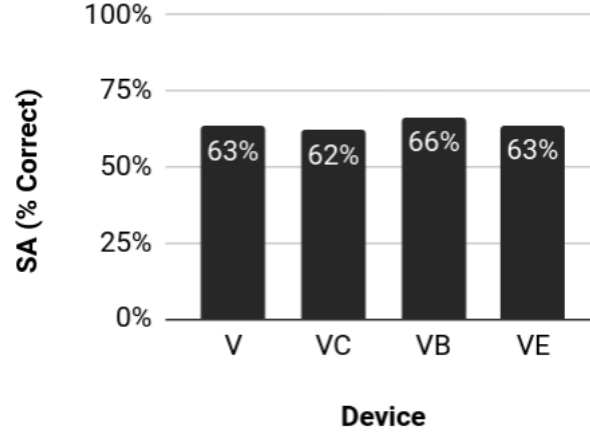
Figure 6.1: Frequency of correct answers to queries in all levels of SA across Devices.

good comprehension of the perceived information concerning the robot and its environment but also develop a notion of future events based on comprehended information and their future intentions.

2. The greatest difference in the *% of SAGAT Correct Answers*, across *Devices*, occurs in SA Level 2 (comprehension), in particular in the *Device VB*. This event was expected as the comprehension of the traction state, the item of interest provided by the haptic devices, is contained in SA Level 2.
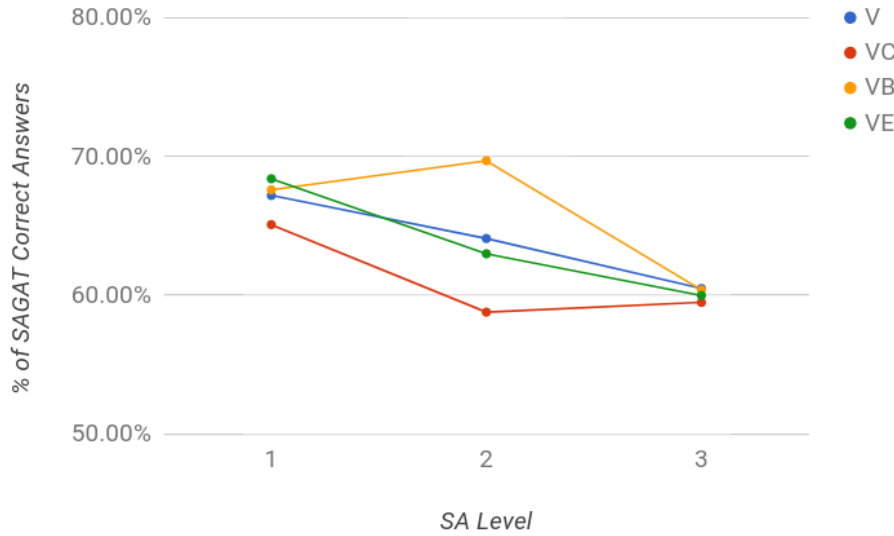
Figure 6.2: *% of SAGAT Correct Answers* to queries in each Device across SA Levels

6.2.2 SAGAT query-by-query Analysis:

When analyzing the *% of SAGAT Correct Answers*, on a query-by-query basis for the *Devices* factor, statistical evidence was found to support that the Traction Cylinder (*VC*) and Vibrotactile Glove (*VB*) improved the SA of the participants regarding comprehension of the UGV's traction state when comparing to the exclusively visual modality (*V*). The obtained results show that the *friction* (*VC*) or *vibration* (*VB*) cues can be used to convey the traction state of the UGV and avoid overloading the visual channel to convey this new information. It should be noted that these results show the viability of adding haptic feedback to the interface, as an alternative sensory modality, and do not evidence that this modality can replace the same information to be provided visually, as that was not the intent of the study. Regarding E-Vita (*VE*), although there is evidence that it might improve the comprehension

of the traction state of the UGV (Figure 6.3a), it is not possible to make any statement supported by statistical significance, at least without more participants.The moving setup mechanism restricted the richness of information provided by to the participants. This setup might have influenced the results regarding E-Vita. With the performed measures, it was not possible to separate the factors regarding the provided textures and the moving mechanism. Therefore the impact of each of these factors on the final solution was not investigated.

(a) *"What is the state of the robot?"* (*Normal, Stuck, Sliding,* and *Don't know*)

(b) *"Is there currently anything that might be preventing the robot desired movement?"* (*Yes, No,* and *Don't Know*)
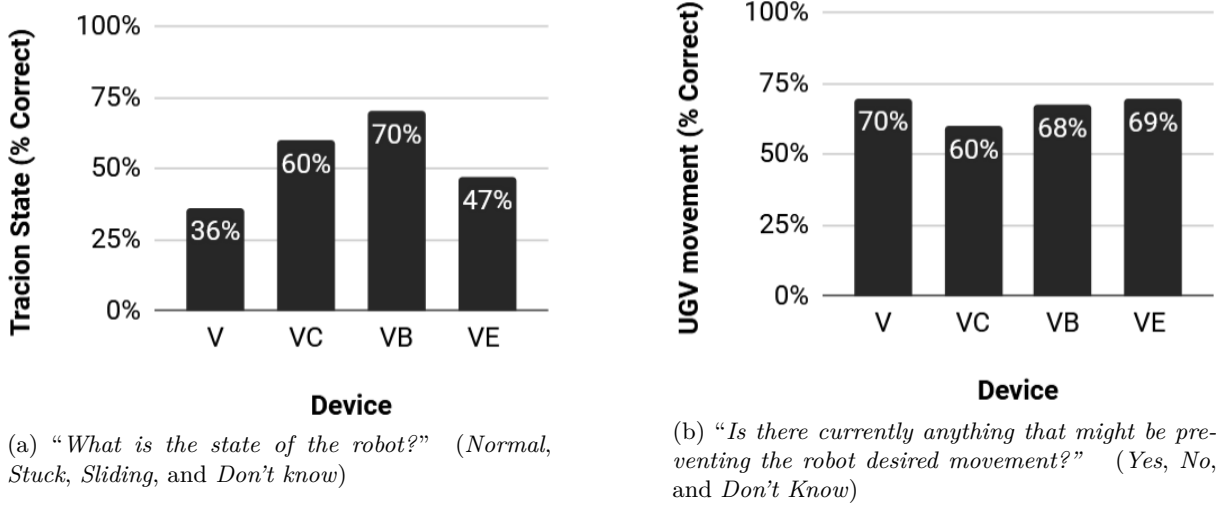
Figure 6.3: Results to two of the SAGAT Queries.

It is interesting to notice that there was no statistically significant difference in the results across the Devices (*V, VC, VB, VE*) for the query *"Is there currently anything that might be preventing the robot desired movement?"*, shown in Figure 6.3b. The obtained results show that participants are capable of comprehending the existence of an impediment to the UGV's movement. However, only when using the Traction Cylinder (*VC*) or the Vibrotactile Glove (*VB*) a statistically significant improvement was obtained in the comprehension of the UGV's traction state. These results address the previously presented issue of confusion and frustration during teleoperation due to loss of traction that this thesis tackles.

Regarding the SAGAT query *"What is the current traction situation of the robot?"*, there was no statistically significant difference across Devices and it was observed a disagreement with the given answers to the SAGAT query regarding the traction state. When inquired regarding traction state and traction situation at the same SAGAT interruption, 61.3% of the times, the participants that answered "Stuck," also answered "With Traction". This incoherence in the answers did not occur for the sliding State. These incoherences might have been caused by a lack of comprehension from the participants regarding the concept of traction, and/or by a weak explanation of the concept during the training period.

The devices only assisted the participants in the comprehension of traction state (Level 2 SA) and did not help in the prediction of future events (Level 3 SA). This effect could have been caused by the population used in the user study. All the participants were non-expert users. The ability to predict future events based on the comprehension of the current state requires a good knowledge of the robotic system. This ability of prediction should be greater when using expert users in the population.

6.3 Qualitative Results: Post-Trial Questionnaires

The collected Data from the Qualitative Post-Trial Questionnaires is available in Annex G. This data was analyzed using a Friedman Test followed by Post hoc analysis with Wilcoxon signed-rank tests with a Bonferroni correction applied.

6.3.1 Difficulty to Understand the Traction States (Sliding and Stuck):

A Friedman Test showed that there was a statistically significant difference in the Difficulty to Understand that the UGV was stuck or sliding depending on the used *Device*: $\chi^2 = 21.773$, exact $p < 0.001$ regarding the stuck State and $\chi^2 = 11.429$, exact $p = 0.005$ regarding the sliding State.

Post hoc analysis with Wilcoxon signed-rank tests was conducted with a Bonferroni correction applied, resulting in a significance level set at $p < 0.0083$ and the respective results are shown in Table 6.1. This Table should be read as follow: *Device X* is lower than *Device Y* (Z, exact p, one-tailed), in the difficulty to understand the $State_n$, where "lower than" means less difficulty to understand the $State_n$. E.g.: *VC* is lower than *V*, in the difficulty to understand the stuck State, where "lower than" means less difficulty to understand the stuck State.

$State_n$	Device X	Device Y	Z	exact p (one-tailed)
	VC	*V*	-2.993	0.0008
Stuck State	*V*	*VE*	-2.892	0.0002
	VC	*VE*	-3.866	< 0.0001
	VB	*VE*	-2.866	0.0016
Sliding State	*VC*	*VE*	-3.025	0.0006

Table 6.1: Results of the performed post hoc analysis with Wilcoxon signed-rank tests regarding the difficulty to understand the traction states (stuck and Sliding) during the trial.

6.3.2 Metrics of the Haptic Devices:

A Friedman Test showed that there was a statistically significant difference in the qualitative evaluation of the several metrics of the haptic devices presented in Table 6.2 depending on the used haptic device. These metrics include level of discomfort (1:no discomfort - 7:very discomforting), level of fatigue (1:no fatigue - 7:very fatiguing), and level of distinguishability (1:indistinguishable - 7:very clear), level of usefulness for the UGV teleoperation (1:not useful - 7:very useful), level of importance for the decision making (1:not import - 7:very important) and number of different patterns felt during each trial.

Post hoc analysis with Wilcoxon signed-rank tests was conducted with a Bonferroni correction applied, resulting in a significance level set at $p < 0.0167$, and the results of this analysis are shown in Table 6.3. This Table should be read as follow: *Device X* is higher than *Device Y* (Z, exact p, one-tailed), regarding $Metric_n$, where higher means greater $Metric_n$. E.g.: *VE* is higher than *VC* ($Z = -3.625$, exact $p < 0.001$, one-tailed) and in *VE* is higher than *VB* ($Z = -3.430$, exact $p < 0.001$, one-tailed) regarding Level of discomfort, where higher means greater discomfort.

	χ^2	exact p
Level of discomfort	25.209	< 0,001
Level of fatigue	14.629	< 0,001
Level of distinguishability	48.136	< 0,001
Level of usefulness	20.558	< 0,001
Level of importance for decision making	20.352	< 0,001
Number of felt sensations	8.711	0.012

Table 6.2: Friedman Test results for the several metrics of the haptic devices.

Metric$_n$	Device X	Device Y	Z	exact p (one-tailed)
Level of	VE	VC	-3.625	< 0,001
discomfort	VE	VB	-3.430	< 0,001
Level of	VE	VC	-2.852	0.002
fatigue	VE	VB	-3.832	0.000
Level of	VC	VB	-2.812	0.002
distinguishability	VC	VE	-4.740	< 0,001
	VB	VE	-4.562	< 0,001
Level of	VC	VE	-4.156	< 0,001
usefulness	VB	VE	-3.493	< 0,001
Level of	VC	VE	-4210	< 0,001
importance	VB	VE	-3.858	< 0,001
Number of Felt	VC	VE	-2.594	0.012
Sensations	VC	VB	-2.829	0.003

Table 6.3: Results of the post hoc analysis with Wilcoxon signed-rank tests for the several metrics of the haptic devices.

6.4 Qualitative Discussion: Post-trial Questionnaires

6.4.1 Difficulty to Understand the Traction States (Sliding and Stuck):

After each trial, participants were qualitatively inquired regarding their ability and difficulty to notice the stuck and sliding states. The stuck state was noticed by the participants 97% of the trials with the Devices (*V*) and (*VC*) and 100% of the trials with (*VC*) and (*VB*), while the sliding state was reported in the trials with the Devices (*V*) 50% of the trials, (*VC*) 81% of the trials, (*VB*) 69% of the trials, and (*VE*) 59,4% of the trials. This difference in reporting the stuck and sliding states might have occurred due to the fact that the sliding state was physically limited by the dimensions of the scenarios, making it a time-limited event, easier to overcome, and less frustrating, and more likely to be forgotten by the end of the trial.

Regarding the difficulty of traction state awareness, the participants described E-Vita (*VE*) as the Device with the greatest difficulty to grasp the stuck state. Participants also commented that the texture associated with the stuck state was very challenging to distinguish from the other provided textures.

6.4.2 Metrics of the Haptic Devices:

Results showed that the Traction Cylinder (*VC*) was reported as the most distinguishable. Comparing these results to the ones obtained on a query-by-query basis, it is observable that there is a difference between the device with greater % *of SAGAT Correct Answers* (*VB*) and the qualitatively reported device with greater distinguishability (*VC*). Participants might have wrongly identified the patterns of the cylinder in cases where the the back and forward pattern occurred in a small period and only a single direction pattern was displayed, while vibrotactile patterns differentiate in terms of actuation point, frequency and, amplitude.

The results obtained from the qualitative post-trial questionnaire, concerning the metrics of the haptic devices (Annex E.2), are shown in Figures 6.4, 6.5, 6.6, 6.7, 6.8 and 6.9. The obtained experimental data also shows that E-Vita (*VE*) was the haptic device with greatest levels of discomfort, fatigue, and lowest level of distinguishability. These results are in agreement with the obtained results from the SAGAT. Based on the comments made by the participants, these greater levels of discomfort and fatigue might have occurred due the fact the most frequent textures during the trials (*Normal* and *Stuck*)

64

displayed high friction. Better distinguishability would require the redesign of the provided textures.

Participants also reported the Traction Cylinder (*VC*) as the haptic device with greatest levels of distinguishability, usefulness and importance for decision making. The Vibrotactile Glove (*VB*) was described as the device with lower level of discomfort, fatigue and limitation.

6.4.3   Preference of Devices and Comments of the Participants

Once the participants completed all 4 Trials, they were inquired regarding their preference and comments on the haptic devices. The following results were obtained:

- ***Do you think adding haptic/tactile feedback was useful to the teleoperation of the robot, comparing to only visual feedback?*** 93.5% (29) of the participants answered *"Yes"* and 6.5% (2) of the participants answered *"No"*.

- ***Which device did you like the most?*** As shown in Figure 6.10, 51.6% (16) of the participants answered *"Vibration Glove"* and 48.4% (15) of the participants answered *"Traction Cylinder"*.

- ***Which device did you like the least?*** As shown in Figure 6.11, 90.3% (28) of the participants answered *"E-Vita"*, 6.5% (2) of the participants answered *"Vibration Glove"* and 3.2% (1) of the participants answered *"Traction Cylinder"*.

- **Comments regarding the Traction Cylinder (*VC*):**
  The positive aspects of the Traction Cylinder are: comfortable and easy to use; useful for teleoperation and decision making; very clear and distinguishable patterns; the most intuitive patterns because the movement of the cylinder matched the motion of the robot.

  The negative aspects of the Traction Cylinder are: not so comfortable during long periods of actuation due to the roughness surface of the rotating cylinder; quite bulky and noisy; when the patterns were conveyed during short periods of time, these became hard to distinguish.

- **Comments regarding the Vibrotactile Glove (*VB*):**
  The positive aspects of the Vibrotactile Glove are: comfortable device that doesn't constrain the movement of the hand, like the remaining devices; distinguishable and clear patterns due to the difference in frequency and actuation point.

  The negative aspects of the Vibrotactile Glove are: patterns are not so intuitive as the one provided by the Traction Cylinder; sometimes the glove was to tight.

- **Comments regarding E-Vita (*VE*):**
  The positive aspect of the E-Vita is: this device is the most sophisticated out of the three.
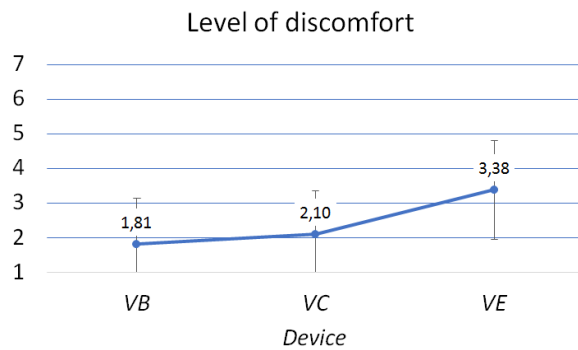
Figure 6.4: Level of discomfort across haptic devices (1:no discomfort - 7:very discomforting).
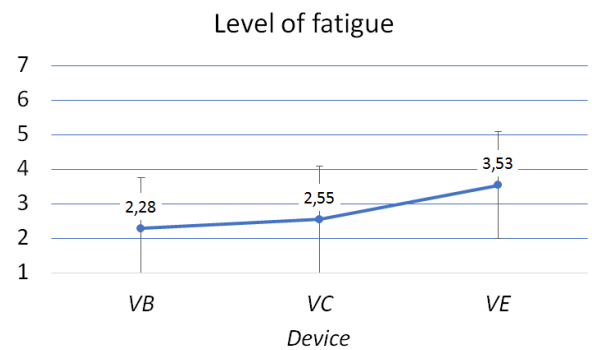
Figure 6.5: Level of fatigue across haptic devices (1:no fatigue - 7:very fatiguing).

Level of distinguishability
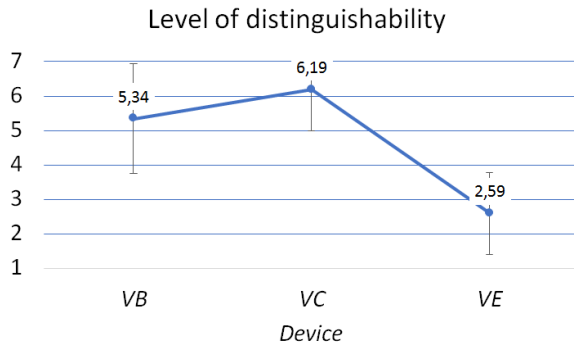
Figure 6.6: Level of distinguishability across haptic devices (1:not distinguishable - 7:very distinguishable).

Level of usefulness
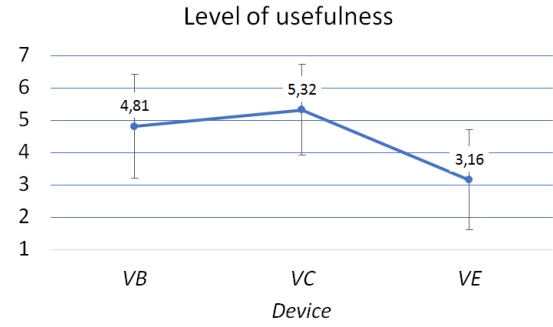
Figure 6.7: Level of usefulness across haptic devices (1:not useful - 7:very useful).
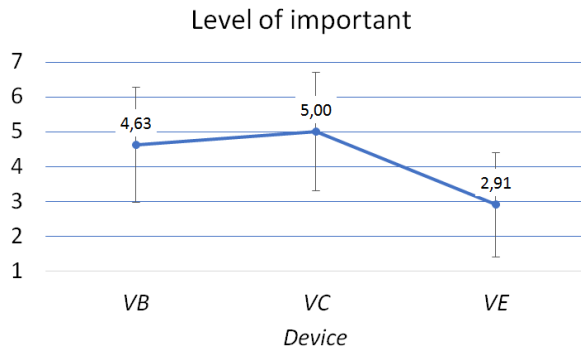
Level of important

Figure 6.8: Level of importance for decision making across haptic devices (1:not important - 7:very important).

Level of limitation
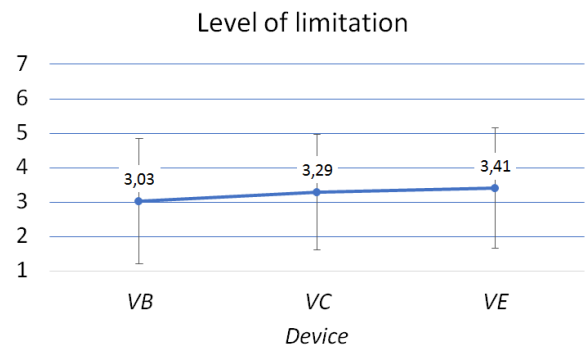
Figure 6.9: Level of Limitation across haptic devices (1:no limiting - 7:very limiting).

The negative aspects of the E-Vita are: very difficult to distinguish the normal and stuck patterns, requiring a lot of attention; the patterns were not so intuitive as the one provided by the Glove or Cylinder; uncomfortable during long periods of time the high friction surface, its movement and noise.

With this user study, it was possible to investigate the viability of adding haptic feedback to the exclusively visual interface, as an alternative sensory modality. Using the SAGAT technique, it was possible to assess and evaluate the Situation Awareness of 32 participants in four different setup conditions (*V, VC, VB, VE*). The obtained results revealed that two of the haptic devices (*VC* and *VB*) improved the participants SA regarding the traction state of RAPOSA-NG. The conducted user study also provided a better understanding of the participants' ability and difficulty to understand the situation of the robot
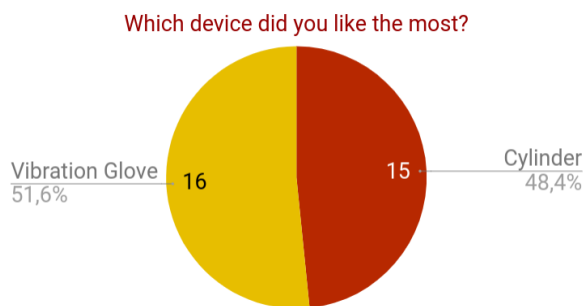
Figure 6.10: Results to the query *Which device did you like the most?*
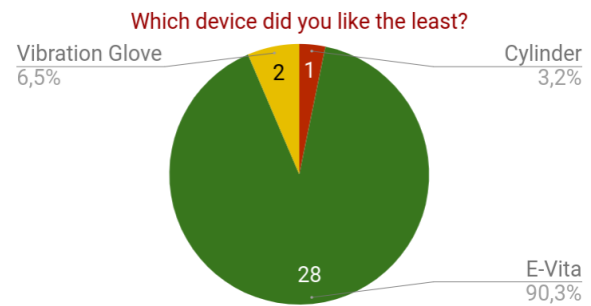
Figure 6.11: Results to the query *Which device did you like the least?*

in scenarios where this one loses traction. Additionally, it was acquired a greater understanding of the way that users interact with the developed haptic devices and possible future improvements.

During the design of the study, several decisions were taken to minimize the bias. Yet, one should keep in mind the study limitations when interpreting the obtained results. It was not possible to guarantee that, in each trial, all participants experienced the same quantity of "stuck" and "sliding" occurrences. Yet, in each trial, all participants experienced every traction states at least once. Due to time constraints, it was not possible to perform a statistical analysis of the results obtained from the NASA-TLX questionnaire. Future analysis of the task load during the different trials should be performed. Finally, the influence of the demographic characteristics of the participants in the results should be investigated. To that a greater number of participants would be necessary. In particular, the possible influence of the usage of the non-dominant hand.

7| Conclusions

7.1   Summary of Thesis Achievements

In this thesis it is presented a teleoperation architecture compromising a laser-based traction detector module and an haptic interface to convey the detected traction states to the human operator, fulfilling the first and second objectives of this thesis. The detected traction states are conveyed to the user through different types of tactile stimuli, provided by three haptic devices (E-Vita, Traction Cylinder, and Vibrotactile Glove). In particular, it is explored three types of tactile stimuli: (1) *friction*, using a rotating cylinder in contact with the operator's hand, (2) *vibration*, using a vibrotactile glove, and (3) *texture*, using a texture rendering device. The integration of this devices on the teleoperation system of RAPOSA-NG which included the physical construction of the above mentioned friction and vibration devices.

A user study was performed to answer two research questions: (*Q1*) "Does the addition of haptic feedback to the exclusively visual interface improves the user SA regarding the UGV traction state?" and (*Q2*) "Which of the presented haptic devices can better convey to the operator the traction state of RAPOSA-NG?", fulfilling the third objective of this thesis.

The experimental results allowed to answer the first research question. It was found an improvement when using the Vibrotactile Glove (*VB*) and the Traction Cylinder (*VC*) regarding comprehension of the UGV's traction state, with respect to the exclusively visual modality (*V*). The obtained results also show that participants are capable of comprehending the existence of an impediment to the UGV's movement. However, only when using the Traction Cylinder (VC) or the Vibrotactile Glove (VB) a statistically significant improvement was obtained in the comprehension of the UGV's traction state. These results address the previously presented issue of confusion and frustration during teleoperation due to loss of traction that this thesis tackles.

Regarding the second research question, no supported answer was obtained. Although it was found a statistically significant improvement of SA, regarding traction state, using the Traction Cylinder (*VC*) and the Vibrotactile Glove (*VB*) when comparing to E-Vita (*VE*), no statistically significant difference was found between *VC* and *VB*. The preferences of the participants, regarding the haptic devices, are in agreement with the obtained results from the SAGAT analysis. The participants preferred the use of Traction Cylinder and the Vibrotactile Glove over the use of E-Vita, but did not reveal preference between these two.

The experimental data also provided insights on how the integration of haptic feedback did not negatively influenced the SA provided by all components of the system. Hence, the tactile modality, regarding the traction state of the UGV, can be introduced to RAPOSA-NG system without deteriorating the SA provided by the remaining components of the interface. The newly integrated feedback modality will avoid overloading the visual sensory channel as more feedback is added to the current interface.

Finally, this work contributes to the HRI research community by presenting a simple but robust approach to a real-world problem of robotics, the lack of traction awareness during the teleoperation of a UGV.

7.2   Future Work

As possible Future Work, it is suggested the possibility of detecting the source of traction loss, additionally to the traction state. For example, when the robot is stuck, it would be interesting to know if there is an obstacle under the body of the robot or if its dimensions are preventing its movement. In the particular case of one the "shoulders" of the robot being stuck, it would be interesting to use the proprioceptive sense to provide information regarding which of them was causing the traction loss by actuating on the corresponding body side of the human operator. In order to accomplish such goal, it would be necessary to use more sensors that could provide such information. Additionally, the developed haptic devices would need redesigning to provide this new information. Based on the comments of the participants of the user study, this new feature would provide a better understanding of the robot situation.

From the conducted user study, it was observed that the design of E-Vita requires further improvement. A possible solution is to design a closed loop system where the user could both receive feedback regarding the traction state of the UGV and perform the control of the robot using E-vita. Therefore, future work includes the design of a new user study to compare the control of RAPOSA-NG, using E-Vita, with and without tactile feedback.

Bibliography

[1] Mica R. Endsley. Measurement of Situation Awareness in Dynamic Systems. *Human Factors: The Journal of the Human Factors and Ergonomics Society*, 37(1):65–84, mar 1995.

[2] Jean Scholtz, Jeff Young, Jill L. Drury, and Holly A. Yanco. Evaluation of human-robot interaction awareness in search and rescue. In *Robotics and Automation*, pages 2327–2332. IEEE, 2004.

[3] Rodrigo Ventura. Two Faces of Human–Robot Interaction: Field and Service Robots. In *Mechanisms and Machine Science*, volume 20, pages 177–192. Springer International, 2014.

[4] Rodrigo Ventura. Joint exercise of ist raposa-ng and gnr/gips - day 2. [Online] Available at: `https://www.youtube.com/watch?v=nFbvKlTBeBM` [Accessed: April - 2018].

[5] Filipe Jesus. Simultaneous Localization and Mapping using Vision for Search and Rescue Robots. Master's thesis, Instituto Superior Técnico, 2012.

[6] Henrique Martins, Ian Oakley, and Rodrigo Ventura. Design and evaluation of a head-mounted display for immersive 3D teleoperation of field robots. *Robotica*, 33(10):2166–2185, dec 2015.

[7] João Reis. Immersive Robot Teleoperation Using an Hybrid Virtual and Real Stereo Camera Attitude Control Master of Science in Electrical and Computer Engineering. Master's thesis, Instituto Superior Técnico, 2012.

[8] From EUROCONTROL | HP Repository. Situation awareness global assessment technique (sagat). [Online] Available at: `https://ext.eurocontrol.int/ehp/?q=node/1601` [Accessed: Oct- 2017].

[9] Mica R Endsley. Direct measurement of situation awareness: validity and use of SAGAT Development of Queries. *Situation Awareness Analysis and Measurement*, pages 1–21, 2000.

[10] Vincent Hayward, Oliver R Astley, Manuel Cruz-Hernandez, Danny Grant, and Gabriel Robles-De-La-Torre. Haptic interfaces and devices. *Sensor Review*, 24(1):16–29, mar 2004.

[11] Mohamad A. Eid and Hussein Al Osman. Affective Haptics: Current Research and Future Directions. *IEEE Access*, 4(c):26–40, 2016.

[12] Sandra Hirche and Martin Buss. Human-oriented control for haptic teleoperation. *Proceedings of the IEEE*, 100(3):623–647, mar 2012.

[13] Gijs Huisman. Social Touch Technology: A Survey of Haptic Technology for Social Touch. *IEEE Transactions on Haptics*, 10(3):391–408, jul 2017.

[14] Lynette A. Jones, Jacquelyn Kunkel, and Edgar Torres. Tactile vocabulary for tactile displays. *Proceedings - Second Joint EuroHaptics Conference and Symposium on Haptic Interfaces for Virtual Environment and Teleoperator Systems, World Haptics 2007*, pages 574–575, 2007.

[15] Lynette A. Jones and Hong Z. Tan. Application of psychophysical techniques to haptic research. *IEEE Transactions on Haptics*, 6(3):268–284, 2013.

[16] Jenna L. Graham, Steven G. Manuel, Matthew S. Johannes, and Robert S. Armiger. Development of a multi-modal haptic feedback system for dexterous robotic telemanipulation. In *2011 IEEE International Conference on Systems, Man, and Cybernetics*, pages 3548–3553. IEEE, oct 2011.

[17] Daniele Leonardis, Michele Barsotti, Claudio Loconsole, Massimiliano Solazzi, Marco Troncossi, Claudio Mazzotti, Vincenzo Parenti Castelli, Caterina Procopio, Giuseppe Lamola, Carmelo Chisari, Massimo Bergamasco, and Antonio Frisoli. An EMG-Controlled Robotic Hand Exoskeleton for Bilateral Rehabilitation. *IEEE Transactions on Haptics*, 8(2):140–151, apr 2015.

[18] Timothy R. Coles, Dwight Meglan, and Nigel W. John. The Role of Haptics in Medical Training Simulators: A Survey of the State of the Art. *IEEE Transactions on Haptics*, 4(1):51–66, jan 2011.

[19] Daniel Lobo, Mine Sarac, Mickeal Verschoor, Massimiliano Solazzi, Antonio Frisoli, and Miguel A. Otaduy. Proxy-based haptic rendering for underactuated haptic devices. In *2017 IEEE World Haptics Conference, WHC 2017*, pages 48–53. IEEE, jun 2017.

[20] Taku Nakamura, Shota Nemoto, Takumi Ito, and Akio Yamamoto. Substituted Force Feedback Using Palm Pressurization for a Handheld Controller. pages 197–199. Springer Nature Singapore Pte Ltd, 2018.

[21] Ali Israr and Ivan Poupyrev. Control space of apparent haptic motion. *2011 IEEE World Haptics Conference, WHC 2011*, (September):457–462, 2011.

[22] Jennifer Casper and R.R. Murphy. Human-robot interactions during the robot-assisted urban search and rescue response at the World Trade Center. *IEEE Transactions on Systems, Man, and Cybernetics, Part B (Cybernetics)*, 33(3):367–385, jun 2003.

[23] Dongseok Ryu, Chang-Soon Hwang, Sungchul Kang, Munsang Kim, and Jae-Bok Song. Wearable haptic-based multi-modal teleoperation of field mobile manipulator for explosive ordnance disposal. In *IEEE International Safety, Security and Rescue Rototics, Workshop, 2005.*, volume 2005, pages 98–103. IEEE, 2005.

[24] D.J. Cox. Mock-up of hazardous material handling tasks using a dual-arm robotic system. In *Proceedings of the 5th Biannual World Automation Congress*, pages 527–532, Orlando, FL, USA, 2002. IEEE.

[25] Boris Trouvain. Teleoperation of Unmanned Vehicles: The Human Factor. Technical report, 2006.

[26] Ben Horan, Doug Creighton, Saeid Nahavandi, and Mo Jamshidi. Bilateral haptic teleoperation of an articulated track mobile robot. *2007 IEEE International Conference on System of Systems Engineering, SOSE*, 2007.

[27] Alexander Owen-Hill, Ramviyas Parasuraman, and Manuel Ferre. Haptic teleoperation of mobile robots for augmentation of operator perception in environments with low-wireless signal. In *2013 IEEE International Symposium on Safety, Security, and Rescue Robotics, SSRR 2013*, pages 1–7. IEEE, oct 2013.

[28] Sangyoon Lee, Gaurav Sukhatme, Gerard Jounghyun Kim, and Chan-Mo Park. Haptic Teleoperation of a Mobile Robot: A User Study. *Presence: Teleoperators and Virtual Environments*, 14(3):345–365, jun 2005.

[29] José Corujeira, José Luís Silva, and Rodrigo Ventura. Effects of Haptic Feedback in Dual-Task Teleoperation of a Mobile Robot. In *Human-Computer Interaction – INTERACT*, pages 267–286. 2017.

[30] Michael Fielding, James Mullins, Ben Horan, and Saeid Nahavandi. OzBotTM -haptic augmentation of a teleoperated robotic platform for search and rescue operations. In *2007 IEEE International Workshop on Safety, Security and Rescue Robotics*, number September, pages 1–6. IEEE, sep 2007.

[31] John A Broderick, Dawn M Tilbury, and Ella M Atkins. Supervisory traction control for a slipping UGV. In *American Control Conference (ACC), 2013*, pages 4350–4355. IEEE, jun 2013.

[32] Eric Vezzoli, Thomas Sednaoui, Michel Amberg, Frédéric Giraud, and Betty Lemaire-Semail. Texture rendering strategies with a high fidelity, capacitive visual-haptic friction control device. *Lecture Notes in Computer Science (including subseries Lecture Notes in Artificial Intelligence and Lecture Notes in Bioinformatics)*, 9774:125–260, 2016.

[33] Weihua Li, Haibo Gao, Liang Ding, and Mahdi Tavakoli. Trilateral Predictor-Mediated Teleoperation of a Wheeled Mobile Robot With Slippage. *IEEE Robotics and Automation Letters*, 1(2):738–745, jul 2016.

[34] Ivan Dryanovski, William Morris, and Andrea Censi. *laser_scan_matcher*, ros wiki, package summary. [Online] Available at: `http://wiki.ros.org/laser_scan_matcher` [Accessed: Fev - 2017].

[35] M. Ferguson and A. Stambler. rosserial_arduino, ros wiki, package summary. [Online] Available at: `http://wiki.ros.org/rosserial_arduino` [Accessed: Mar- 2017].

[36] Motomama, itead wiki. [Online] Available at: `https://www.itead.cc/wiki/MotoMama` [Accessed: May - 2017].

[37] Eric Vezzoli, Thomas Sednaoui, Michel Amberg, Frédéric Giraud, and Betty Lemaire-Semail. Texture rendering strategies with a high fidelity, capacitive visual-haptic friction control device. *Lecture Notes in Computer Science (including subseries Lecture Notes in Artificial Intelligence and Lecture Notes in Bioinformatics)*, 9774:125–260, 2016.

[38] Eric Vezzoli, Thomas Sednaoui, Michel Amberg, Frédéric Giraud, and Betty Lemaire-Semail. Texture rendering strategies with a high fidelity, capacitive visual-haptic friction control device. *Lecture Notes in Computer Science (including subseries Lecture Notes in Artificial Intelligence and Lecture Notes in Bioinformatics)*, 9774:125–260, 2016.

[39] Claudio Pacchierotti, Stephen Sinclair, Massimiliano Solazzi, Antonio Frisoli, Vincent Hayward, and Domenico Prattichizzo. Wearable Haptic Systems for the Fingertip and the Hand: Taxonomy, Review, and Perspectives. *IEEE Transactions on Haptics*, XX(X):1–1, 2017.

[40] Susan J. Lederman and Lynette a. Jones. Tactile and Haptic Illusions. *IEEE Transactions on Haptics*, 4(4):273–294, 2011.

[41] Jaedong Lee, Youngsun Kim, and Gerard Jounghyun Kim. Rich Pinch: Perception of Object Movement with Tactile Illusion. *IEEE Transactions on Haptics*, 9(1):80–89, 2016.

[42] Neville Stanton, Alan Hedge, Karel Brookhuis, Eduardo Salas, and Hal Hendrick. *Handbook of Human Factors and Ergonomics Methods*. CRC Press LLC, 2005.

[43] Vincent Hayward and Oliver R Astley. Performance Measures for Haptic Interfaces. *Robotic Research: the 7th International Symposium*, pages 195–207, 1996.

[44] L A Jones, J Kunkel, and E Piateski. Vibrotactile pattern recognition on the arm and back. *Perception*, 38(1):52–68, 2009.

[45] Oliver S Schneider, Ali Israr, and Karon E Maclean. Tactile Animation by Direct Manipulation of Grid Displays. *Proceedings of the 28th Annual ACM Symposium on User Interface Software & Technology - UIST '15*, pages 21–30, 2015.

[46] Annie W Y Ng and Alan H S Chan. Finger Response Times to Visual, Auditory and Tactile Modality Stimuli. *Proceedings of the International MultiConference of Engineers and Computer Scientists*, II:1449–1454, 2012.

[47] Jennifer L. Burke, Matthew S. Prewett, Ashley A. Gray, Liuquin Yang, Frederick R. B. Stilson, Michael D. Coovert, Linda R. Elliot, and Elizabeth Redden. Comparing the effects of visual-auditory and visual-tactile feedback on user performance: A Meta-analysis. *Proceedings of the 8th international conference on Multimodal interfaces*, (January 2006):108, 2006.

[48] Meredith Ringel Morris, Jacob O. Wobbrock, and Andrew D. Wilson. Understanding users' preferences for surface gestures. *Proceedings of Graphics Interface 2010*, pages 261–268, 2010.

[49] Mica R Endsley. Situation awareness global assessment technique (SAGAT). *Aerospace and Electronics Conference, 1988. NAECON 1988., Proceedings of the IEEE 1988 National*, pages 789–795, 1988.

[50] Jaedong Lee, Youngsun Kim, and Gerard Jounghyun Kim. Rich Pinch: Perception of Object Movement with Tactile Illusion. *IEEE Transactions on Haptics*, 9(1):80–89, 2016.

[51] M.R. Endsley. Situation awareness global assessment technique (SAGAT). In *Proceedings of the IEEE 1988 National Aerospace and Electronics Conference*, pages 789–795. IEEE, 1988.

[52] Ben Horan, Doug Creighton, Saeid Nahavandi, and Mo Jamshidi. Bilateral haptic teleoperation of an articulated track mobile robot. *2007 IEEE International Conference on System of Systems Engineering, SOSE*, 2007.

[53] Hyoung Il Son, Antonio Franchi, Lewis L. Chuang, Junsuk Kim, Heinrich H. Bülthoff, and Paolo Robuffo Giordano. Human-centered design and evaluation of haptic cueing for teleoperation of multiple mobile robots. *IEEE Transactions on Cybernetics*, 43(2):597–609, apr 2013.

[54] Ildar Farkhatdinov, Jee Hwan Ryu, and Jinung An. A preliminary experimental study on haptic teleoperation of mobile robot with variable force feedback gain. In *2010 IEEE Haptics Symposium, HAPTICS 2010*, 2010.

[55] Alison Gibson, Andrea Webb, and Leia Stirling. Analysis of a wearable, multi-modal information presentation device for obstacle avoidance. *IEEE Aerospace Conference Proceedings*, 2017.

[56] Christopher D Wickens. Multiple resources and performance prediction. *Theoretical Issues in Ergonomics Science*, 3(2):159–177, jan 2002.

[57] Paul Nadrag, Lounis Temzi, Hichem Arioui, and Philippe Hoppenot. Remote control of an assistive robot using force feedback. In *2011 15th International Conference on Advanced Robotics (ICAR)*, pages 211–216. IEEE, jun 2011.

A| Instructions of the User Study

Haptic Feedback in Robot Teleoperation

Purpose

Common robot teleoperation interfaces are usually limited to the visual feedback provided by the robot cameras. In this study are provided three haptic devices to the participant. These devices will transmit information about the robot traction situation through the sense of touch as an addition the visual feedback from the cameras. The participant will use the developed haptic devices during several navigation challenges.

Description

In this study the robot and the participant will be separated. The robot will be placed in 4 different scenarios (simulated Search and Rescue environments) that should be explored by the participant. The participant will be sitting in front of computer receiving a visual feedback from the robot's camera. He/she will use a gamepad to control the robot in all 4 setup conditions and will receive traction feedback through the devices in 3 of the setup conditions. The participant can only use its left hand to teleoperate (use the gamepad) and when provided, should use its right hand to grasp the devices. During the study the participant will pass through a training session and through 4 different setup conditions:

- <u>Training Session</u> where the participant can get accustomed to teleoperation of the robot. In this session the participant can see both the robot and interface, to get familiar with the teleoperation controls and devices as well as how the robot reacts to the control inputs. The participant will also be shown the SAGAT queries and receive clear instructions and explanation on how to answer each one.

- <u>Experiment Session</u> where the participant will perform four navigation challenges each for each setup condition. During and after these four conditions the participant must answer a set of questions. Between each of the conditions the participant will rest.

- <u>Setup Combinations</u> (random order)

    - Visual Feedback

    - Visual Feedback + Haptic Feedback: Cylinder

    - Visual Feedback + Haptic Feedback: E-Vita

    - Visual Feedback + Haptic Feedback: Vibration Glove

- <u>Instructions</u> on the necessary steps will be provided to the participant during the study.

Procedure

1. **Demographic Questionnaire:**

- The user must answer to a demographic questionnaire where it's going be asked some basic information (age, gender, nationality and english level) and information about its everyday navigation.

- The collected information is for research purposes only and will not be used for any other purpose.

2. **Training Session:**

- Minimum Time of training: 15min

- In the training session the user will get familiar with teleoperation interface, the robot operation and the different devices. During this period the participant can see the robot and is free to control it while having access to the visual feedback from the cameras and the different devices.

- The participant will be shown the different possible traction situations of the robot and the implications to its movement.

- In the beginning of each navigation challenge the participant will be shown the normal function of the haptic devices (in the case that it is being used).

3. **Navigation Challenge:**

- Maximum time of the challenge: 8 minutes

- The experiment consists on executing 4 navigation challenges.

- In each navigation challenge the user should follow the red 'X', presented on the environment floor, until the STOP sign has been crossed.

- Each of these challenges will be randomly stopped and the participant should answer to a short list of questions regarding the robot and its environment, after which he/she should return to the navigation challenge.

- After crossing the STOP sign the user must answer a new list of questions regarding its overall perception and the used devices.

4. **Break Period:**

- Minimum time of Break: 2 minutes

- Between each challenge the user will have a resting period.

- This period will depend on the user, as he/she feels calm and ready to start.

5. **Final Evaluation:**

- Once all the 4 challenges are complete the user will be asked to give a very brief opinion regarding the used devices during the navigation challenges.

Observations for the User:

- During the experiment there will be some situations where the user will get stuck that might become frustrating, in these moments the user should keep in mind:

Try not to give up

The navigation challenge is limited to 8 minutes

The challenge will be completed with Success in both situations:

- The user teleoperates the robot during the 8 minutes
- The user crosses the STOP sign

B| Informed Consent

- I understood what this study consisted of. I had the opportunity to ask questions if necessary and to get answers to them.

- I understood that participation in this study was voluntary and that I can withdraw at any time without giving an explanation. If this happens, no penalty will occur and my data will be removed and destroyed.

- During this study audio and video recordings were carried out with the exclusive purpose of scientific research.

- I authorize the treatment of data collected under this project for the purpose of analysis, research and dissemination of results in magazines or conferences in the area of renown, by the researchers of the project.

- I understood that the data collected in this study will be used as previously mentioned.

- As described above, I authorize my participation in the study and accept the conditions thereof.

I accept the terms of this consent,
Name .... Date ....
Signature ....

....
For more information, please contact:
Rute Luz (Responsible for the Study)
      rute.luz@tecnico.ulisboa.pt
Professor Rodrigo Ventura
      rodrigo.ventura@isr.tecnico.ulisboa.pt
Instituto Técnico de Lisboa, Universidade de Lisboa & ISR
Professor José Luís Silva
      jose.l.silva@m-iti.org
ISCTE – Instituto Universitário de Lisboa

ONE COPY OF THE CONSENT IS FOR THE PARTICIPANT AND ONE FOR THE INVESTIGATORS.

C| Demographic Questionnaire

1. Gender

   - Female
   - Male
   - Others
   - Rather not say

2. Age

   - ....

3. Nationality

   - ....

4. English Level

   - English Basic User
   - English Independent User
   - Proficient English User
   - Mother Tongue

5. Dominant Hand

   - Right
   - Left

6. How often do you travel new (unknown) routes?

   - Never
   - Less than once a year
   - Once or twice a year
   - 3-5 times a year
   - Bi-monthly
   - Monthly
   - Weekly
   - Daily

7. How often do you use teleoperation (drones, teleoperated cars, etc.)?

   - Never
   - Less than once a year
   - Once or twice a year

- 3-5 times a year
- Bi-monthly
- Monthly
- Weekly
- Daily

8. How often do you play video games?

- Never
- Less than once a year
- Once or twice a year
- 3-5 times a year
- Bi-monthly
- Monthly
- Weekly
- Daily

D| SAGAT Questionnaire

Notes to the participants

- All the questions are referring to the immediate moment before the interruption

- Concepts descriptions are available at the end of the questionnaire and are marked in the questions with Greek letters.

Level 1 SA: Perception

1) What is the current Roll Value (Fig.D.1) of the robot (δ)?

- 1: [-90º ; -60º [
- 2: [-60º ; -30º [
- 3: [-30º ; 0º [
- 4: [0º ; 30º [
- 5: [30º ; 60º [
- 6: [60º ; 90º]
- Don't know
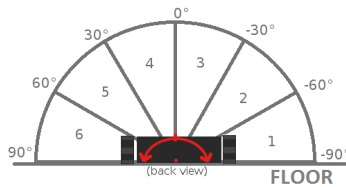
Figure D.1: Roll value.

2) What is the current Pitch Value (Fig.D.2) of the robot (δ)?

- 1: [-90º ; -60º [
- 2: [-60º ; -30º [
- 3: [-30º ; 0º [
- 4: [0º ; 30º [
- 5: [30º ; 60º [
- 6: [60º ; 90º]
- Don't know

3) What is the current Arm Position (Fig.D.3) of the robot (δ)?

- 1: [-90º ; -60º [
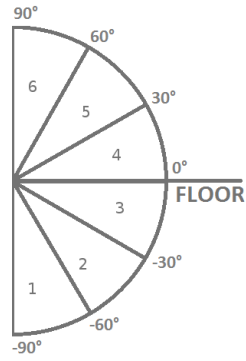
Figure D.2: Pitch value.

- 2: [-60º ; -30º [
- 3: [-30º ; 0º [
- 4: [0º ; 30º [
- 5: [30º ; 60º [
- 6: [60º ; 90º]
- Don't know
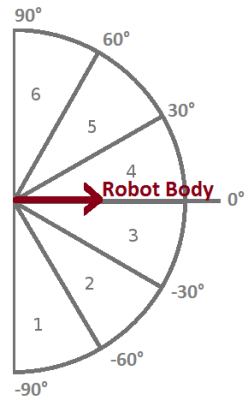
Figure D.3: Arm position value.

4) What type of movement can you identify from the image of the camera? (*V*: Visual)

- 1: No movement
- 2: Back or forward motion
- 3: Rotation
- 4: Both 2 and 3
- 5: Don't know

4) What is the current pattern you can identify from the haptic device? (*VC*: Visual & Cylinder)

- No rotation
- Constant rotation
- Back and forward
- Don't know

4) What is the current pattern you can identify from the haptic device? (*VB*: Visual & Vibrotactile Glove)

- No vibration
- Start/Stop vibration
- Continuous vibration
- Don't know

4) What is the current pattern you can identify from the haptic device? (*VE*: Visual & E-Vita)

- Rough texture
- Smooth texture
- Both rough and smooth textures
- Don't know

5) Is there any obstacle (e.g. blocks, boxes) in sight?

- Yes
- No
- Don't know

6) Is the red 'X' (navigation indicator) in sight?

- Yes
- No
- Don't know

Level 2 SA: Comprehension

7) What is the state of the robot (β)?

- Stopped
- Moving
- Stuck
- Sliding
- Don't know

8) Is there currently anything that might be preventing the robot desired movement?

- Yes
- No
- Don't know

9) What is the current traction (α) situation of the robot?

- With Traction
- Without Traction
- Don't know

10) Is the robot moving accordingly to the tracks/wheels movement?

- Yes
- No
- Don't know

11) Are the dimensions of the robot currently affecting its movement?

- Yes
- No
- Don't know

Level 3 SA: Projection

12) If the robot moves exclusively forward during the next 15 seconds will it at any moment lose traction (α)?

- Yes
- No
- Don't know

13) If the robot maintain exclusively rotational movement during the next 15 seconds will it at any moment lose traction (α)?

- Yes
- No
- Don't know

14) Will the current state of the robot (β) constrain its movement in the next 15 seconds?

- Yes
- No
- Don't know

15) Can maintaining the current attitude (δ) of the robot (roll and pitch) lead to a dangerous or unstable situation (γ)?

- Yes
- No
- Don't know

16) Will you reach a red 'X' (navigation indicator) in the next 15 seconds?

- Yes
- No
- Don't know

Concepts

(α) **Traction**: the adhesive friction between the wheels and the floor.

(β) **States of the Robot:**

- *Stopped*: both the robot and the tracks/wheels don't have any movement.

- *Moving*: movement of the wheels correspond to the robot movement (normal operation).

- *Stuck*: movement of the wheels but the robot is unable to move (e.g. object under robot preventing its movement making it stuck).

- *Sliding*: robot moving when the wheels are stopped or robot moving in a difference direction of the wheels movement (e.g. sliding during climbs).

(λ) **Dangerous or Unstable Situation**: situation that might lead the robot to roll over or permanently damage it.

(δ) **Robot's Attitude (Pitch and Roll) and Arm Position (Figure D.4).**
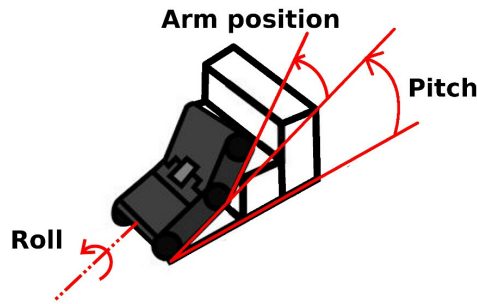
Figure D.4: Attitude (roll and pitch) and arm position of the robot.

E| Post-Trial Qualitative Questionnaire

E.1 Overall Perception of the Traction States

1) At any moment did you noticed the robot was Stuck?

- Yes
- No

2) How difficult was to understand that the robot was stuck?

- Scale: [1 - Very easy, 7 - Very Difficult]

3) How difficult was to overcome the stuck state of the robot?

- Scale: [1 - Very easy, 7 - Very Difficult]

4) At any moment did you noticed the robot Sliding?

- Yes
- No

2) How difficult was to understand that the robot was sliding?

- Scale: [1 - Very easy, 7 - Very Difficult]

3) How difficult was to overcome the sliding state of the robot?

- Scale: [1 - Very easy, 7 - Very Difficult]

E.2 Metrics of the Haptic Devices

1) Level of discomfort during the device operation?

- Scale: [1 - No Discomfort, 7 - Very Discomforting]

2) Level of fatigue during the device operation?

- Scale: [1 - No Fatigue, 7 - Very Fatiguing]

3) Level of limitation of motion/control due to the presence of the device?

- Scale: [1 - Not Limiting, 7 - Very Limiting]

4) How many patterns/sensations did you identified/felt during this task?

- Scale: [1, 7]

5) How clear were the different sensations given by the device?

- Scale: [1 - Not Clear, 7 - Very Clear]

6) How useful was the device for the robot teleoperation?

  - Scale: [1 - Not Useful, 7 - Very Useful]

7) How important was the device for your decision making?

  - Scale: [1 - Not Important, 7 - Very Important]

E.3 Preference on the Devices

1. Do you think adding haptic/tactile feedback was useful to the teleoperation of the robot, comparing to only visual feedback?

  - Yes
  - No

2. Which device did you prefer?

  - Traction Cylinder
  - Vibrotactile Glove
  - E-Vita

3. Can you justify your previous choice?

  - ....

4. Which device did you like the least?

  - Traction Cylinder
  - Vibrotactile Glove
  - E-Vita

5. Can you justify your previous choice?

  - ....

6. What are the positive aspects of the Device:

  - Traction Cylinder
    - ....
  - Vibrotactile Glove
    - ....
  - E-Vita
    - ....

7. What are the negative aspects of the Device:

  - Traction Cylinder
    - ....
  - Vibrotactile Glove
    - ....
  - E-Vita
    - ....

F| SAGAT Collected Data

The obtained SAGAT Data is summarized in Tables F.3, F.4, F.5 and F.6, concerning the Trials Conditions Exclusively Visual (*V*), Visual & Traction Cylinder (*VC*), Visual & Vibrotactile Glove (*VB*) and Visual & E-Vita (*VE*) respectively. Participants' answers to the SAGAT queries were scored as either correct (1) or incorrect (0). Queries asked the participant but not answered were considered incorrect (0). Queries not asked during a given stop were not evaluated (-). This classification was performed by comparing the participants' answers with the actual status, obtained from the recorded data and expert judgment.

For each participant it was evaluated its answers of all queries in all Trial Conditions as shown in Table F.1. This information was then summarized in a Table as shown in Table F.2 from each it was obtained a weighted average of *% SAGAT Correct Answers*.

Condition I	Stop 1	Stop 2	*Total answers*	*Average (%)*
Query 1	1	0	2	0.5
Query 2	1	-	1	1
Etc.	...	...	...	...

Table F.1: Example Data from a Participant in Condition I.

Condition I	Participant 1	Participant 2	Participant *n*	*Weighted Average (%)*
Query 1	0.5	0	...	...
	2	2	...	-
Query 2	1	1	...	...
	1	2	...	-
Etc.	*Average (%)*	*Average (%)*	...	...
	Total answers	*Total answers*	...	...

Table F.2: Query summed across participants in Condition I.

The data obtained in the user study is represented in Tables F.3, F.4, F.5 and F.6, where the Queries correspond to ones presented in Annex D. For each Query it is presented the *Average (%)* in the top row and the *Total answers* in the bottom row for each Trial Condition across participants.

Trial V	1	2	3	4	5	6	7	8	9	10	11	12	13	14	15	16	17	18	19	20	21	22	23	24	25	26	27	28	29	30	31	32
Query 1	0,5	0,5	0,5	1	0	0	1	0	0	0	1	1	1	1	0,5	1	0,5	1	1	1	1	1	0	1	1	1	1	1	1	1	1	0
Query 2	1	1	1	0	0,5	1	0	1	0	0	1	1	1	1	1	1	1	1	1	1	1	1	0	1	1	1	1	1	1	1	1	1
Query 3	0	0	1	1	1	1	0	1	1	1	0	1	0	1	1	1	1	2	1	1	0	0,5	0	0	0	0	0	0,5	0	1	1	0
Query 4	1	2	2	2	1	0	1	2	1	1	0	2	0,5	1	1	2	2	2	1	2	1	1	1	1	1	0,5	1	1	1	1	1	1
Query 5	0	0	0	0	1	1	1	0	1	0,5	0	0,5	1	1	0	1	0	0,5	1	0,5	1	0	0	0,5	0,5	0,5	0	0,5	1	1	0,5	0
Query 6	0,5	2	1	1	1	1	1	1	1	1	1	1	1	1	0,5	1	1	2	2	1	1	1	1	1	1	1	1	1	1	1	1	1
Query 7	0	0,5	1	0,5	0,5	0	1	2	1	1	0	0	1	1	-	1	0,5	2	0,5	0	1	0,5	0,5	1	0,5	0,5	0	1	1	1	0,5	0
Query 8	1	1	1	1	1	2	2	2	2	2	1	1	1	1	2	2	1	1	0	1	1	1	1	1	2	1	2	1	1	2	1	1
Query 9	1	1	0	1	0,5	0	1	1	1	1	1	1	1	0	1	2	0	0	0	2	1	1	0	1	0,5	1	1	1	1	0,5	1	1
Query 10	2	1	1	1	0	0	1	1	0	1	0	0	1	0	1	1	-	1	2	0	1	0	0	0	0	1	2	1	1	2	1	1
Query 11	1	1	1	0	0	0	1	0	0	0	0,5	0,5	1	1	1	-	1	1	1	2	0	2	2	1	0	0	1	1	0,5	1	1	0,5
Query 12	0	1	0,5	0	1	0	1	1	1	1	1	1	1	1	-	0	-	0	0	1	1	0	2	1	0	1	2	1	1	1	1	1
Query 13	0	1	1	0	0	1	1	1	2	1	1	1	1	1	0	0,5	0	1	1	2	1	1	1	1	0,5	1	1	0,5	1	1	1	1
Query 14	0	1	1	2	0	0	0	0	1	1	0	0	0	0	1	1	0	0	0	1	0,5	1	1	0	0	0	1	1	1	1	1	0
Query 15	0	1	2	-	0,5	1	1	1	1	1	2	1	1	1	1	0	-	0,5	0	0	1	1	0	1	0	0,5	0	1	1	0	0	2
Query 16	0,5	2	1	0	0	0	1	1	1	1	1	1	1	2	-	1	1	1	2	1	1	1	1	1	1	1	1	1	0,5	1	1	0

Table F.3: SAGAT Collected Data from the Exclusively Visual Trial (V).

90

Table F.4: SAGAT Collected Data from the Visual & Traction Cylinder Trial (*VC*).

Trial VC	1	2	3	4	5	6	7	8	9	10	11	12	13	14	15	16	17	18	19	20	21	22	23	24	25	26	27	28	29	30	31	32
Query 1	0	1	1	1	1	1	1	1	1	0	0	1	1	0,5	1	1	1	1	0	1	1	1	0	1	1	0,5	1	0	1	1	1	1
	1	1	2	2	2	1	1	2	2	1	1	2	1	2	2	1	1	1	1	1	2	2	1	1	1	2	1	1	1	1	1	1
Query 2	0	0	1	1	0,5	1	1	0	1	0,5	0	1	1	1	1	0	1	1	0,5	1	0,5	1	0	1	1	0	1	0	1	0	1	1
	2	1	1	1	2	1	2	1	2	2	2	1	1	1	1	1	1	1	2	1	2	1	1	1	1	1	1	1	2	1	1	1
Query 3	0	-	0,5	0	0,5	1	1	0	0	0	0	0	0	1	1	1	1	0	0	0	1	1	1	1	1	0,5	1	0,5	1	0	1	0
	2	-	2	1	2	1	1	1	1	1	2	2	2	1	2	1	2	1	2	2	1	1	1	1	1	2	1	2	1	1	2	2
Query 4	1	1	1	1	1	1	0	0	0	1	0	0	-	0	1	1	0	1	1	0	0	1	1	1	1	1	1	0,5	1	1	0,5	0
	1	1	1	1	2	1	1	1	1	1	1	1	-	2	1	2	1	1	1	1	1	1	2	2	2	1	1	2	2	2	2	1
Query 5	0	0	0	1	-	1	0	0	1	0	0	0	1	1	1	0,5	1	0	-	1	1	1	0	1	0,5	1	0,5	1	1	1	0	1
	1	1	1	2	-	2	2	2	1	2	1	1	2	1	1	2	1	2	-	2	1	2	1	2	2	1	2	1	1	2	1	1
Query 6	1	-	1	1	-	0,5	1	1	1	1	1	0	1	1	1	1	1	0	-	1	1	1	0,5	1	1	0	1	1	1	1	1	0,5
	2	-	1	1	-	2	1	1	1	1	1	1	2	1	1	1	2	2	-	1	1	2	2	1	1	2	2	1	1	1	1	2
Query 7	0,5	1	1	1	0,5	0	0	-	1	0	1	1	0	1	1	1	1	0	1	0	1	1	0	1	1	0	0	1	1	0	0	1
	2	1	1	1	2	1	2	-	1	1	1	1	1	1	1	1	1	2	1	1	1	1	1	1	1	1	1	1	1	1	1	1
Query 8	0	0	0	0	0,5	1	1	0	1	0,5	0	1	0,5	1	1	0	1	0	1	0	1	1	0,5	0	1	1	0,5	1	0	1	1	0
	1	1	2	1	2	1	1	2	1	2	1	1	2	2	1	1	1	1	1	1	1	1	2	1	1	1	2	1	1	1	1	1
Query 9	1	1	1	0,5	-	0	1	0	0	1	1	0,5	1	1	0	1	1	1	0	0	0,5	1	-	1	1	0	1	1	0,5	0	1	1
	1	1	1	2	-	2	1	2	1	1	1	2	1	1	1	1	2	1	1	2	2	2	-	1	2	1	1	1	2	1	1	1
Query 10	1	1	0	1	1	0	0	0	1	1	0	1	1	0	0,5	0,5	0	0	0	0	1	1	0	1	1	0,5	1	1	1	1	0,5	0
	1	-	1	1	2	1	1	2	1	1	2	1	1	1	2	2	1	1	2	1	1	1	1	2	1	2	1	2	1	2	2	1
Query 11	1	-	0	1	-	1	1	1	0,5	1	0	0	1	1	1	0	0	0	0	0	1	0	1	1	1	0	0	0	0	1	1	0,5
	1	-	1	1	-	1	1	2	2	1	1	1	1	1	1	2	1	1	1	1	1	1	2	1	2	1	2	1	1	1	1	2
Query 12	1	-	1	1	-	1	1	0	0	1	0	0	1	1	1	1	0	0	0	1	1	0	1	0	1	1	1	1	0	0	1	1
	1	-	1	1	-	2	2	2	1	2	1	1	1	1	1	1	1	1	2	1	1	1	1	1	1	2	2	1	1	1	1	1
Query 13	1	1	1	0,5	-	0	1	1	1	1	1	0	0	0,5	1	0	0	1	1	0	0	1	1	0	1	0,5	1	0	0	0	1	1
	1	1	1	2	-	2	1	2	1	2	1	1	1	2	1	2	1	2	1	1	1	1	1	1	1	2	1	1	1	1	1	1
Query 14	0,5	-	1	1	0	1	0	1	0,5	0	0	0	1	0	1	1	0	0	1	1	1	0	0,5	1	1	1	0	1	0	0	1	0,5
	2	-	1	1	2	2	1	2	2	1	2	2	2	1	2	1	2	1	1	2	1	1	2	1	2	1	1	1	1	1	1	2
Query 15	0	0	0	0,5	0,5	-	0	-	0	0	0	0	0	1	1	0,5	0	1	1	0	1	1	0	0	1	1	1	0	1	1	1	1
	1	1	2	2	2	-	1	-	1	1	1	1	1	1	1	2	1	1	1	1	1	1	1	1	1	1	1	1	2	1	1	1
Query 16	0	-	1	1	0	-	0	-	1	1	1	1	1	1	0	0	0	1	1	0	1	1	0	1	1	0	1	0	1	1	1	0
	1	-	1	1	2	-	1	-	1	1	1	1	1	1	1	1	1	1	1	1	1	1	1	2	1	1	1	1	2	1	2	1

Trial emphVB	1	2	3	4	5	6	7	8	9	10	11	12	13	14	15	16	17	18	19	20	21	22	23	24	25	26	27	28	29	30	31	32
Query 1	0,5	0	0,5	1	1	1	1	1	1	1	1	1	1	1	1	0,5	1	0,5	1	1	1	1	1	1	1	1	1	1	1	1	1	1
	2	1	2	2	1	1	1	2	2	1	1	1	1	1	1	1	2	2	1	2	1	1	2	1	1	1	2	1	1	2	2	1
Query 2	0	1	1	1	1	0	1	1	1	0	1	1	1	1	1	1	0	1	0	1	1	0	1	0,5	1	1	1	1	1	1	1	1
	1	1	2	2	1	2	2	1	2	1	1	1	1	1	1	1	1	1	1	1	1	2	1	2	2	1	1	1	1	1	1	2
Query 3	1	0,5	0	0,5	0,5	1	1	0,5	0	1	1	0	1	1	2	0,5	1	1	0	1	1	1	0	1	1	1	1	0,5	0	0,5	1	1
	1	2	2	2	2	1	1	2	1	1	1	1	1	1	2	2	1	1	1	1	1	1	2	1	1	1	1	2	1	2	1	1
Query 4	1	1	1	1	1	1	1	1	1	1	1	1	1	1	1	1	1	0,5	1	1	1	1	1	1	0,5	1	1	1	1	1	0	1
	2	2	2	2	2	2	2	2	1	1	1	2	2	2	2	1	2	1	1	1	1	1	1	1	1	2	1	2	1	1	2	1
Query 5	0	0	0	0	0	0,5	1	0	0	0	0	0,5	1	0,5	0	0	0	1	0,5	1	0,5	1	0	0	0,5	0	1	0,5	0	0,5	0	0
	1	1	1	1	1	1	1	1	1	1	1	1	1	1	1	1	1	1	1	1	2	1	1	1	1	1	1	1	1	1	1	2
Query 6	2	1	1	0	0	1	1	1	1	0	1	1	1	0,5	1	0	0	0,5	0	1	0	0	0	0	1	0,5	1	0,5	1	1	0	0
	2	2	1	2	2	2	2	2	2	2	1	2	2	1	1	2	2	2	2	2	2	2	2	2	2	2	1	2	1	2	2	2
Query 7	1	1	1	2	1	1	1	1	0,5	0,5	1	0,5	1	1	0,5	0,5	1	1	1	1	1	1	1	0,5	1	1	0,5	1	1	1	1	1
	1	1	2	2	2	2	2	1	2	2	1	2	1	1	2	2	2	1	1	1	1	1	2	2	2	1	2	2	1	1	1	1
Query 8	1	1	0	0,5	0	0,5	1	1	0,5	0	1	0	1	0,5	1	1	1	0,5	0	1	1	1	1	1	1	1	0,5	0,5	1	1	1	1
	1	1	2	1	2	1	2	1	1	1	1	1	1	2	1	1	1	1	1	1	1	1	1	1	1	1	1	1	1	1	1	1
Query 9	0,5	1	1	1	1	1	1	0	0,5	0	1	1	1	0	1	1	1	0	0	1	0,5	1	1	0,5	1	1	0,5	0,5	1	0,5	0,5	1
	2	1	1	1	1	1	1	2	2	1	1	1	1	1	2	1	1	1	1	2	1	1	2	1	1	1	2	2	1	1	1	1
Query 10	1	1	1	1	0	0	0	1	1	0	1	0	1	0	1	1	1	1	0	0,5	0	1	0	0,5	1	1	1	1	1	1	1	1
	2	2	1	1	1	1	1	1	1	1	1	1	1	1	1	1	1	2	1	1	2	1	2	2	1	1	1	1	1	1	1	1
Query 11	1	1	0	1	0	0	0	0	0	1	0	1	1	1	1	1	1	1	1	1	1	1	1	1	1	1	1	1	1	1	1	1
	1	1	1	1	1	1	1	1	1	1	1	2	1	1	1	1	1	1	1	1	2	1	1	1	1	1	1	1	1	1	1	2
Query 12	0	0	1	1	1	1	0,5	1	0	0	0	1	1	1	1	1	0,5	0	0	1	0	0	0	1	1	1	0,5	1	0	0	0	1
	1	1	1	1	2	1	2	1	2	1	1	1	1	1	1	1	2	2	2	1	1	1	2	1	1	1	2	1	1	1	1	1
Query 13	0,5	1	1	2	1	1	1	1	1	1	-	1	0,5	1	0	0	1	1	1	1	1	0	1	0,5	1	1	1	1	0,5	1	0	1
	2	1	1	2	1	1	1	1	1	1	-	1	2	1	1	1	1	1	1	1	1	1	1	1	1	1	1	2	2	2	2	2
Query 14	0	0	1	0,5	1	0	1	1	1	1	1	1	0	0	1	1	1	1	1	1	1	1	1	1	1	1	0	1	0	0	0	0
	1	1	1	2	1	1	1	1	1	1	-	1	1	1	1	1	1	1	1	1	2	1	2	1	1	1	2	1	1	1	1	1
Query 15	0	1	0	0	0	1	1	1	1	0,5	0	1	1	0,5	0	0	0	1	1	1	1	1	1	1	1	1	1	0,5	0,5	0	0,5	0
	1	1	2	2	1	1	1	2	1	2	1	1	2	2	1	1	2	1	1	1	1	1	1	1	1	1	1	2	2	2	2	1
Query 16	0	0	1	1	1	1	1	1	0,5	1	1	1	1	1	1	1	1	1	1	1	1	1	1	1	1	1	1	1	1	1	1	1
	1	2	1	1	1	1	1	2	2	1	1	1	1	1	2	1	1	1	2	2	1	2	1	1	1	1	1	1	1	1	1	1

Table F.5: SAGAT Collected Data from the Visual & Vibrotactile Glove Trial (VB).

Table F.6: SAGAT Collected Data from the Visual & E-Vita Trial (*VE*).

Trial *VE*	1	2	3	4	5	6	7	8	9	10	11	12	13	14	15	16	17	18	19	20	21	22	23	24	25	26	27	28	29	30	31	32
Query 1	0	1	0	0	1	1	1	1	1	1	1	1	1	1	1	1	1	1	0	1	0	1	1	1	0,5	1	1	0,5	1	-	1	0
	1	2	1	1	1	1	1	1	1	1	1	1	1	2	1	1	1	1	1	1	1	1	1	1	2	2	2	2	1	-	1	1
Query 2	0	1	1	1	1	1	1	0	1	0	0,5	1	1	1	1	1	1	1	1	1	1	0,5	1	1	1	1	1	1	1	1	1	0
	1	1	1	1	1	1	1	1	1	1	2	1	1	1	1	2	1	2	1	1	1	2	1	1	1	1	2	1	1	1	2	1
Query 3	0	0	0	0	0	1	0	1	0	0	0	0	0,5	0	1	1	0	1	0	1	1	1	1	1	1	1	1	0	0	-	1	0,5
	1	1	2	1	2	1	1	1	2	2	2	1	2	1	1	1	1	2	1	1	1	1	2	2	1	1	1	1	2	-	1	2
Query 4	0,5	0,5	0,5	0	1	1	1	1	1	1	1	0	1	1	1	1	1	1	0,5	1	1	1	1	1	1	1	0	1	0	1	1	0
	2	2	2	2	2	2	2	2	1	1	1	1	1	1	2	2	2	1	2	1	2	1	1	2	2	2	1	2	1	1	1	1
Query 5	0	1	0	1	0	0	1	0	0,5	1	1	-	0,5	0	1	1	1	0,5	1	1	1	0,5	0	0,5	0	1	1	1	0,5	1	0	0,5
	1	1	1	1	1	1	1	1	2	2	1	-	2	1	2	1	2	2	2	2	1	2	1	2	1	1	1	1	2	1	2	2
Query 6	1	0	1	0,5	0	0,5	1	0,5	0	0	1	-	0	0,5	0	0	1	-	0	1	0,5	0	0	0,5	0	0	1	0	1	1	1	1
	2	1	1	2	1	2	1	2	1	1	2	-	1	2	1	1	1	-	1	2	2	1	2	2	1	1	1	1	1	1	1	1
Query 7	1	0	1	0	0	1	1	0	0	1	1	0	0,5	1	0,5	1	1	1	0	1	0	1	1	1	1	1	1	0	1	-	1	1
	1	1	1	1	1	1	1	1	1	1	1	1	2	1	2	1	2	1	1	1	1	1	1	2	1	1	1	1	1	-	1	2
Query 8	0	1	0	1	1	0,5	1	1	1	0	1	-	1	1	0	1	0	1	1	1	1	1	0,5	1	1	1	0	1	1	1	0	0
	1	2	1	1	1	2	1	1	1	1	1	-	1	2	1	2	1	1	1	1	2	1	2	1	1	1	2	1	1	1	1	1
Query 9	1	0	0	1	1	1	1	0,5	0	0	0,5	1	1	0	0	0	1	0	1	1	1	0	1	1	1	0,5	1	0,5	0,5	-	1	0
	1	1	1	1	1	1	1	2	1	1	2	1	1	1	1	1	1	1	1	1	1	2	1	1	2	2	1	2	2	-	1	1
Query 10	0	0	1	1	0	1	0	1	1	0	0	-	0	0	0	0	1	0	0	1	0	0	0	0	1	1	1	0	0	-	0	1
	2	1	1	1	1	1	1	1	1	1	1	-	1	1	1	1	1	1	2	1	1	2	1	1	2	1	1	1	1	-	2	1
Query 11	0	0	1	0,5	0	0	0	0	0,5	1	1	1	1	1	1	0	1	0	0	1	0	0	0	0	1	1	1	0	0	1	1	1
	1	1	2	2	1	1	1	1	2	2	1	1	1	1	1	1	1	1	2	2	1	1	2	1	1	1	1	1	1	1	1	1
Query 12	1	1	1	0,5	1	1	1	1	0,5	1	0,5	1	0	1	1	0	1	0	0,5	1	1	0	0	1	0	0,5	1	0	0	1	0	0
	1	1	2	2	1	1	1	2	2	2	2	1	1	1	1	1	1	2	2	1	1	2	1	1	1	2	1	2	1	1	1	2
Query 13	1	1	1	1	1	1	1	0	0	1	1	1	1	0,5	1	0	0	1	0	0	1	1	1	1	0	0	0	1	0,5	1	0	0
	1	1	1	2	1	2	1	2	1	1	1	1	1	2	2	1	1	1	1	1	2	1	1	2	1	1	1	1	2	1	1	1
Query 14	1	1	0	1	0	1	1	-	1	1	0	1	0	0	0	0	0	0	1	0	0	0	0	0	0	0	0	0	1	1	0	1
	1	1	1	2	1	2	2	-	1	1	1	1	1	1	1	1	1	1	1	1	1	1	1	1	1	1	1	1	1	1	1	1
Query 15	1	0,5	0	1	1	1	1	0,5	0	0,5	1	-	1	1	1	0	1	1	1	1	1	1	1	1	0,5	0	1	0	1	0	1	1
	1	2	1	1	2	2	1	2	1	2	1	-	2	1	1	2	1	1	1	2	1	1	1	1	2	1	2	1	1	1	2	1
Query 16	0	0	1	0	0	0	1	-	1	0	1	1	1	1	0	1	1	1	0	1	1	1	1	0	1	0	1	0	1	-	1	1
	2	1	1	1	1	1	1	-	2	1	1	1	1	1	1	1	1	1	1	1	1	1	1	1	1	1	1	1	1	-	1	1

G| Qualitative Questionnaires Collected Data

G.1 Qualitative Post-Trial Questionnaire

After each trial, the participants answered the post-trial questionnaire presented in Annex E.1 to assess their overall perception of the Traction States. The Collected Data is summarized in Table G.1 where the mentioned Queries are listed below:

Query 1 At any moment did you noticed the robot was Stuck?

Query 2 How difficult was to understand that the robot was stuck?

Query 3 How difficult was to overcome the stuck state of the robot?

Query 4 At any moment did you noticed the robot Sliding?

Query 5 How difficult was to understand that the robot was sliding?

Query 6 How difficult was to overcome the sliding state of the robot?

G.2 Qualitative Devices' Metrics

After each trial, the participants answered the post-trial questionnaire presented in Annex E.2 to qualitative evaluate some metrics of the Haptic Devices. The Collected Data is summarized in Table G.2 where the mentioned Queries are listed below:

Query 1 Level of discomfort during the device operation?

Query 2 Level of fatigue during the device operation?

Query 3 Level of limitation of motion/control due to the presence of the device?

Query 4 How many patterns/sensations did you identified/felt during this task?

Query 5 How clear were the different sensations given by the device?

Query 6 How useful was the device for the robot teleoperation?

Query 7 How important was the device for your decision making?

Table G.1: Qualitative Post-Trial Questionnaire: Collected Data from all Trials.

Participant	1	2	3	4	5	6	7	8	9	10	11	12	13	14	15	16	17	18	19	20	21	22	23	24	25	26	27	28	29	30	31	32
V Query 1	Yes	Yes	Yes	Yes	Yes	Yes	Yes	Yes	Yes	No	Yes	Yes	Yes	Yes	Yes	Yes	No	-	No	Yes	No	No	Yes	Yes	Yes	No	No	No	No	Yes	Yes	No
V Query 2	3	2	5	6	3	2	3	4	5	-	4	6	3	5	3	7	3	-	6	3	3	3	6	4	1	1	6	2	3	1	3	1
V Query 3	7	6	5	6	6	5	5	6	5	-	4	5	5	4	4	7	5	5	6	6	6	3	3	6	4	4	6	4	6	4	5	6
V Query 4	No	Yes	No	No	No	No	No	No	Yes	-	No	No	No	No	Yes	No	No	No	No	No	No	No	No	No	Yes	No	No	No	No	No	No	No
V Query 5	-	2	-	-	6	-	3	2	5	-	4	5	-	6	3	-	-	2	-	-	-	-	5	5	-	-	-	2	3	-	5	-
V Query 6	-	4	-	-	-	-	5	6	6	6	5	6	-	1	4	-	5	5	2	-	-	5	-	5	-	-	-	5	7	-	6	-
VC Query 1	Yes	Yes	Yes	Yes	Yes	Yes	Yes	Yes	Yes	No	Yes	Yes	Yes	Yes	Yes	Yes	Yes	-	Yes	Yes	Yes	Yes	Yes	Yes	Yes	Yes	Yes	Yes	Yes	Yes	Yes	Yes
VC Query 2	1	1	4	3	1	2	1	6	5	1	3	6	5	1	2	6	2	-	2	1	1	2	2	2	1	1	1	1	4	1	2	1
VC Query 3	7	3	5	6	5	3	6	3	7	7	7	6	3	2	6	6	6	5	5	6	4	3	5	4	4	7	3	3	7	7	4	5
VC Query 4	Yes	Yes	Yes	No	No	Yes	Yes	Yes	Yes	No	Yes	Yes	Yes	No	No	No	No	-	No	Yes	Yes	Yes	Yes	Yes	Yes	Yes	Yes	Yes	Yes	Yes	Yes	Yes
VC Query 5	2	1	3	-	1	4	1	6	1	3	3	2	1	-	2	-	3	-	1	1	1	1	1	2	1	4	3	2	3	3	1	1
VC Query 6	-	4	4	-	5	5	3	7	3	6	4	3	3	-	2	-	3	-	-	3	2	4	4	2	5	5	4	4	-	3	3	6
VB Query 1	Yes	Yes	Yes	Yes	Yes	Yes	Yes	Yes	Yes	No	Yes	Yes	Yes	Yes	Yes	No	Yes	Yes	Yes	Yes	Yes	Yes	Yes	Yes	Yes	No	No	No	Yes	No	Yes	No
VB Query 2	1	2	4	5	1	1	1	4	6	2	6	6	3	7	2	5	2	5	1	6	2	4	6	6	1	7	1	5	3	1	2	4
VB Query 3	1	5	5	5	4	2	7	6	6	1	7	6	3	2	3	5	4	5	4	2	4	6	6	6	7	-	3	5	7	1	4	4
VB Query 4	No	Yes	Yes	Yes	Yes	Yes	No	Yes	Yes	Yes	No	No	No	No	No	No	Yes	Yes	Yes	Yes	No	No	Yes	Yes	Yes	-	No	No	Yes	No	Yes	No
VB Query 5	-	1	4	3	1	1	1	3	2	-	2	-	-	-	2	-	4	4	1	5	-	4	4	3	-	-	2	2	5	-	3	-
VB Query 6	-	2	5	1	4	7	7	4	-	4	4	-	-	-	2	-	4	2	5	1	3	6	2	6	4	-	5	4	-	2	5	-
VE Query 1	Yes	Yes	Yes	No	Yes	No	No	Yes	Yes	Yes	Yes	Yes	Yes	No	Yes	Yes	Yes	Yes	Yes	No	No	No	No	Yes	Yes	No	No	No	No	Yes	Yes	No
VE Query 2	5	2	4	7	3	5	5	4	3	7	4	2	3	1	6	2	5	1	6	5	6	7	5	3	2	2	7	2	3	1	6	4
VE Query 3	5	3	5	5	3	3	5	5	6	6	4	4	3	3	3	5	2	5	5	6	6	4	5	5	5	5	5	7	7	7	5	6
VE Query 4	Yes	Yes	Yes	No	Yes	No	No	Yes	Yes	Yes	No	No	No	No	Yes	Yes	No	No	Yes	No	No	No	No	Yes	Yes	No	No	No	No	Yes	Yes	No
VE Query 5	3	2	4	-	3	-	-	5	3	2	4	4	-	2	6	5	-	6	1	-	-	-	-	2	7	-	-	-	-	6	5	6
VE Query 6	6	4	5	-	5	-	-	7	4	4	3	5	-	1	6	6	-	6	4	-	-	-	-	6	4	-	-	-	-	4	3	6

96

Table G.2: Qualitative Devices' Metrics: Collected Data from all Trials.

	Participant	1	2	3	4	5	6	7	8	9	10	11	12	13	14	15	16	17	18	19	20	21	22	23	24	25	26	27	28	29	30	31	32
VC	Query 1	4	2	3	2	1	1	2	2	1	1	5	1	1	1	2	3	1	-	2	1	3	2	2	2	3	1	2	1	1	5	2	5
	Query 2	1	6	3	1	1	1	2	2	1	3	5	1	3	4	2	2	3	-	2	1	3	4	4	2	1	1	2	1	4	5	2	6
	Query 3	2	6	4	2	1	1	4	3	1	6	5	5	1	4	2	4	5	-	2	1	4	4	2	5	6	4	2	1	4	4	2	5
	Query 4	3	4	3	2	3	3	3	3	3	2	3	3	3	2	2	3	5	-	3	3	2	2	2	3	3	3	2	2	2	2	3	3
	Query 5	7	6	6	7	7	6	7	6	7	7	5	7	5	7	6	6	7	-	6	7	7	5	7	6	6	3	6	7	7	5	7	7
	Query 6	7	6	4	3	7	5	7	6	7	6	5	6	3	6	2	3	6	-	5	7	7	5	6	5	6	6	6	5	4	3	5	6
	Query 7	7	6	4	2	6	5	5	5	7	7	5	5	2	6	2	2	6	-	5	7	7	6	6	4	2	5	7	5	3	4	5	7
	Query 1	1	2	2	1	1	1	1	2	1	1	1	1	1	1	2	2	1	1	1	1	1	3	4	6	3	1	1	5	1	1	3	4
	Query 2	1	2	3	1	1	1	4	2	1	1	3	1	2	1	2	3	2	1	2	1	1	5	5	6	2	3	1	1	4	2	3	5
	Query 3	1	2	4	3	2	1	5	3	1	5	4	3	1	7	1	2	5	2	2	1	1	5	5	6	5	4	1	2	2	1	5	5
	Query 4	2	3	3	2	3	3	3	2	3	2	2	2	2	2	2	2	3	2	3	2	3	2	3	1	3	2	2	2	1	2	3	2
	Query 5	7	6	5	7	7	6	7	5	7	5	7	6	6	7	6	5	4	7	6	5	5	1	5	3	3	3	6	5	2	7	4	6
	Query 6	7	6	5	5	6	7	5	6	5	7	4	7	5	3	2	4	3	2	6	3	7	4	5	2	3	5	6	5	2	6	5	6
	Query 7	7	6	5	4	7	6	6	6	3	6	4	5	5	4	2	2	3	2	6	4	6	2	5	3	3	4	6	6	2	6	5	7
VB	Query 1	5	3	5	2	4	3	4	4	1	3	4	2	3	1	5	5	1	5	2	1	5	5	4	3	4	4	2	1	5	3	5	4
	Query 2	1	3	5	1	3	4	3	5	1	3	4	3	2	3	3	5	3	5	3	1	6	6	5	5	2	2	2	5	4	4	5	6
	Query 3	2	2	4	2	2	2	4	4	2	6	4	4	1	2	4	5	2	1	2	1	3	6	5	6	6	4	1	1	6	5	3	6
	Query 4	3	3	3	1	3	2	3	3	2	3	2	3	1	3	3	3	1	1	3	1	2	1	1	3	2	2	1	2	2	2	3	3
	Query 5	3	6	3	2	3	4	2	2	4	2	2	5	1	4	2	4	3	1	2	1	2	1	2	3	2	3	2	2	2	2	2	4
	Query 6	3	6	5	1	4	2	2	4	3	4	1	5	1	4	2	5	4	1	5	1	2	2	3	5	3	5	2	2	5	2	2	5
	Query 7	3	6	3	1	4	2	2	4	4	4	1	3	1	4	1	3	2	1	5	1	3	2	4	4	3	5	2	1	4	2	2	6
VE	Query 1	5	3	5	2	4	3	4	4	1	3	4	2	3	1	5	5	1	5	2	1	5	5	4	3	4	4	2	1	5	3	5	4
	Query 2	1	3	5	1	3	4	3	5	1	3	4	3	2	3	3	5	3	5	3	1	6	6	5	5	2	2	2	5	4	4	5	6
	Query 3	2	2	4	2	2	2	4	4	2	6	4	4	1	2	4	5	2	1	2	1	3	6	5	6	6	4	1	1	6	5	3	6
	Query 4	3	3	3	1	3	2	3	3	2	3	2	3	1	3	3	3	1	1	3	1	2	1	1	3	2	2	1	2	2	2	3	3
	Query 5	3	6	3	2	3	4	2	2	4	2	2	5	1	4	2	4	3	1	2	1	2	1	2	3	2	3	2	2	5	2	2	4
	Query 6	3	6	5	1	4	2	2	4	3	4	1	5	1	4	2	5	4	1	5	1	2	2	3	5	3	5	2	2	5	2	2	5
	Query 7	3	6	3	1	4	2	2	4	4	4	1	3	1	4	1	3	2	1	5	1	3	2	4	4	3	5	2	1	4	2	2	6